April 2001

Applied MICROWAVE & WIRELESS

www.amwireless.com

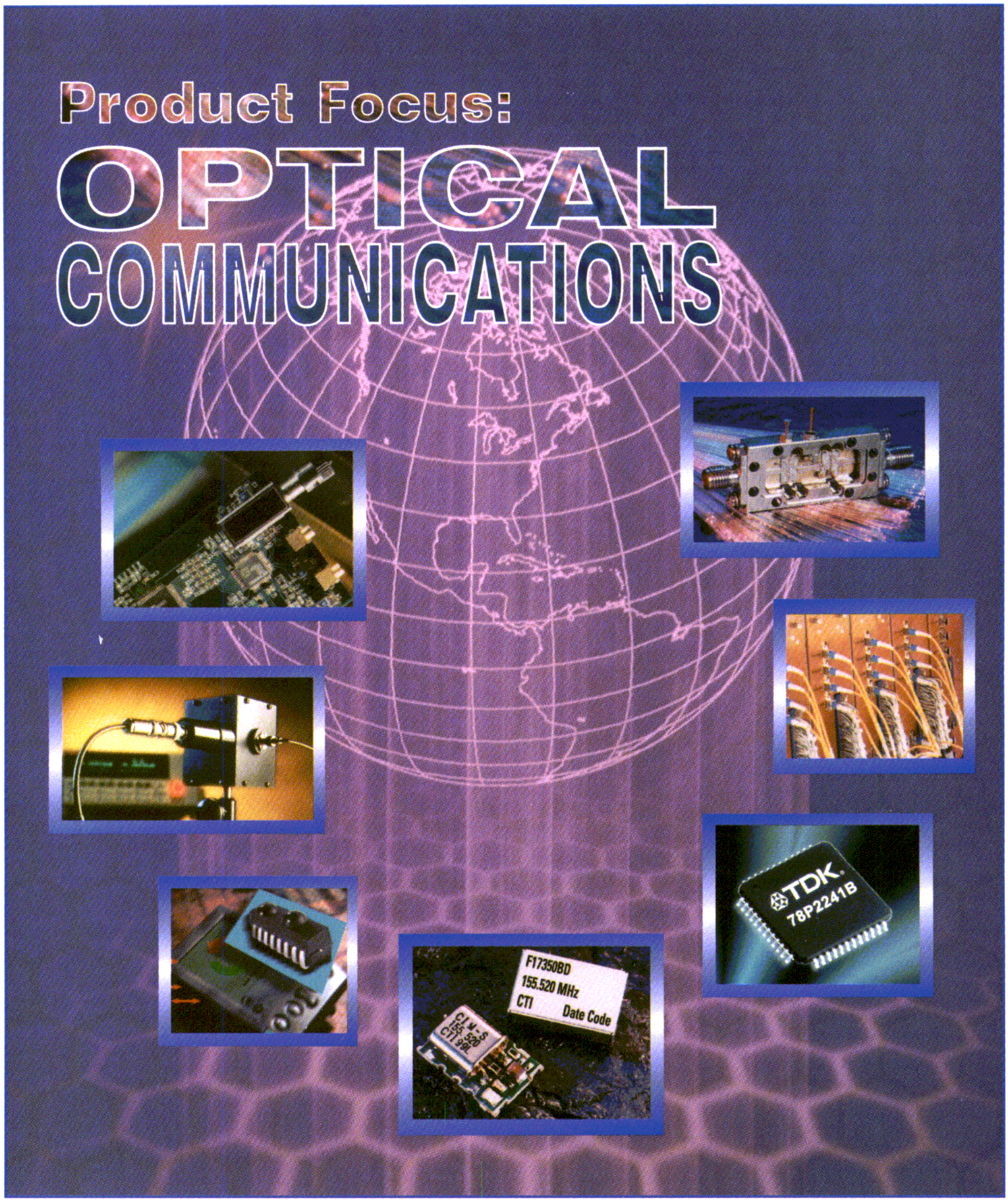

Test & Measurement

Narrow Band Ultra-Low VSWR Cable Assemblies

Design Techniques

A Comparison of Bipolar Transistor Biasing Techniques

Guest Editorial

Maximizing the Potential of the Radio Spectrum

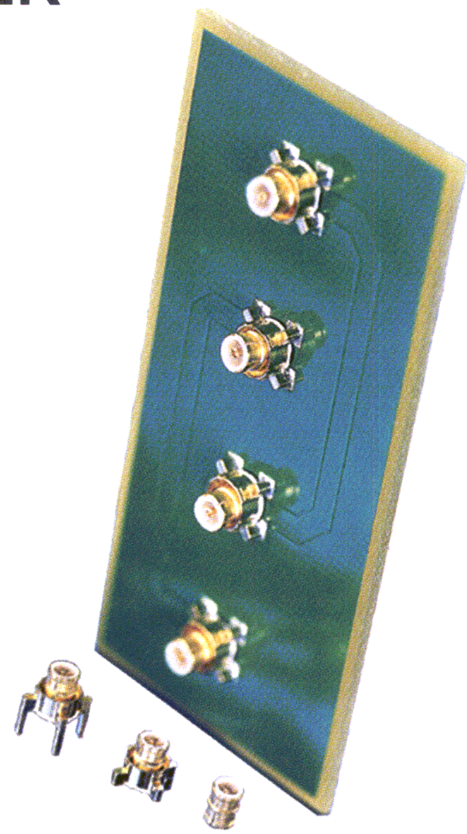

THE WORLD'S LARGEST SELECTION

POWER SPLITTERS/ COMBINERS

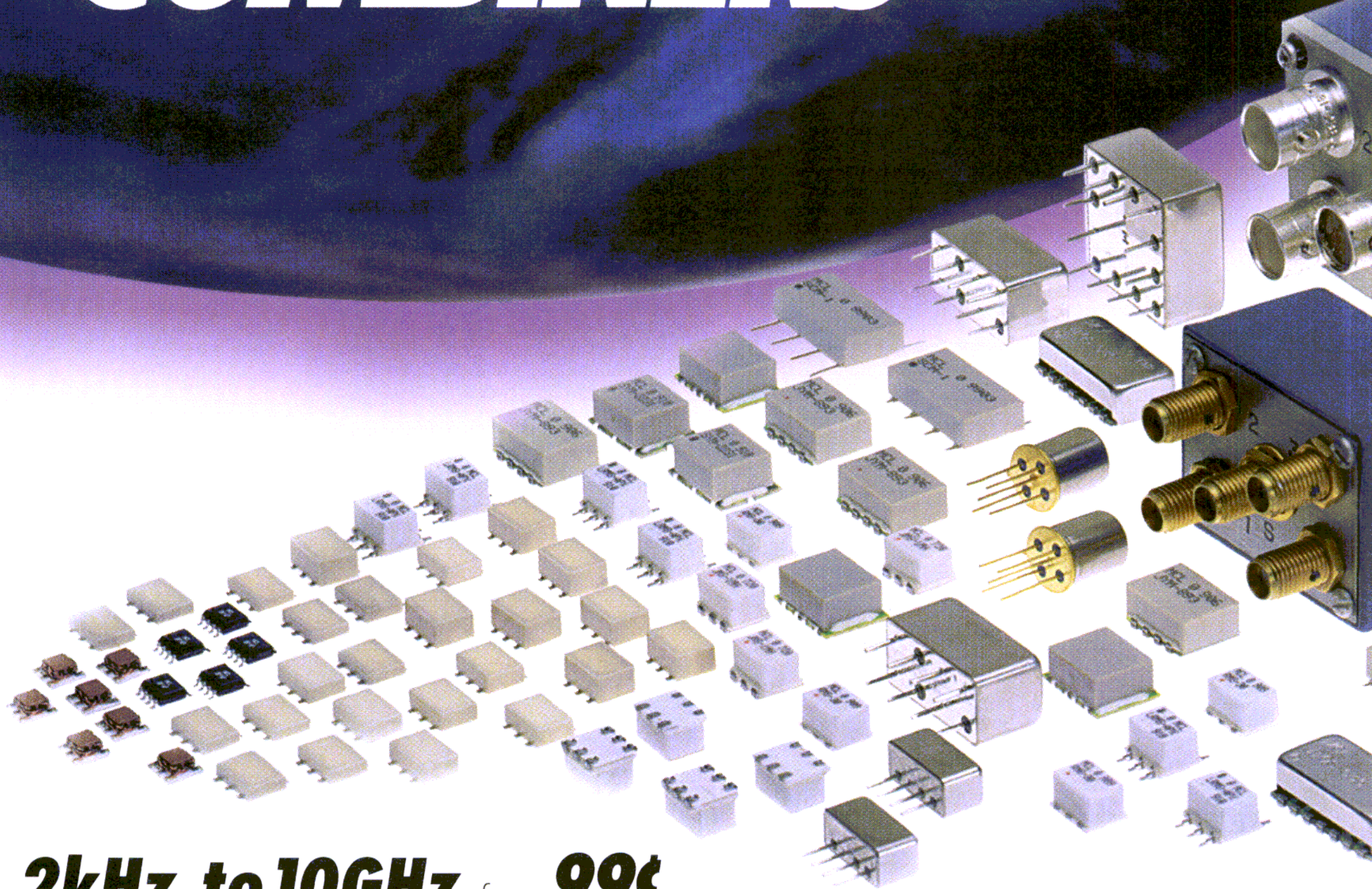

2kHz to 10GHz *from* 99¢

Choose from over 550 standard off-the-shelf models from 2way and 3way to 48way; 0°, 90°, and 180°; 50 and 75 ohms covering 2kHz to 10GHz. Mini-Circuits will also supply your special needs and custom designs such as wider bandwidths, higher isolation, lower insertion loss and phase matched ports...all at catalog prices with rapid turnaround time. Case styles include surface mount, plug-in, flat pack, and coaxial connectorized... and custom case styles are no problem! Super-miniature and ultra-low profile surface mount units provide excellent solutions in cellular communications, cable systems, and countless wireless applications. And all units come with a 1 year guarantee and skinny 4.5 sigma performance repeatability unit-to-unit and production run to production run. Add fast delivery, unsurpassed applications support and value pricing, and the decision is easy. Call Mini-Circuits today!

Mini-Circuits...we're redefining what VALUE is all about!

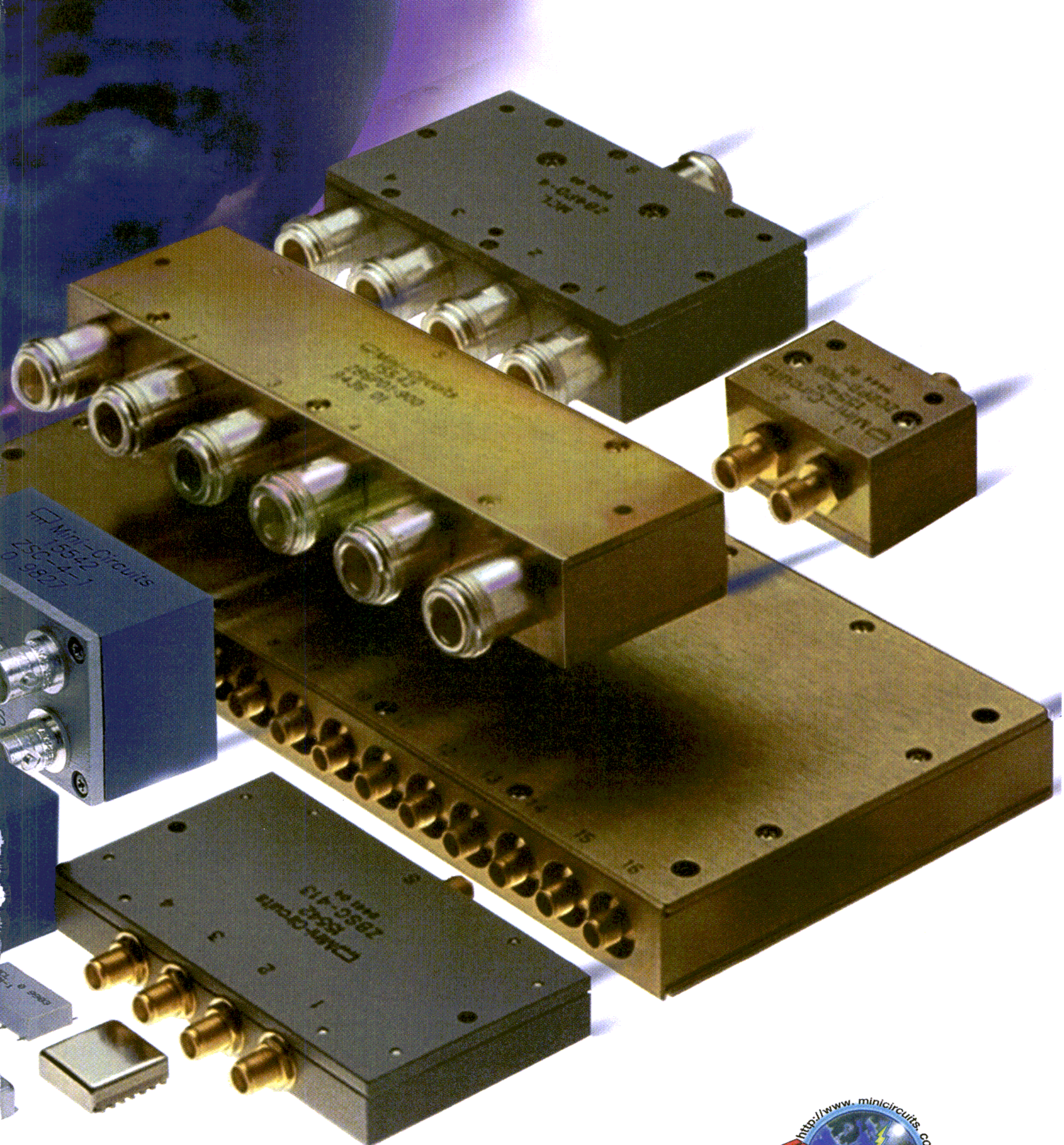
Mini-Circuits
15542
ZSC-4-1

Economize.

At prices as low as 29¢ each*, Stanford Microdevices' affordable SGA series gain blocks present a cost-effective solution to designers with high-volume requirements in wireless data products and thousands of general-purpose applications up to 5 GHz.

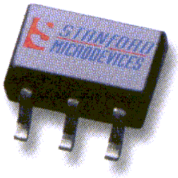

SOT-363 Package

And, the SGA series' economy goes beyond price. The units' low-voltage operation and low DC current requirement make them ideal for today's vast range of wireless devices requiring power-efficient performance.

The broadband units also offer exceptional IP3 performance and superior linearity for the power consumed.

Part Number	Bandwidth (GHz)	Gain @ 1 GHz (dB)	Gain (dB)	P1dB (dBm)	OIP3 (dBm)	Noise Figure (dB)	Vd (V)	Id (mA)
Low Voltage Gain Blocks								
SGA-0163	DC-4.5	13	12	-2	+9	4.7	2.1	8
SGA-0363	DC-5.0	20	17	+2	+14	3.0	2.5	11
High Reverse Isolation Gain Blocks								
SGA-1163	DC-6.0	12	11	-3	+8	3.1	4.6	12
SGA-1263	DC-4.0	16	15	-8	+3	2.7	2.8	8
General Purpose Gain Blocks								
SGA-2163	DC-5.0	10	10	+7	+21	4.2	2.2	20
SGA-2263	DC-3.5	15	14	+8	+20	3.2	2.2	20
SGA-2363	DC-2.8	17	16	+8	+19	2.9	2.7	20
SGA-2463	DC-2.0	20	17	+9	+20	2.7	2.7	20

For more information, visit us at stanfordmicro.com.

*500,000 pieces

STANFORD MICRODEVICES

www.stanfordmicro.com • 800.764.6642

Circle 25

Applied
MICROWAVE & WIRELESS

April 2001
Vol. 13 No. 4

CONTENTS

TECHNICAL FEATURES

Applied MICROWAVE & WIRELESS

April 2001
Vol. 13 No. 4

PRODUCTS & TECHNOLOGIES

GUEST EDITORIAL

DEPARTMENTS

Publisher
Gary A. Breed
Associate Publisher
Scott Spencer
Director of Operations
Dennis Ford
Managing Editor
Shannon O'Connor
Senior Consulting Editor
Dr. Joseph F. White
Editorial Advisors
Dr. Peter Staecker
Dr. James C. Rautio
Dr. Frederick H. Raab
Dr. Les Besser
Dr. Peter Rizzi
Dr. T.B. Ramachandran
Ben Robinson
Art Director
Joan Clipp
Assistant Editors
Kristine Phillips
Sarah Sturm
Associate Editor
Martina Voigt
Data Manager
Nancy Breed
Office Assistant
Stephanie Hayden
Advertising Sales — East
Scott Spencer
Tel: 603-472-8261
Fax: 603-471-0716
Advertising Sales — West
Tim Burkhard
Tel: 707-544-9977
Fax: 707-544-9375
Classified & Spotlight Ads, Reprints and List Rentals
Aileen Kronke
Tel: 770-449-6774
Fax: 770-448-2839
New Subscriptions and Address Changes
Mail: 630 Pinnacle Court
Norcross, GA 30071
Fax: 770-448-2839
Back Issues
Tel: 770-449-6774

BPA INTERNATIONAL®

NOBLE PUBLISHING

Applied Microwave & Wireless
Noble Publishing Corporation
630 Pinnacle Court
Norcross, GA 30071
Tel: 770-449-6774
Fax: 770-448-2839
E-mail: amw@amwireless.com
www.amwireless.com

AMPLIFIERS

FOR EVERY APPLICATION

- HIGH RELIABILITY
- COMPETITIVELY PRICED
- QUICK DELIVERY

Model#	Freq Range (GHz)	Gain (dB min)	N/F (dB max)	Gain Flat (+/-dB)	1 dB comp. pt. (dBm min)	3rd Order ICP min	VSWR In/Out max	DC Current (mA)
MEDIUM POWER AMPLIFIERS (UP TO 2 WATTS)								
JCA01-P01	0.5-1.0	25	3.5	1	30	40	2.0:1	250
JCA12-P01	1.0-2.0	32	3	1	30	40	2.0:1	800
JCA34-P01	3.7-4.2	30	3	1	30	40	2.0:1	750
JCA56-P01	5.9-6.4	30	3	1	30	40	2.0:1	850
JCA78-P01	7.9-8.4	30	4	1	30	40	2.0:1	900
JCA812-P02	8.3-11.7	40	5	1.5	33	40	2.0:1	1700
JCA910-P01	9.5-10.0	30	4	1	33	40	2.0:1	1300
JCA1011-P01	10.7-11.7	30	4	1	30	40	2.0:1	950
JCA1819-P01	18.1-18.6	30	5	1	27	37	2.0:1	800
RADAR & COMMUNICATION BAND LOW NOISE AMPLIFIERS								
JCA23-302	2.2-2.3	30	0.8	0.5	10	20	2.0:1	80
JCA34-301	3.7-4.2	30	1	0.5	10	20	2.0:1	80
JCA56-502	5.4-5.9	50	1	0.5	10	20	2.0:1	160
JCA78-305	7.25-7.75	27	1.2	0.5	13	23	2.0:1	100
JCA910-305	9.0-9.5	27	1.4	0.5	13	23	1.5:1	150
JCA1112-305	11.7-12.2	27	1.5	0.5	13	23	1.5:1	150
JCA1415-305	14.0-14.5	26	1.6	0.5	13	23	1.5:1	160
JCA1819-305	18.1-18.6	22	2.0	0.5	10	20	1.5:1	160
JCA2021-600	20.2-21.2	30	2.2	1	13	23	1.5:1	240
TRI-BAND AMPLIFIERS (5.85 TO 14.5)								
JCA514-201	5.85-14.5	8	7	1.5	10	20	2.0:1	100
JCA514-300	5.85-14.5	14	6	1.5	10	20	2.0:1	150
JCA514-302	5.85-14.5	22	6	1.5	20	30	2.0:1	350
JCA514-400	5.85-14.5	25	6	1.5	10	20	2.0:1	250
JCA514-403	5.85-14.5	32	6	1.5	23	33	2.0:1	500
JCA514-501	5.85-14.5	35	6	1.5	16	26	2.0:1	375
JCA514-503	5.85-14.5	41	6	1.5	23	33	2.0:1	500
ULTRA-BROAD BAND AMPLIFIERS (2.0 TO 18 GHZ)								
JCA218-200	2.0-18.0	15	5	2.5	10	20	2.0:1	90
JCA218-300	2.0-18.0	23	5	2.5	10	20	2.0:1	110
JCA218-400	2.0-18.0	29	5	2.5	10	20	2.0:1	150
JCA218-500	2.0-18.0	39	5	2.5	10	20	2.0:1	180

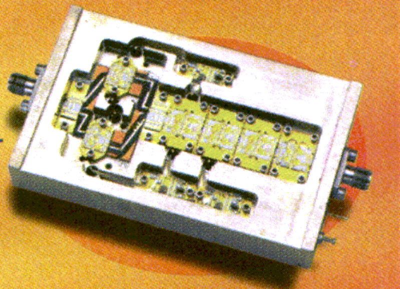

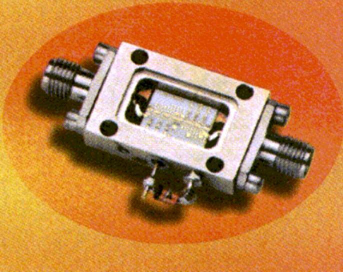

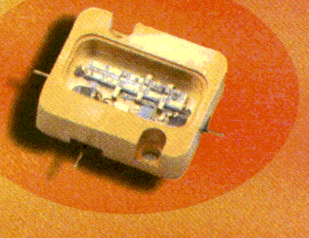

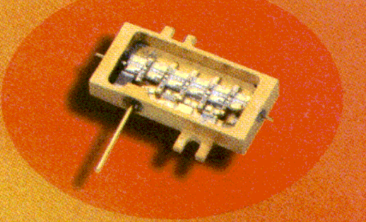

JCA's catalog can now be downloaded from the Web at www.jcatech.com

JCA TECHNOLOGY

DELIVERY IN 2-4 WEEKS ARO

4000 Via Pescador, Camarillo, CA 93012
Phone: (805) 445-9888 • Fax: (805) 987-6990
Email: jca@jcatech.com

Circle 49

Editorial

Are Standards Really Needed for Wireless Data Applications?

By Gary A. Breed
Publisher

Several years ago, when the IEEE 802.11 Committee meetings were rowdy, contentious affairs, I began wondering whether it was worth the trouble. If standards are delayed, compromised and watered-down, will they still be viable at the end of the process? Wireless data products based on IEEE 802.11 should have been on the market six years ago. Instead, they are appearing only now. The IEEE 802.11 experience is a perfect example of a process that was based on the belief that standards would help create a new market. Instead, the standards battle may have prevented a market from developing as fast as it should have.

Coming from a different direction is Bluetooth. Its success as a standard has come as a result of a commercial, industry-driven process. In part, Bluetooth arose out of frustration with the IEEE 802.11 process. The profit motive is more powerful than the politics of an independent standards committee. The first widely available products using Bluetooth technology will show up in stores later this year.

In the meantime, many companies (and a few consumers) have been using wireless data without regard to standards. A vast number of specific needs have been met without concern for off-the-shelf technology or interoperability. If a company wants to install a 10 Mb/s wireless data link between its main office and the new R&D lab across the freeway, many proprietary solutions are available.

If I want to connect my upstairs computer to the one in the downstairs office, I can either wait for a standards-based unit to appear at an affordable price, or can go out today and buy some company's 900 MHz or 2.4 GHz ISM band wireless unit that uses a proprietary communications protocol. As long as my units talk to each other, why should I care if they are compliant with some standard?

In the long run, standards are required. Sometime in the future, wireless interconnections will be commonplace, and different users will need to communicate with a common modulation format and data transfer protocol. But even then, the standard will be unimportant once the user is outside that wireless network. ■

Letters

Readers comment on FSK article

Editor:

K. Jegnathan's article (*Design Ideas, "A Transistor-Controlled FSK Modulator/Transmitter," December 2000*) suggests that a 25 MHz crystal oscillator can be pulled 5 MHz or so by the addition of inductor Lx — or, at least, that is what the data in Figure 5 suggests.

If the crystal motional capacitance C1 is 1E-15 farads as you suggest, then the change in reactance from 25 MHz to 30 MHz is about –j1E6 ohms! This suggests that the crystal is actually NOT part of the frequency determining elements. Remove the crystal from your circuit and re-run your simulations. I think you will find that the circuit still behaves the same.

Charlie Thompson
Maxim Austin Design Center

The author replies:

I acknowledged the simulation circuit could provide some misinterpretation easily. The resistance and the inductance parallel to the crystal oscillator should not be included during the simulation. Rather, these components are mainly needed for practical purposes only. The corrected circuit and the simulation results are given at right. As a matter of fact, the crystal oscillators can only be pulled for a few kilohertz only. If more deviation is required, then the harmonics of the fundamental can be tuned out through a relevant filter. The circuit shown at right provides a frequency deviation of about 5.3 kHz for the fundamental frequency.

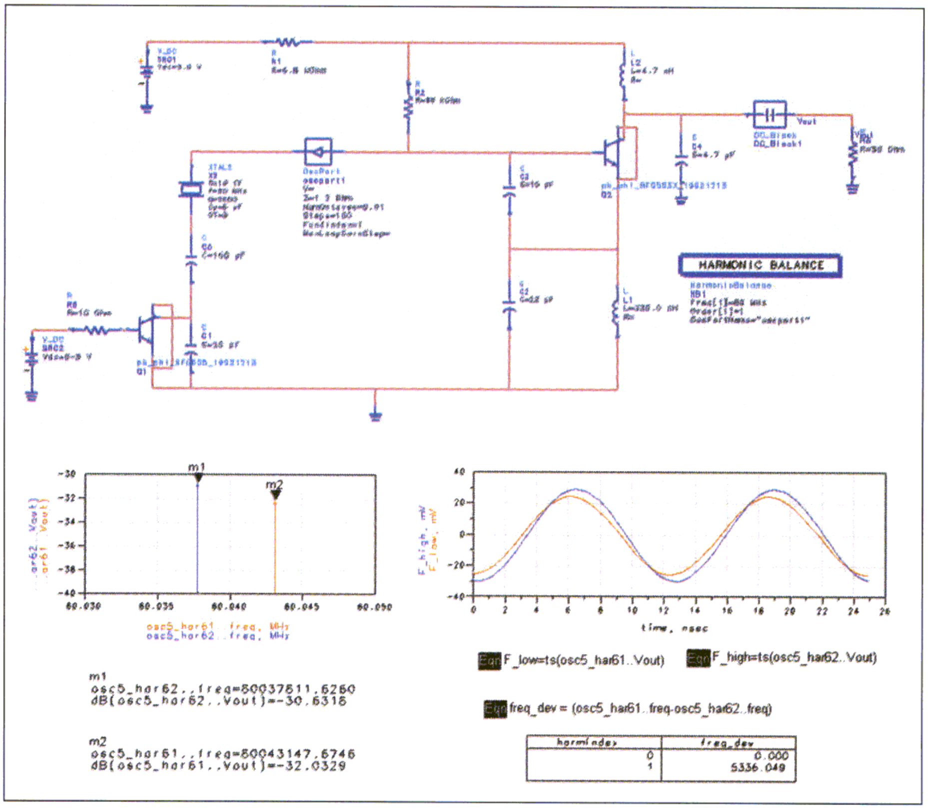

▲ **Corrected circuit and simulation results for a 25 MHz crystal oscillator.**

Editor:

In 1991, a client of mine (Worthington Data Systems, Santa Cruz, CA) asked me to design a pen barcode reader that would be completely wireless. I successfully accomplished this by using the very same modulator described in this article, along with two other innovations I thought were unique at that time. I came up with the idea of GMSK filtering and transmission and also a stabilized DC balancing circuit that allowed completely un-scrambled data to be sent even though the data contained strings of zeros or ones. A patent application was written that included all of these circuits, but as far as I know it was not filed with the USPO. It's probably good it wasn't filed, because I've been told these ideas were very likely prior art to my disclosure in 1991. I still have the EESOF Libra simulations and the FCC lab Part 15 testing results showing this combination of modulation with this modulator/transmitter indeed worked very well.

Jeffrey Pawlan
Pawlan Communications

Amateur radio draws interest

Editor:

I read with interest your October 2000 editorial, asking, "How can we get kids interested in wireless technology careers?" In my opinion, one good way to get fresh blood is amateur radio. By getting youngsters interested in Ham Radio very early, most of them get hooked and will choose courses enabling them to work in the wireless field. For example, I got interested in Ham Radio when I was 13. Until then, I'd never been a math-inclined pupil, but I saw that math would be very useful for my hobby. I then began to get good grades in math simply because I understood its usefulness for my hobby. Naturally, the hobby pushed me in my school courses in a way I would not have investigated before.

A few years ago, two men received the Nobel Prize in Physics for their studies. One of them commented that without being interested in Ham Radio when he was a kid, he would never have won the prize.

Best wishes and thanks very much for the nice magazine.

Dom DeHays
Instructor, ENAC France

Calendar

CONFERENCES

APRIL

April 20-21, 2001
Topical Workshop on Flip Chip Technology
Palo Alto, CA
Information: IMAPS
Tel: 703-758-1060; Fax: 703-758-1066
E-mail: imaps@imaps.org
Internet: http://www.imaps.org

April 21-26, 2001
National Association of Broadcasters Conference and Exhibition (NAB2001)
Las Vegas, NV
Information: NAB
Internet: http://www.nab.org

April 23-25, 2001
49th International Relay Conference
Oak Brook, IL
Information: ECA
Tel: 703-907-7547
Internet: http://www.ec-central.org

April 24-25, 2001
Second European Workshop on Conformal Antennas
The Hague, The Netherlands
Information: Wim L. Smith
E-mail: iec@fel.tno.nl
Internet: http://www.tno.nl/instit/fel/felnews/conformal_antennas

MAY

May 1-3, 2001
2001 IEEE Radar Conference
Atlanta, Georgia
Information: Georgia Institute of Technology
E-mail: conted@gatech.edu
Internet: http://www.conted.gatech.edu/home

May 8-10, 2001
Mikrowellen und Optronik (Microwaves and Optronics), The German Wireless Week (MIOP)
Stuttgart, Germany
Information: Dr. Martin Schallner
E-mail: martin.schallner@marconi.com

May 13-16, 2001
Fourth Conference on Electromagnetic Wave Interaction with Water and Moist Substances
Information: Dr. Klaus Kupfer
E-mail: klaus.kupfer@mfpa.de
Internet: http://www.mfpa.de

May 13-17, 2001
International Symposium on Electromagnetic Theory
Victoria, British Columbia, Canada
Information: Secretariat
Tel: 613-993-9431; Fax: 613-993-7250
E-mail: URSI-B2001@nrc.ca
Internet: http://www.nrc.ca/confserv/URSI-B2001

May 20-25, 2001
2001 IEEE MTT-S International Microwave Symposium
Phoenix, AZ
Information: LRW Associates
Tel: 704-841-1915; Fax: 704-845-3078
E-mail: lrwassoc@carolina.rr.com
Internet: http://www.ims2001.org

May 22-24, 2001
Automated Manufacturing Exposition
Greenville, SC
Information: Marlene Cobia
Tel: 803-779-7123, x. 17; Fax: 803-779-7167
E-mail: mcobia@tecinconline.com
Internet: http://www.am-expo.com

May 25, 2001
57th ARFTG Microwave Measurements Conference
Phoenex, AZ
Information: David Walker
Tel: 303-497-5490; Fax: 303-497-3970
E-mail: dwalker@boulder.nist.gov
Internet: http://www.arftg.org

JUNE

June 6-8, 2001
IEEE International Conference on Third Generation Wireless and Beyond (3Gwireless'01)
San Francisco, CA
Information: H. Janny
E-mail: janny@delson.org
Internet: http://www.3Gwireless.com/3Gwireless01

June 6-8, 2001
IEEE Frequency Control Symposium & PDA Exhibition
Seattle, WA
Information: ECA
Tel: 703-907-7547
Internet: http://www.ec-central.org

June 6-8, 2001
2001 Virginia Tech Symposium on Wireless Personal Communications
Blacksburg, VA
Information: Jenny Frank
Tel: 540-231-2971
E-mail: mprg@vt.edu

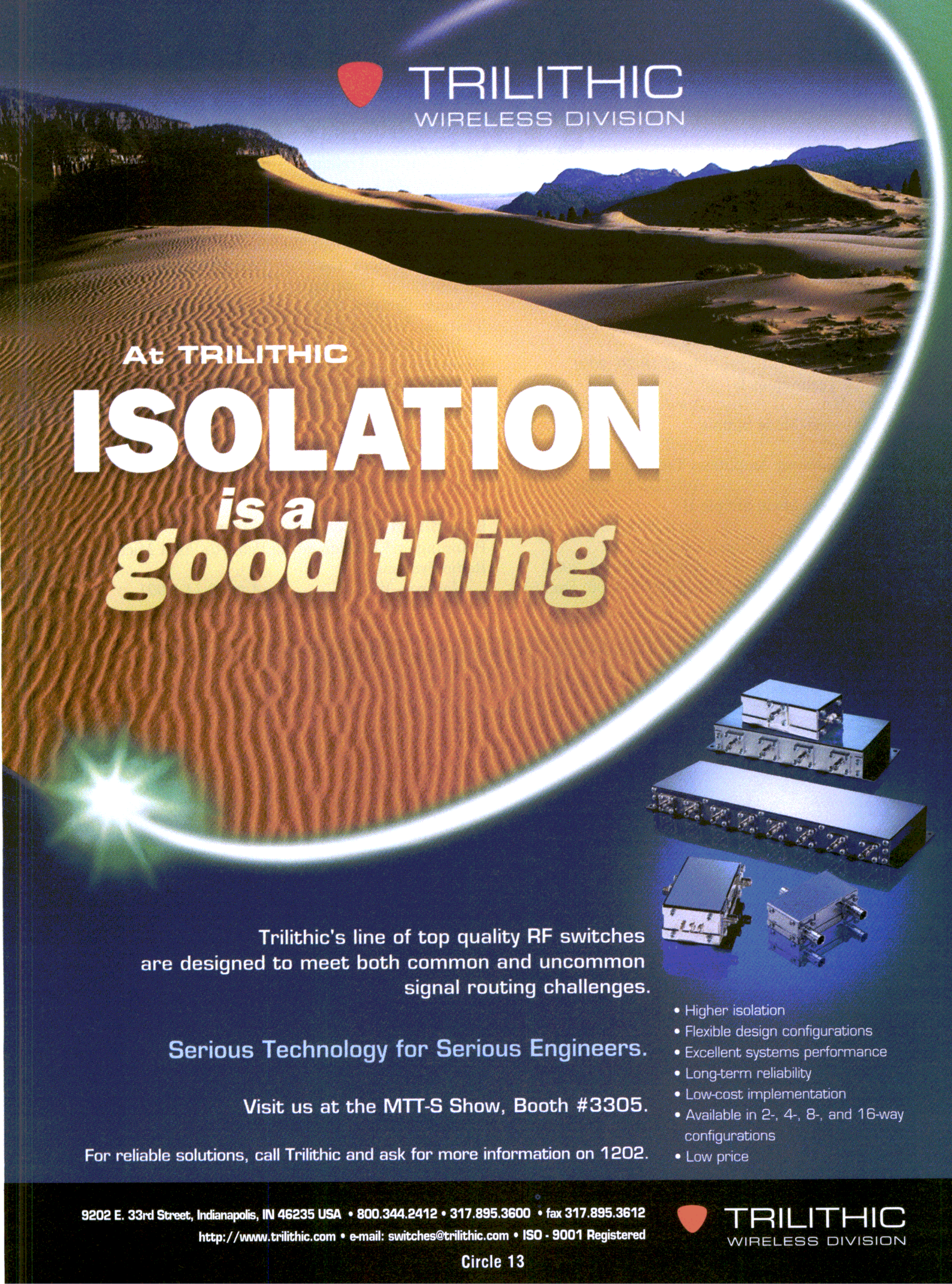
TRILITHIC
WIRELESS DIVISION
At TRILITHIC
ISOLATION
is a
good thing
Trilithic's line of top quality RF switches
are designed to meet both common and uncommon
signal routing challenges.
Serious Technology for Serious Engineers.
Visit us at the MTT-S Show, Booth #3305.
For reliable solutions, call Trilithic and ask for more information on 1202.
• Higher isolation
• Flexible design configurations
• Excellent systems performance
• Long-term reliability
• Low-cost implementation
• Available in 2-, 4-, 8-, and 16-way configurations
• Low price
9202 E. 33rd Street, Indianapolis, IN 46235 USA • 800.344.2412 • 317.895.3600 • fax 317.895.3612
http://www.trilithic.com • e-mail: switches@trilithic.com • ISO - 9001 Registered
Circle 13
TRILITHIC
WIRELESS DIVISION

SHORT COURSES

Besser Associates

Fiber Optics Made Simple
Mountain View, CA . . . . . .April 2-3, 2001
Broadband Networking Made Simple
Mountain View, CA . . . . . .April 4-5, 2001
Antennas and Array Design for Wireless Communications
Mountain View, CA . . . . . .April 9, 2001
Filters for Wireless Applications
Mountain View, CA . . . . . .April 16-17, 2001
DSP Made Simple for Engineers
Mountain View, CA . . . . . .April 18-20, 2001
Applied RF Techniques I
Boston, MA . . . . .April 23-27, 2001
RF and Wireless Made Simple
Boston, MA . . . . .April 24-25, 2001
Advanced RF Power Amplifiers Techniques
Boston, MA . . . . .April 24-27, 2001
RF and Wireless Made Simple II
Boston, MA . . . . .April 26-27, 2001
Modern Digital Modulation Techniques
Mountain View, CA . . . . . .April 30-May 4, 2001
Information: Annie Wong, Tel: 650-949-3300; Fax: 650-949-4400; E-mail: info@bessercourse.com; Internet: www.bessercourse.com.

TTi Technology Training Initiative (Tustin Technical Institute, Inc.)

Calibration Processes
Santa Barbara, CA . . . . . .April 2-4, 2001
Physical Measurement Techniques
Santa Barbara, CA . . . . . .April 9-11, 2001
Measurement Uncertainty
Santa Barbara, CA . . . . . .April 11-13, 2001
Thermal Analysis and Heat Transfer
Santa Barbara, CA . . . . . .April 18-20, 2001
Grounding and Shielding for EMI/EMC/ESD
Santa Barbara, CA . . . . . .April 25-27, 2001
Test Procedures for EMI/EMC/ESD
Santa Barbara, CA . . . . . .April 30-May 2, 2001
Information: Brian P. Slatery, Tel: 805-682-7171; Fax: 805-687-6949; E-mail: brian@ttiedu.com; Internet: www. ttiedu.com.

University of Wisconsin at Madison

Planning and Implementing Point-to-Point Microwave Radio Systems
Madison, WI . . . . .April 9-11, 2001

For Point-to-Multipoint Applications...
...MMDS and UNII RF Heads
WJ MMDS Point-to-Multipoint RF Unit
2.5–2.7GHz
Up to 60MHz Tx, Rx
MDS Tx Option
WJ UNII Point-to-Multipoint RF Unit
5.725–5.825GHz
25MHz Tx, Rx Bands
WJ Communications – a Cisco Technology Partner
Other features include:
Full duplex operation
Integral antennas
Single cable interface from IDU to ODU
Optional duplexer configurations
For more details, call our toll free number, fax us at 408-577-6620 or e-mail us at sales@wj.com. Data sheets are available in PDF download file format by visiting our web site at www.wj.com.
broadband wireless internet forum
1-800-WJ1-4401
Visit us on the web at www.wj.com
Circle 60
The Communications Edge™
wj communications

Information: Katie Peterson, Tel: 1-800-462-0876; Fax: 608-263-3160; E-mail: custserv@epd.engr.wisc.edu; Internet: http://epd.engr.wis.edu.

University of California at Los Angeles Extension

Digital Signal Processing: Theory, Algorithms and Implementation
Los Angeles, CA . . . . .April 9-13, 2001

Charge-Coupled Devices/CMOS Imaging Sensors and Cameras
Los Angeles, CA . . . . .April 30-May 4, 2001

Information: UCLA Extension, Short Course Program Office, Tel: 310-825-3344; Fax: 310-206-2815.

University of Missouri-Rolla

Grounding and Shielding Electronic Systems
Columbus, OH . . . . .April 17-18, 2001

Circuit Board Layout to Reduce Noise Emission and Susceptibility
Columbus, OH . . . . .April 19, 2001

Information: Sue Turner, Tel: 573-341-6061; Fax: 573-341-4992; E-mail: suet@umr.edu; Internet: www.umr.edu/~conted.

Georgia Institute of Technology

Phased-Array Radar System Design
Smyrna, GA . . . . .April 17-20, 2001

Basic Radar Concepts
Smyrna, GA . . . . .April 24-26, 2001

Information: Georgia Tech Distance Learning, Continuing Education and Outreach, Tel: 404-894-2547; Fax: 404-894-7398; E-mail: conted@gatech.edu; Internet: www.conted.gatech.edu.

R.A. Wood Associates

Introductory RF & Microwaves
Baltimore, MD . . . . .April 19-25, 2001

RF and Microwave Receiver Design
Baltimore, MD . . . . .April 23-25, 2001

RF Power Amplifiers, Classes A through S
Baltimore, MD . . . . .April 19-20, 2001

Information: R.A Wood Associates, Tel: 315-735-4217; Fax: 315-735-4328; E-mail: RAWood@rawood.com; Internet: www.rawood.com.

Submit calendar items to amw@amwireless.com

RIDE THE

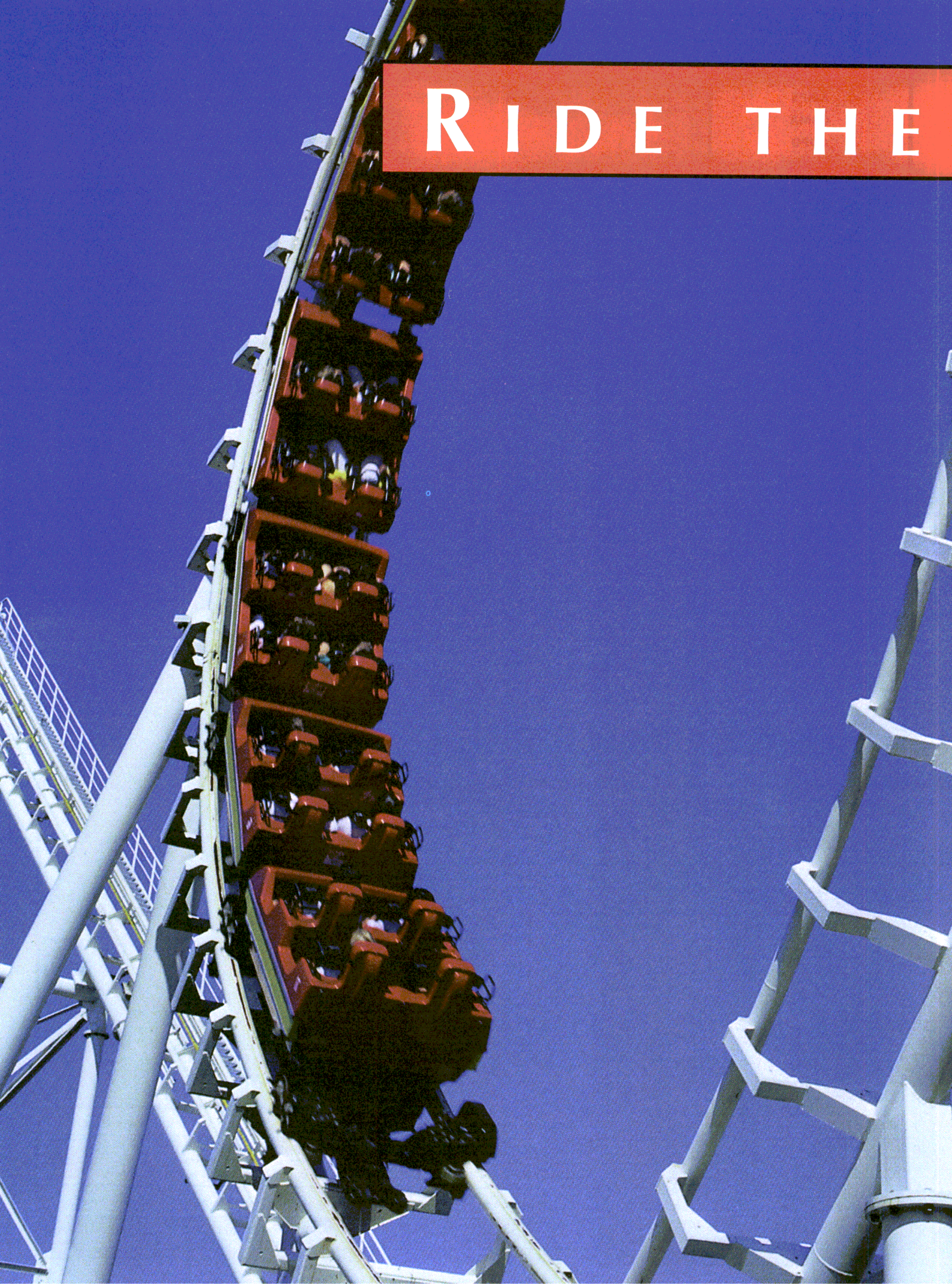

BRIEFS

• Adhesives Research has launched a Web site for its Electronics Business Unit as part of the company's corporate Web site at www.adhesiveresearch.com. The site provides information about the products, services and market applications offered by the unit, as well as links to the company's product catalog.

• Anritsu Company's new Web site, www.us.anritsu.com, offers information on the company's communications test solutions, optical and microwave components and devices, network solutions and industrial automation products.

• Vicor has introduced Power Express™, a service for rapid delivery of production quantities of its products. Most products are now eligible for Power Express and will be available with lead times of less than four weeks. Vicor plans to expand the service to include the company's entire product line.

• KNÜRR Group of Munich, Germany, has announced the acquisition of Quante's production facility in Newmarket, Cambridgeshire, UK. The UK site will manufacture KNÜRR's leading edge Miracle 19 inch racks and outdoor enclosure systems and provide integration services for its communication OEM customers.

• IMAPS, the International Microelectronics and Packaging Society, has announced that its Industry Guide is now available electronically and free of charge at www.imaps.org/indguide. The guide, a comprehensive listing of products and services for over 600 organizations, provides a searchable database of microelectronics and packaging companies.

Submit information for our News section to: Shannon O'Connor, *Applied Microwave & Wireless*, 630 Pinnacle Court, Norcross, GA, 30071; Fax: 770-448-2839; E-mail: amw@amwireless.com.

Andrew to supply communications system for Madrid airport-area metro stations

Andrew Corporation has been selected by the Madrid Metro as the supplier of a distributed communications system to be used in rail stations in the area around Barajas Aeropuerto, the international airport in Madrid, Spain.

▲ **Andrew Corporation will supply a distributed communications system for rail stations in and around Madrid's airport.**

The new system will support TETRA and GSM 900/1800 communications within the public areas of the airport line metro stations and adjoining running tunnels. It can also be upgraded for future UMTS technology, the next generation of mobile communications. The system is scheduled to be installed and operational by July 2001.

The system will provide wireless communications for the Madrid Metro's existing Mar de Cristal, Campo de las Naciones, Barajas Aeropuerto and Barajas Pueblo stations and their adjoining tunnels.

Andrew Corporation, located in Orland Park, IL, supplies communications systems equipment and services worldwide.

NEC to spin off semiconductor division

NEC Corporation plans to spin off its Compound Semiconductor Device Division into a new company, effective October 2001. NEC will retain full ownership of the new enterprise.

The new company will operate on a fabless semiconductor company business model and will be headquartered in Kawasaki, Kanagawa Prefecture, Japan. Manufacturing will initially be done at current NEC and contractor facilities.

NEC is based in Tokyo, Japan. Its Compound Semiconductor Device Division designs and manufactures silicon and GaAs RF and microwave semiconductor devices, as well as optical semiconductor devices.

OFDM Forum, CABA sign reciprocal membership agreement

The OFDM Forum, an association organized to promote a single-standard for high-speed wireless communications, has signed a reciprocal membership agreement with the Continental Automated Buildings Association (CABA).

The reciprocal membership is most applicable to the forum's LAN, PAN and HMM working group, which is focused on improving existing standards and facilitating the acceptance of Orthogonal Frequency Division Multiplexing as the technology of choice for the wireless LAN, PAN and home multi-media markets. In addition, the forum will be able to participate in CABA's Standards Committee, whose main objective is to facilitate and encourage industry-wide interoperability for protocols and standards.

The OFDM Forum is a market development association comprised of hardware manufacturers, software firms, telecommunications companies and other users interested in OFDM technology in wireless applications.

CABA's mission is to encourage the development, promotion and adoption of business opportunities in the home and building automation industry.

Freshfield helps Orange UK optimize network performance

Freshfield Communications Ltd. has completed a network measurement campaign on behalf of Orange UK, assessing the performance of all four GSM personal communications networks on selected mainline railways in the UK.

The campaign covered 1,500 calls on each of the four UK GSM networks along the main rail routes in several metropolitan areas. To simulate peak usage hours, calls were monitored continuously from 8 a.m. until 8 p.m.

Using Optima, Freshfield's multiband (GSM 900 and 1800 MHz) network monitoring and optimization tool, network performance was measured and assessed for typical rail passengers. Data from all four networks were simultaneously monitored without disruption to passengers or train service.

Freshfield, based in Surrey, UK, is a wireless consulting company offering solutions for network operators and infrastructure vendors.

Superconductor Technologies, Paradigm announce alliance

Superconductor Technologies Inc. and Paradigm Wireless Systems, Inc., have signed a strategic alliance under which they will jointly develop complete solutions that combine their respective technologies to deliver the first balanced link solutions to wireless operators seeking to optimize their networks.

Superconductor Technologies' systems improve the signal between the cell phone and the cellular tower or base station, while Paradigm's power amplifiers improve the signal between the base station and the cell phone. The two companies have combined their complementary technologies to create their first joint product, SuperLink™, which enables carriers to handle an additional 50 percent or more traffic on their existing networks, with their existing spectrum.

Superconductor Technologies, based in Santa Barbara, CA, manufactures superconducting products for wireless networks. Paradigm, based in Irvine, CA, provides multicarrier power amplifiers and RF technologies for wireless networks.

Honeywell debuts products using SOI technology

The Honeywell Solid State Electronics Center (SSEC) has introduced a variety of customized RF and microwave design and foundry services for designers and manufacturers in the wireless communication and high-speed fiber optic networks.

The Honeywell SSEC, located in Plymouth, MN, manufactures integrated circuits, sensors and electronic components for military, space and commercial applications.

BUSINESS AND FINANCE

IMPSAT signs agreement with Nextel

IMPSAT Fiber Networks, Inc., has signed a $22 million dollar agreement with Nextel Argentina under which IMPSAT will provide Lambda connectivity over its broadband network to support Nextel's transmission capacity for its voice and value added services.

This capacity will allow Nextel Argentina to extend the coverage of its digital mobile services to the principal commercial centers in Argentina, linking Buenos Aires and Mendoza along two fully redundant routes that also connect the cities of Santa Fe, Rosario, Cordoba and San Luis. In addition, IMPSAT will provide two 155 Mbps connections over complementary routes to smaller cities outside the main footprint.

The agreement marks the commencement of Lambda Channel offering in Argentina and confirms the Company's leadership in connectivity service provision for telecommunications carriers.

IMPSAT, based in Buenoe Aries, Argentina, provides Internet and private network integrated data and voice telecommunications services in Latin America.

Andrew receives three antenna contracts

Andrew Corporation has been awarded antenna-related contracts with Siemens, Loxley Ltd. and Alan Dick and Company.

- The Siemens contract calls for Andrew to supply an ALP Series II slotted antenna for the Bangkok Entertainment Company in Bangkok, Thailand. The 12-bay, medium power ALP antenna is the first and smallest of its type to be sold in Thailand.
- Under the agreement with Loxley Ltd., a Thai conglomerate, Loxley will equip the Royal Thai Navy with three Andrew HF antennas to boost ship-to-shore communications. The installation is due for completion in mid-2001.
- Andrew has agreed to market Alan Dick and Company's television transmitting antennas in North America. Alan Dick is Britain's leading supplier of masts, towers and antenna systems

Andrew Corporation, located in Orland Park, IL, is a global supplier of communications systems equipment and services.

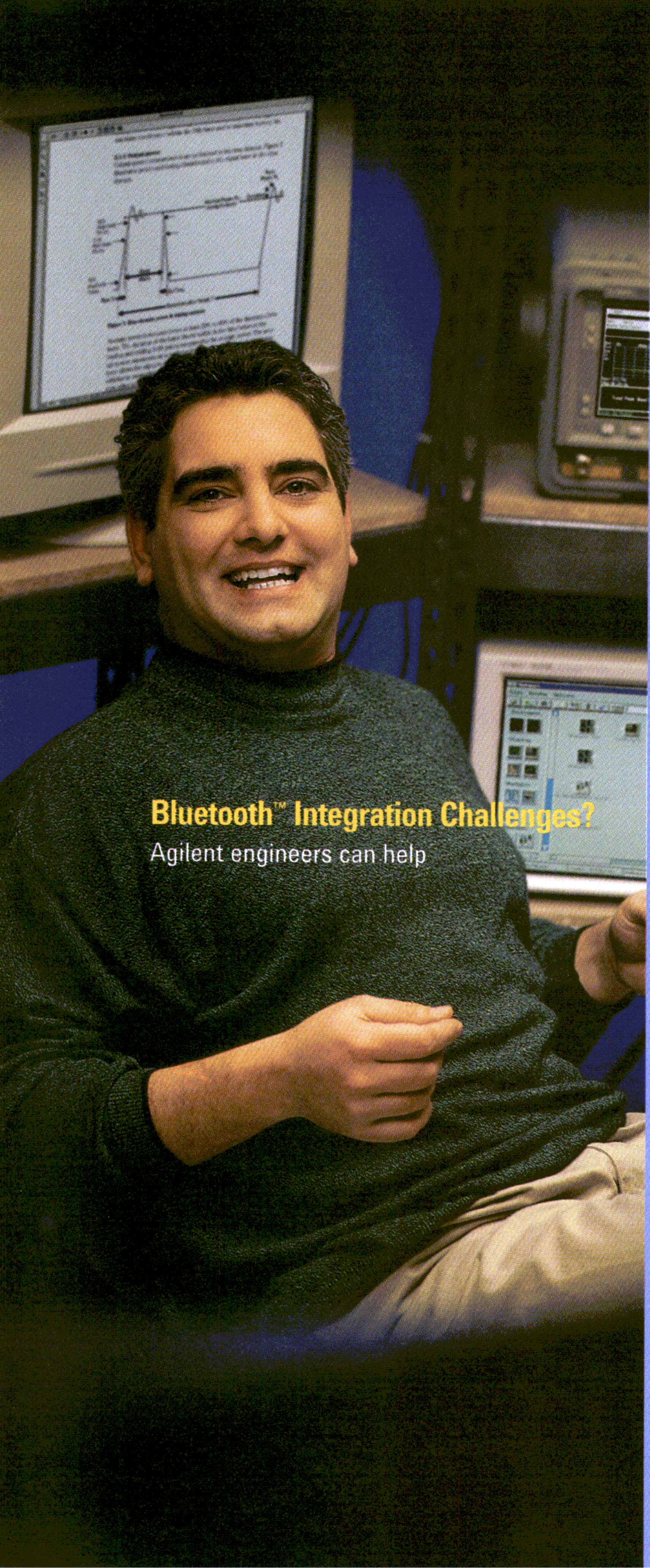

Bluetooth™ Integration Challenges?

Agilent engineers can help

It probably started with a conversation over in marketing: "*Bluetooth* wireless technology is the next big thing! We have to put it in all our products! Details? Bah, all you do is add an antenna. The engineers will figure it out. Let's go see if they're finished yet."

And now you and a few thousand other engineers are figuring out that *Bluetooth* integration is not a trivial task. From baseband DSP to RF interference, you've got an integration challenge worthy of legendary King Harald himself.

Welcome to the wild world of RF. New to RF? We've pooled the talents of our digital, DSP and RF experts to identify the most important signal checks you'll need to make when integrating *Bluetooth* designs. Our online resources include everything from an RF basics seminar to advanced measurement techniques.

Something for the RF experts, too. If you have the luxury of approaching *Bluetooth* from an RF background, we can offer advice on the most-efficient test procedures and toolsets to tackle a wide range of *Bluetooth* measurements.

The *Bluetooth* big picture. Most of the *Bluetooth* work we're seeing today involves the integration of a *Bluetooth* module into a new product design:

- Evaluating module performance and characterizing interoperability
- Understanding host-module integration issues
- Designing and debugging the host-module interface
- Conducting pre-qualification RF testing
- Getting *Bluetooth* Qualification
- Manufacturing quality products

Some of the more interesting problems show up in the second stage, as you bring the RF transceiver into your host products.

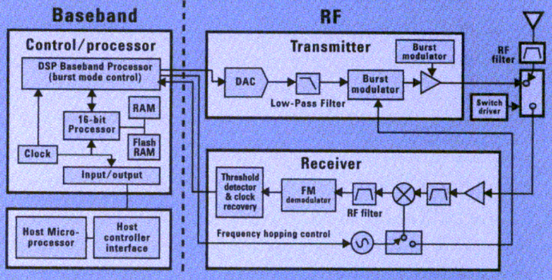

Watch out for some interesting interoperability problems when you integrate a Bluetooth module into your host device

Bluetooth

www.agilent.com/find/bt

u.s. 1-800-452-4844, ext. 7456
canada 1-877-894-4414, ext. 7471

Baseband signal integration. Challenges here include verifying transmission and receipt of data packets, viewing the actual data values transmitted, quantifying system bottlenecks, identifying logic errors, and resolving DSP and mixed-signal issues.

For instance, once you've found the preamble, you can identify the entire bit stream, including the access code, header and payload. Learn more in our free *Bluetooth* baseband application note.

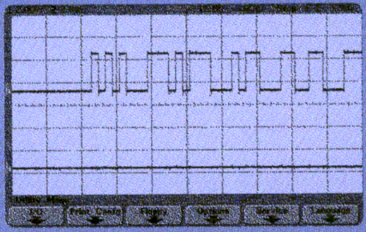

The first two pulses in this idealized transmit signal correspond to the 0101 pattern of the preamble; the access code follows immediately after

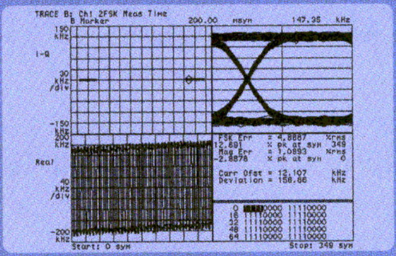

Bluetooth measurement tools range from powerful design analysis to fast, automated tests for the production line. Above, a modulation characteristics test verifies proper performance of the modulation circuitry to ensure reliable data transfer over the Bluetooth communication link.

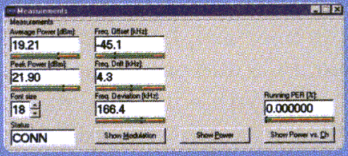

At left, an automated test combines pass/fail indications with numerical readouts

RF receiver tests. RF receiver performance is key to both *Bluetooth* qualification and overall product performance. For example, a sensitive radio that is immune to interference will reduce file transfer times and therefore increase battery life. You need to make sure the RF receiver will not be adversely impacted by the harmonics of high-frequency digital signals or other noise sources likely to be present in your system.

Receiver performance is tested in a number of ways for qualification, including carrier/interference and blocking tests. You probably won't need to run all the tests if you're integrating someone else's module, but they can be complicated so clear information and simplified procedures are important.

RF transmitter tests. The *Bluetooth* specification covers a wide range of transmitter tests, some to insure interoperability between *Bluetooth* devices (e.g., modulation characteristics) and others to meet regulatory limits (e.g., spurious emissions). Given the concerns about interference with other wireless systems, output spectrum tests are also important.

Integrating a module can create problems that affect transmitter performance, sometimes in unexpected ways. For example, power supply ripple coupled through your system can degrade the modulation characteristics.

You must be able to show that your device stays within both *Bluetooth* and regulatory limits, and the more of this work you can do on your design bench, the better. Some of the tests are complex and potentially time-consuming to understand and perform. Our free online application resources can help you look for and fix problems quickly.

Get the complete *Bluetooth* test story—FREE. Talk to one of our *Bluetooth* measurement specialists to learn more or tap into our free technical resources at www.agilent.com/find/bt.
Among the features you'll find there:

- A comprehensive measurement guide: *Performing Bluetooth RF Measurements Today* featuring descriptions and examples of the many RF measurements you might need
- Interactive measurements that show some key *Bluetooth* measurements in action, starting with frequency drift and frequency settling—explore these real-life measurements before you need to make them on your own system

We can't do much about your enthusiastic friends in marketing, but we can definitely help you through the *Bluetooth* integration experience.

Visit www.agilent.com/find/bt for a FREE *Bluetooth* CD-ROM packed with application notes, measurement tips and solution guides.

Circle 24

Agilent Technologies

A Comparison of Various Bipolar Transistor Biasing Circuits

An up-to-date review of bias techniques

By Al Ward and Bryan Ward
Agilent Technologies

The bipolar junction transistor (BJT) is often used as a low noise amplifier in cellular, PCS and pager applications because of its low cost. With a minimal number of external matching networks, the BJT can produce an LNA with RF performance considerably better than an MMIC. Of equal importance is the DC performance. Although the device's RF performance may be quite closely controlled, the variation in device DC parameters can be quite significant because of normal process variations.

It is not unusual to find a 2 or 3 to 1 ratio in device h_{FE}. Variation in h_{FE} from device to device will generally not appear as a difference in RF performance. In other words, two devices with widely different h_{FE} can have similar RF performance, as long as the devices are biased at the same V_{CE} and I_C. The primary purpose of the bias network is to keep V_{CE} and I_C constant as DC parameters vary from device to device.

The bias circuitry is often overlooked because of its apparent simplicity. With a poorly designed fixed bias circuit, the variation in I_C from lot to lot can have the same maximum to minimum ratio as the h_{FE} variation from lot to lot. If there is no compensation I_C will double when h_{FE} is doubled. It is the task of the DC bias circuit to maximize the circuit's tolerance to h_{FE} variations. In addition, transistor parameters can vary over temperature causing a drift in I_C at temperature. The low power supply voltages typically available for handheld applications also make it more difficult to design a temperature stable bias circuit.

One solution to the biasing dilemma is the use of active biasing. Active biasing often makes use of an IC or a PNP transistor and a variety of resistors, effectively setting V_{CE} and I_C regardless of variations in device h_{FE}. Although the technique of active biasing would be the best choice for control of device to device variability and over temperature variations, associated costs are usually high.

Other biasing options include various forms of passive biasing. This article discusses various passive biasing circuits, including their advantages and disadvantages.

Various BJT passive bias circuits

Passive biasing schemes usually consist of two to five resistors properly arranged about the transistor. Various passive biasing schemes are shown in Figure 1. The simplest form of passive biasing is shown as Circuit #1 in Figure 1. The collector current I_C is simply h_{FE} times the base current I_B. The base current is determined by the value of R_B. The collector voltage V_{CE} is determined by subtracting the voltage drop across resistor R_C from the power supply voltage V_{CC}. As the collector current is varied, the V_{CE} will change based on the voltage drop across R_C. Varying h_{FE} will cause I_C to vary in a fairly direct manner. For constant V_{CC} and constant V_{BE}, I_C will vary in direct proportion to h_{FE}. For example, as h_{FE} is doubled, collector current, I_C, will also double. Bias circuit #1 provides no compensation for variation in device h_{FE}.

Bias circuit #2 provides voltage feedback to the base current source resistor R_B. The base current source is fed from the voltage V_{CE}, as opposed to the supply voltage V_{CC}. The value of the base bias resistor R_B is calculated based upon nominal device V_{BE} and the desired V_{CE}. Collector resistor R_C has both I_C and I_B flowing through it.

The operation of this circuit is best explained

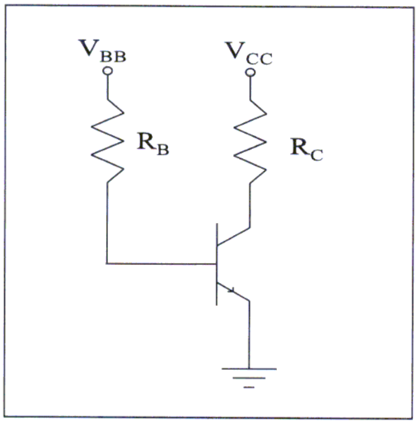

▲ **Figure 1(a). Circuit #1: nonstabilized BJT bias network.**

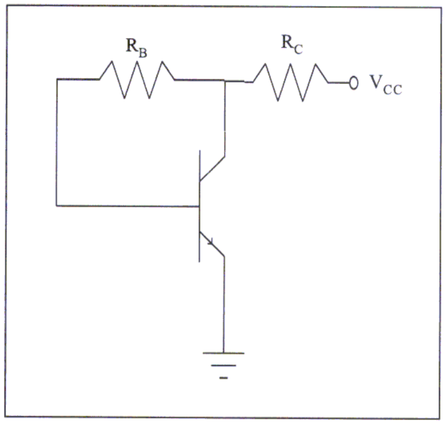

▲ **Figure 1(b). Circuit #2: voltage feedback BJT bias network.**

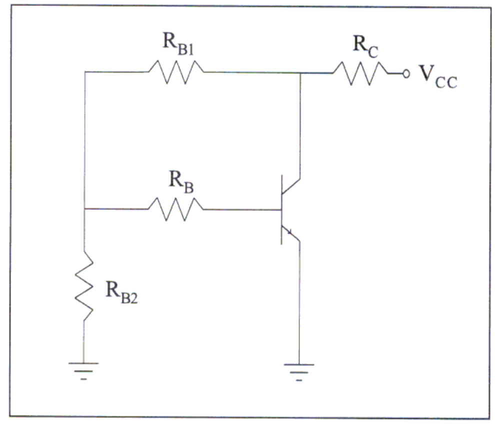

▲ **Figure 1(c). Circuit #3: voltage feedback with current source BJT bias network.**

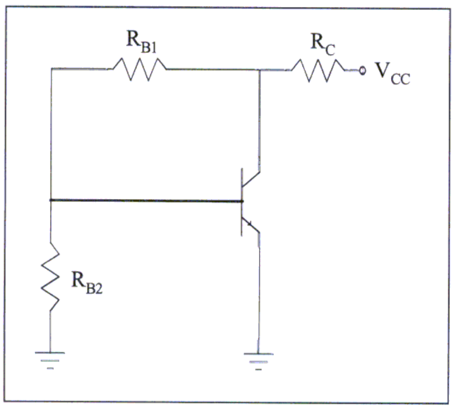

▲ **Figure 1(d). Circuit #4: voltage feedback with voltage source BJT bias network.**

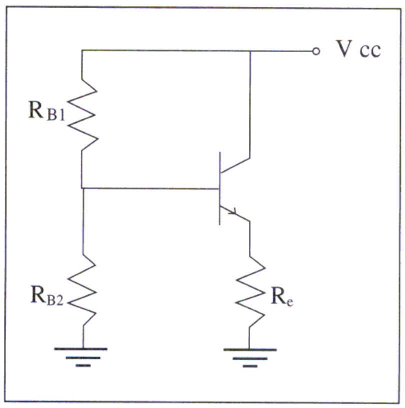

▲ **Figure 1(e). Circuit #5: emitter feedback BJT bias network.**

as follows. An increase in h_{FE} will tend to cause I_C to increase. An increase in I_C causes the voltage drop across resistor R_C to increase. The increase in voltage across R_C causes V_{CE} to decrease. The decrease in V_{CE} causes I_B to decrease because the potential difference across base bias resistor R_B has decreased. This topology provides a basic form of negative feedback which tends to reduce the amount that the collector current increases as h_{FE} is increased.

Bias circuit #3 has been discussed in past literature but predominately when very high V_{CC} (> 15 volts) and V_{CE} (> 12 volts) were used [1]. The voltage divider network consisting of R_{B1} and R_{B2} provide a voltage divider from which resistor R_B is connected. Resistor R_B then determines the base current. I_B times h_{FE} provides I_C. The voltage drop across R_C is determined by the collector current I_C, the base current I_B and the current consumed by the voltage divider, consisting of R_{B1} and R_{B2}. This circuit provides similar voltage feedback to that of bias circuit #2.

Bias circuit #4 is similar to bias circuit #3 with the exception that the series current source resistor R_B is omitted. This circuit is seen in bipolar power amplifier design with resistor R_{B2} replaced by a series silicon power diode providing temperature compensation for the bipolar device. The current flowing through resistor R_{B1} is shared by both resistor R_{B2} and the base emitter junction V_{BE}. The greater the current through resistor R_{B2}, the greater the regulation of the base emitter voltage V_{BE}.

Bias circuit #5 is the customary textbook circuit for biasing BJTs. A resistor is used in series with the device emitter lead to provide voltage feedback. This circuit ultimately provides the best control of h_{FE} variations from device to device and over temperature. The disadvantage of this circuit is that the emitter resistor must be properly bypassed for RF. The typical bypass capacitor often has internal lead inductance which can create unwanted regenerative feedback. The feedback can create device instability. Despite the problems associated with using the emitter resistor technique, this biasing scheme generally provides the best control on h_{FE} and over temperature variations.

The sections that follow begin with a discussion of the BJT model and its temperature dependent variables. From the basic model, various equations are developed to predict the device's behavior over h_{FE} and temperature variations. This article is an update to the original article written by Kenneth Richter of Hewlett-Packard [2] and Hewlett-Packard Application Note 944-1 [3].

BJT modeling

The BJT is modeled as two current sources, as shown in Figure 2. The primary current source is $h_{FE}I_B$. In parallel is a secondary current source I_{CBO} (1+ h_{FE}) that

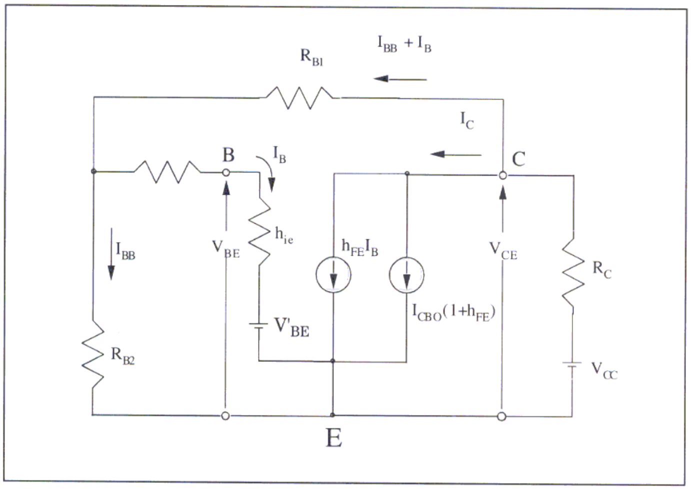

▲ **Figure 2. Gummel-Poon model of BJT with voltage feedback and constant base current source network.**

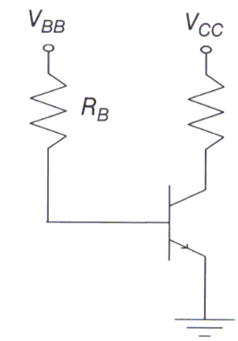

$$R_B = \frac{V_{CC} - V_{BE}}{I_B} \qquad R_C = \frac{V_{CC} - V_{CE}}{I_C}$$

$$I_C = \frac{h_{FE} \cdot (V_{CC} - V'_{BE})}{h_{ie} + R_B} + I_{CBO} \cdot (1 + h_{FE})$$

▲ **Figure 3. Equations for nonstabilized bias network.**

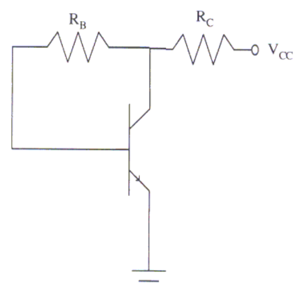

$$R_B = \frac{V_{CE} - V_{BE}}{I_B} \qquad R_C = \frac{V_{CC} - V_{CE}}{I_C + I_B}$$

$$I_C = \frac{h_{FE} \cdot (V_{CC} - V'_{BE}) + I_{CBO} \cdot (1 + h_{FE}) \cdot (h_{ie} + R_B + R_C)}{h_{ie} + R_B + R_C \cdot (1 + h_{FE})}$$

▲ **Figure 4. Equations for voltage feedback bias network.**

describes the leakage current flowing through a reverse biased PN junction. I_{CBO} is typically 1×10^{-7} A at 25 degrees C for an Agilent Technologies HBFP-0405 transistor. V'_{BE} is the internal base emitter voltage with h_{ie} representing the equivalent Hybrid PI input impedance of the transistor. h_{ie} is also equal to $h_{FE} / \lambda I_C$ where λ = 40 at +25 degrees C. V_{BE} will be defined as measured between the base and emitter leads of the transistor. It is equivalent to $V'_{BE} + I_B h_{ie}$. V_{BE} is approximately 0.78 volts at 25 degrees C for the HBFP-0405 transistor.

The device parameters that exhibit the greatest change as temperature is varied are h_{FE}, V'_{BE}, and I_{CBO}. These temperature dependent variables have characteristics which are process dependent and fairly well understood. h_{FE} typically increases with temperature at the rate of 0.5 percent/degrees C. V'_{BE} has a typical negative temperature coefficient of –2 mV/degrees C. This indicates that V_{BE} decreases 2 mV for every degree increase in temperature. I_{CBO} typically doubles for every 10 degree C rise in temperature. Each one of these parameters contributes to the net resultant change in collector current as temperature is varied.

For each bias network shown in Figure 1, several sets of simplified circuit equations have been generated to allow calculation of the various bias resistors. These are shown in Figures 3, 4, 5, 6 and 7. Each of the bias resistor values are calculated based on various design parameters such as desired I_C, V_{CE}, power supply voltage V_{CC} and nominal h_{FE}. I_{CBO} and h_{ie} are assumed to be zero for the basic calculation of resistor values.

Additional information, usually provided by the designer, is required for the three circuits that use the voltage divider consisting of R_{B1} and R_{B2}. For the bias network that uses voltage feedback with current source, the designer must choose the voltage across R_{B2} (V_{RB2}) and the bias current through resistor R_{B2}, which will be termed I_{RB2}. If $V_{CE} > V_{RB2} > V_{BE}$, then a suggested V_{RB2} would be 1.5 volts and a suggested I_{RB2} would be 10 percent of I_C, or 0.5 mA.

The voltage feedback with a voltage source network and the emitter feedback network also require that the designer choose I_{RB2}. The ratio of I_C to I_{RB2} can play a major role in bias stability.

An equation was then developed for each circuit that calculates collector current, I_C, based on nominal bias resistor values and typical device parameters, including h_{FE}, I_{CBO}, and V'_{BE}. MATHCAD 7 was used to help develop the I_C equation. Although the I_C equation begins simply, it develops into a rather lengthy equation

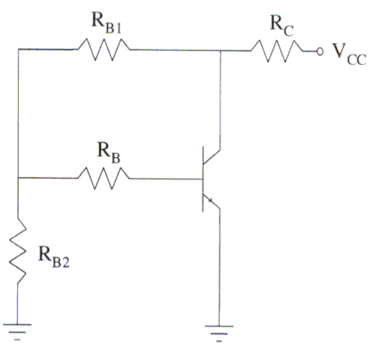

$$R_B = \frac{V_{RB2} - V_{BE}}{I_B} \qquad R_C = \frac{V_{CC} - V_{CE}}{I_C + I_{B2} + I_B}$$

$$R_{B1} = \frac{V_{CE} - V_{RB2}}{I_{B2} + I_B} \qquad R_{B2} = \frac{V_{RB2}}{I_{B2}}$$

Designer must choose I_{B2} and V_{RB2} such that $V_{CE}>V_{RB2}>V_{BE}$

$$I_C = \left[\frac{-V'_{BE}\cdot(R_{B1}+R_{B2}+R_C) - R_{B2}\cdot[R_C\cdot I_{CBO}\cdot(1+h_{FE}) - V_{CC}]}{(R_B+h_{ie})\cdot(R_{B1}+R_{B2}+R_C) + R_{B2}\cdot(h_{FE}\cdot R_C + R_C + R_{B1})}\right]\cdot h_{FE} + I_{CBO}\cdot(1+h_{FE})$$

▲ **Figure 5. Equations for voltage feedback with current source bias network.**

for some of the more complicated circuits. MATHCAD helped to simplify this task.

Design example using the Agilent HBFP-0405 BJT

The HBFP-0405 transistor is used as a test example for each of the bias circuits. The HBFP-0405 is described in [4] as a low noise amplifier for 1800 to 1900 MHz applications. The HBFP-0405 will be biased at a V_{CE} of 2.7 volts and a drain current I_C of 5 mA. A power supply voltage of 3 volts will be assumed. The nominal h_{FE} of the HBFP-0405 is 80. The minimum is 50 while the maximum is 150. The calculated bias resistor values for each bias circuit are described in Table 1.

With the established resistor values, I_C is calculated based on minimum and maximum h_{FE}. The performance of each bias circuit with respect to h_{FE} variation is shown in Table 2. Bias circuit #1 clearly has no compensation for varying h_{FE}, allowing I_C to increase 85 percent as h_{FE} is taken to its maximum. Circuit #2 with very simple collector feedback offers considerable compensation due to h_{FE} variations allowing an increase of only 42 percent. Circuit #3 offers very little improvement over circuit #2. Circuit #4 provides considerable improvement in h_{FE} control by only allowing a 9 percent increase in I_C. Circuit #4 offers an improvement over the previous circuits by providing a stiffer voltage source across the base emitter junction. As we will see later, this circuit has worse performance over temperature as compared to circuits #2 and #3. However, when both h_{FE} and temperature are considered, circuit #4 will appear to be the best performer for a grounded emitter configuration. As expected, circuit #5 provides the best control on I_C with varying h_{FE} allowing only a 5.4 percent increase in I_C. Results are power supply dependent, and with higher V_{CC}, results may vary significantly.

BJT performance over temperature

Since all three temperature dependent variables (I_{CBO}, h_{FE} and V'_{BE}) exist in the I_C equation, differentiating the I_C equation with respect to each of the parameters provides insight into their effect on I_C. The partial derivative of each of the three parameters represents a stability factor. The various stability factors and their calculation are shown in Table 3. Each circuit has three distinctly different stability factors which are then multiplied times a corresponding change in either V'_{BE}, h_{FE}, or I_{CBO} and finally summed. These changes or deltas in V'_{BE}, h_{FE}, and I_{CBO} are calculated based on

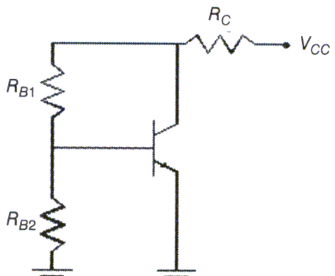

$$R_{B2} := \frac{V_{BE}}{I_{B2}} \qquad R_C := \frac{V_{CC} - V_{CE}}{I_C + I_B + I_{B2}}$$

$$R_{B1} := \frac{V_{CE} - (I_{B2}\cdot R_{B2})}{I_B + I_{B2}}$$

Designer must choose I_{B2}

$$I_C := \frac{-\left[\frac{-R_C}{h_{FE}}\cdot I_{CBO} - R_C\cdot I_{CBO} + \frac{R_C}{R_{B2}}\cdot V'_{BE} - \frac{R_C}{(R_{B2}\cdot h_{FE})}\cdot h_{ie}\cdot I_{CBO} - \frac{R_C}{R_{B2}}\cdot h_{ie}\cdot I_{CBO} - \frac{R_{B1}}{h_{FE}}\cdot I_{CBO} - R_{B1}\cdot I_{CBO} + \frac{R_{B1}}{R_{B2}}\cdot V'_{BE} - \frac{R_{B1}}{(R_{B2}\cdot h_{FE})}\cdot h_{ie}\cdot I_{CBO} - \frac{R_{B1}}{R_{B2}}\cdot h_{ie}\cdot I_{CBO} + V'_{BE} - \frac{1}{h_{FE}}\cdot h_{ie}\cdot I_{CBO} - h_{ie}\cdot I_{CBO} - V_{CC}\right]}{\left[R_C + \frac{R_C}{h_{FE}} + \frac{R_C}{(R_{B2}\cdot h_{FE})}\cdot h_{ie} + \frac{R_{B1}}{h_{FE}} + \frac{R_{B1}}{(R_{B2}\cdot h_{FE})}\cdot h_{ie} + \frac{1}{h_{FE}}\cdot h_{ie}\right]}$$

▲ **Figure 6. Equations for voltage feedback with voltage source bias network.**

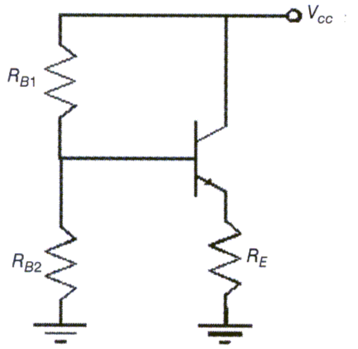

$$R_E = \frac{V_{CC} - V_{CE}}{I_C\left(1 + \frac{1}{h_{FE}}\right)} \qquad R1 = \frac{V_{CC} - I_{B2} \cdot R_2}{I_{B2} + I_B}$$

Pick I_{B2} to be 10 percent of I_C, which is equal to .0005 A

$$R_2 = \frac{V_{RB2}}{I_{B2}} \qquad V_{RB2} = V_{BE} + (I_B + I_C) \cdot R_E$$

$$I_C = \frac{-\left[V'_{BE} - \frac{1}{h_{FE}} \cdot h_{ie} \cdot I_{CBO} - h_{ie} \cdot I_{CBO} - \frac{R_E}{h_{FE}} \cdot I_{CBO} - R_E \cdot I_{CBO} - \frac{R_1}{R_2} \cdot V'_{BE} - \frac{R_1}{R_2 \cdot h_{FE}} \cdot h_{ie} \cdot I_{CBO} - \frac{R_1}{R_2} \cdot h_{ie} \cdot I_{CBO} - \frac{R_1}{R_2} \cdot \frac{R_E}{h_{FE}} \cdot I_{CBO} - \frac{R_1}{R_2} \cdot R_E \cdot I_{CBO} - \frac{R_1}{h_{FE}} \cdot I_{CBO} - R_1 \cdot I_{CBO} - V_{CC}\right]}{\frac{1}{h_{FE}} \cdot h_{ie} + \frac{R_E}{h_{FE}} + R_E + \frac{R_1}{R_2 \cdot h_{FE}} \cdot h_{ie} + \frac{R_1}{R_2} \cdot \frac{R_E}{h_{FE}} + \frac{R_1}{R_2} \cdot R_E + \frac{R_1}{h_{FE}}}$$

▲ **Figure 7. Equations for emitter feedback bias network.**

variations in these parameters based on the manufacturing processes.

A comparison of each circuit's stability factors will certainly provide insight as to which circuit compensates best for each parameter. MATHCAD was again used to calculate the partial derivatives for each desired stability factor. The stability factors for bias circuit #1 are shown in Table 4. The stability factors for the remaining circuits are shown in the Appendix.

Resistor	Non-Stabilized Bias Network	Voltage Feedback Bias Network	Voltage Feedback with Current Source Bias Network	Voltage Feedback with Voltage Source Bias Network	Emitter Feedback Bias Network
R_C	140 Ω	138 Ω	126 Ω	126 Ω	
R_B	30770 Ω	19552 Ω	11539 Ω		
R_{B1}			889 Ω	2169 Ω	2169 Ω
R_{B2}			3000 Ω	1560 Ω	2960 Ω
R_E					138 Ω

▲ **Table 1. Bias resistor values for HBFP-0405 biased at V_{CE} = 2 volts, V_{CC} = 2.7 volts, I_C = 5 mA, h_{FE} = 80 for the various bias networks.**

Bias Circuit	Non-Stabilized Bias Network	Voltage Feedback Bias Network	Voltage Feedback with Current Source Bias Network	Voltage Feedback with Voltage Source Bias Network	Emitter Feedback Bias Network
I_c(mA)@ minimum h_{FE}	3.14	3.63	3.66	4.53	4.70
I_c(mA)@ typical h_{FE}	5.0	5.0	5.0	5.0	5.0
I_c(mA)@ maximum h_{FE}	9.27	7.09	6.98	5.44	5.27
Percentage change in I_c from nominal I_c	+85% –37%	+42% –27%	+40% –27%	+9% –9%	+5.4% –6%

▲ **Table 2. Summary of I_C variation versus h_{FE} for various bias networks for the HBFP-0405, V_{CC} = 2.7 volts, V_{CE} = 2 volts, I_C = 5 mA, T_j = +25 degrees C.**

The change in collector current from the nominal design value at 25 degrees C is then calculated by taking each stability factor and multiplying it times the corresponding change in each parameter. Each product is then summed to determine the absolute change in collector current.

As an example, the collector current of the HBFP-0405 will be analyzed as temperature is increased from +25 degrees C to +65 degrees C. For the HBFP-0405, I_{CBO} is typically 100 nA at +25 degrees C and typically doubles for every 10 degrees C temperature rise. Therefore, I_{CBO} will increase from 100 nA to 1600 nA at +65 degrees C. The difference or ΔI_{CBO} will be 1600 – 100 = 1500 nA. The 1500 nA will then be multiplied times its corresponding I_{CBO} stability factor.

V_{BE} at 25 degrees C was measured at 0.755 volts for the HBFP-0405. Since V_{BE} has a typical negative temperature coefficient of –2 mV per degree C, V_{BE} will be 0.675 volts at +65 degrees C. The difference in V_{BE} will then be 0.675 – 0.755 = –0.08 volts. The –0.08 volts will then be multiplied by its corresponding V_{BE} stability factor.

$$I_{CBO} = \frac{\partial I_C}{\partial I_{CBO}} \quad h_{FE}, V'_{BE} = \text{constant}$$

$$V'_{BE} = \frac{\partial I_C}{\partial V'_{BE}} \quad I_{CBO}, h_{FE} = \text{constant}$$

$$h_{FE} = \frac{\partial I_C}{\partial h_{FE}} \quad I_{CBO}, V'_{BE} = \text{constant}$$

First calculate the stability factors for V'_{BE}, I_{CBO} and h_{FE}. Then, to find the change in collector current at any temperature, multiply the change from 25 degrees C of each temperature dependent variable with its corresponding stability factor and sum.

$$\Delta I_C = SI_{CBO} \times \Delta I_{CBO} + SV'_{BE} \times \Delta V'_{BE} + Sh_{FE} \times \Delta h_{FE}$$

▲ **Table 3. Calculation of the stability factors and their combined effect on I_C.**

Collector Current at any Temperature (I_C)	$\dfrac{h_{FE} \cdot (V_{CC} - V'_{BE})}{(h_{ie} + R_B)} + I_{CBO} \cdot (1 + h_{FE})$
I_{CBO} Stability Factor $I_{CBO} = \dfrac{\partial I_C}{\partial I_{CBO}} \Big\vert h_{FE}, V'_{BE} = \text{constant}$	$1 + h_{FE}$
V'_{BE} Stability Factor $V'_{BE} = \dfrac{\partial I_C}{\partial V'_{BE}} \Big\vert I_{CBO}, h_{FE} = \text{constant}$	$\dfrac{-h_{FE}}{h_{ie} + R_B}$
h_{FE} Stability Factor $h_{FE} = \dfrac{\partial I_C}{\partial h_{FE}} \Big\vert I_{CBO}, V'_{BE} = \text{constant}$	$\dfrac{V_{CC} - V'_{BE}}{h_{ie} + R_B} + I_{CBO}$

▲ **Table 4. Stability factors for non-stabilized bias network #1.**

h_{FE} is typically 80 at +25 degrees C and typically increases at a rate of 0.5 percent per degree C. Therefore, h_{FE} will increase from 80 to 96 at +65 degrees C, making Δh_{FE} equal to 96 – 80 = 16. Again the Δ is multiplied by its corresponding stability factor.

Once all stability terms are known, they can be summed to give the resultant change in collector current from the nominal value at +25 degrees C. The results of the stability analysis are shown in Table 5. The nonstabilized circuit #1 allows I_C to increase about 27 percent, while circuits 2 and 3 show a 19 to 20 percent increase in I_C. Somewhat surprising is that circuit #4 shows a nearly 30 percent increase in I_C with temperature because V'_{BE} is the major contributor to stability. This is probably due to the impedance of the R_{B1} and R_{B2} voltage divider working against V'_{BE}. Both circuits #2 and #3 have very similar performance over temperature. Both offer a significant improvement over circuit #1 and #4. Predictably, circuit #5 offers the best performance over temperature by nature of the emitter feedback. Emitter feedback can be used effectively if the resistor can be adequately RF bypassed without producing stability problems.

The degree of control that each bias circuit has on controlling I_C due to h_{FE} variations and the intrinsic temperature dependent parameters is defined by the design of the bias circuit. Increasing the voltage differential between V_{CE} and V_{CC} can enhance the circuit's ability to control I_C. In handset applications, this becomes difficult with 3-volt batteries as power sources. The current that is allowed to flow through the various bias resistors can also have a major effect on I_C control.

In order to analyze the various configurations, an AppCAD [5] module was generated. AppCAD consists of various modules developed to help RF designers with microstrip, stripline, detector, pin diode, MMIC biasing, RF amplifier, transistor biasing and system level calculations, as well as other design modules. The AppCAD BJT biasing module allows the designer to fine-tune each bias circuit design for optimum performance. AppCAD also allows the designer to input device variation parameters peculiar to a certain manufacturer's semiconductor process. A sample screen showing a typical bias circuit is shown in Figure 8. The data from AppCAD is used to create the graphs in the following sections.

The first exercise is to graphically illustrate the percentage

Bias Circuit	Non-stabilized	#2 Voltage Feedback	#3 Voltage Feedback w/Current Source	#4 Voltage Feedback	#5 Emitter Feedback
I_{CBO} stability factor	81	52.238	50.865	19.929	11.286
V'_{BE} stability factor	-2.56653×10^{-3}	-2.568011×10^{-3}	-3.956×10^{-3}	–0.015	-6.224378×10^{-3}
h_{FE} stability factor	6.249877×10^{-5}	4.031×10^{-5}	3.924702×10^{-5}	1.537669×10^{-5}	8.707988×10^{-6}
ΔI_C due to I_{CBO}(mA)	0.120	0.078	0.076	0.030	0.017
ΔI_C due to V'_{BE}(mA)	0.210	0.205	0.316	1.200	0.497
ΔI_C due to h_{FE}(mA)	0.999	0.645	0.628	0.246	0.140
Total I_C(mA)	1.329	0.928	1.020	1.476	0.654
Percentage change in I_C from nominal I_C	26.6%	18.6%	20.4%	29.5%	13.1%

▲ **Table 5. Bias stability analysis at +65 degrees C using the HBFP-0405, where V_{cc} = 2.7 volts, V_{CE} = 2 volts and I_c = 5 mA.**

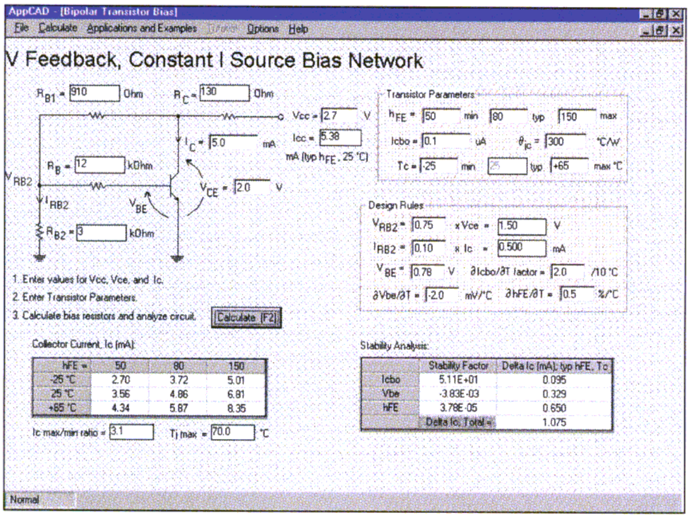

▲ **Figure 8. Agilent Technologies AppCAD module for BJT biasing.**

change in I_C versus h_{FE}. AppCAD is used to calculate the resistor values for each of the five bias networks. The HBFP-0405 transistor is biased at a V_{CE} of 2 volts, I_C of 5 mA, and V_{CC} of 2.7 volts. Various values of h_{FE} are substituted into AppCAD; results are presented in Figure 9. The data clearly shows that the emitter feedback and voltage feedback with voltage source networks are superior to the remaining circuits with regards to controlling h_{FE} at room temperature. These networks provide a 4:1 improvement over the other two voltage feedback networks.

AppCAD is then used to simulate a temperature change from T_j = –25 de-grees C to +65 de-grees C with h_{FE} held constant. Whereas the original Matchcad analysis assumed that $T_c = T_j$, AppCAD takes into account that T_j is greater than T_c. AppCAD calculates the thermal rise based on DC power dissipated and the thermal impedance of the device. The results of the analysis are shown in Figure 10. The voltage feedback with voltage source network performed nearly as poorly as the non-stabilized circuit. This is due to the temperature induced V_{BE} decrease and the bias circuit trying to keep V_{BE} constant. Power bipolar designers will often utilize a silicon diode in place of R_{B2} so that the bias voltage will track the V_{BE} of the transistor. Depending on the impedance of the voltage divider network, V_{BE} could rise, causing I_C to increase. The emitter feedback network performed very well as expected. The simple voltage feedback network appeared to be optimum when considering the simplicity of the circuit.

Bias networks 3 through 5 make use of an additional resistor that shunts some of the total power supply current to ground. Properly chosen, this additional bias current can be used to assist in controlling I_C over temperature and h_{FE} variations from device to device. AppCAD is set up such that the designer has various choices regarding the amount of bias resistor current that is allowed to flow from the power supply. AppCAD is used to analyze each bias circuit.

The graphs in Figures 11 and 12 plot the percentage change in I_C versus the ratio of I_C to I_{RB1}. I_{RB1} is the current flowing through resistor R_{B1}, which is the summation of base current I_B and current flowing through resistor R_{B2}. The maximum permissible ratio of I_C to I_{RB1} is limited by the h_{FE} of the transistor. Figure 11 represents the worst case condition, where I_C increases at maximum h_{FE} and highest temperature. Figure 12 shows the opposite scenario, in which the lowest I_C results from lowest h_{FE} and lowest temperature. The percentage change is certainly more pronounced at high h_{FE} and high temperature.

Although some of the predicted results are somewhat surprising, the bias network with emitter resistor feedback, as expected, offers the best performance overall. For a ratio of I_C to I_{RB1} of 10 to 1 or less, the resultant change in collector current is less than 20 percent. The voltage feedback with voltage source network performs best with an I_C to I_{RB1} ratio between 6 and 10 with a worst case change of 41 percent in collector current.

To complete the comparison, two additional points representing the nonstabilized and the voltage feedback networks have been added to the graphs. They are

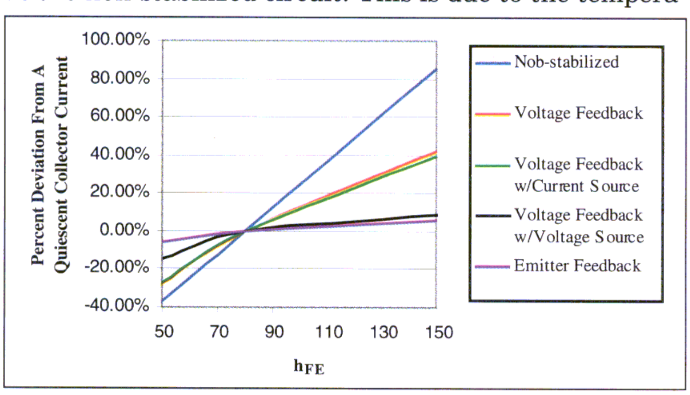

▲ **Figure 9. Percent change in quiescent collector current versus h_{FE} for the HBFP-0405 where V_{CC} = 2.7 volts, V_{CE} = 2 volts, I_C = 5 mA and T_j = +25 degrees C.**

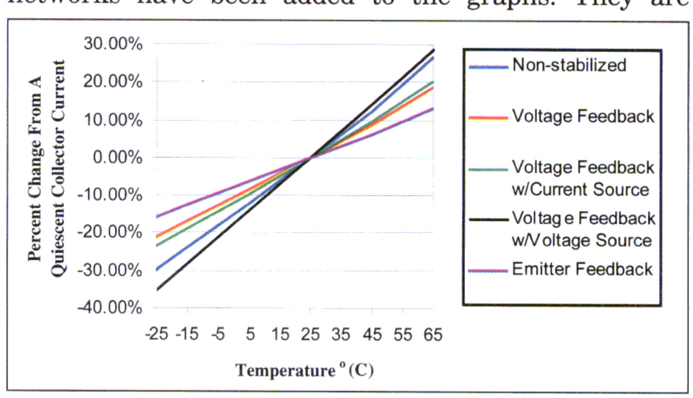

▲ **Figure 10. Percent change in quiescent collector current versus temperature for the HBFP-0405 where V_{CC} = 2.7 volts, V_{CE} = 2 volts, I_C = 5 mA and T_j = +25 degrees C.**

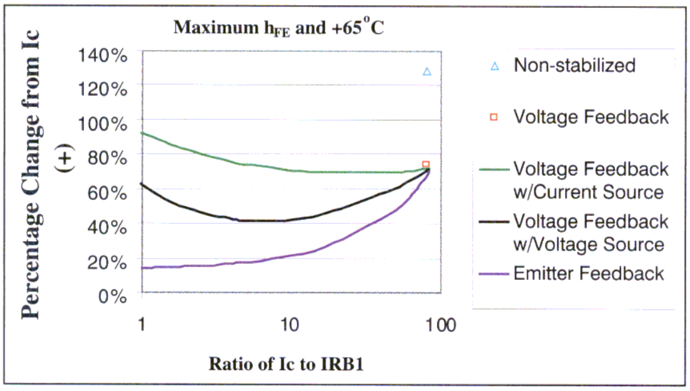

▲ **Figure 11. Percent change in quiescent collector current versus ratio of I_C to I_{RB1} for maximum h_{FE} and T_j = +65 degrees C for the HBFP-0405, where V_C = 2.7 volts, V_{CE} = 2 volts and I_C = 5 mA.**

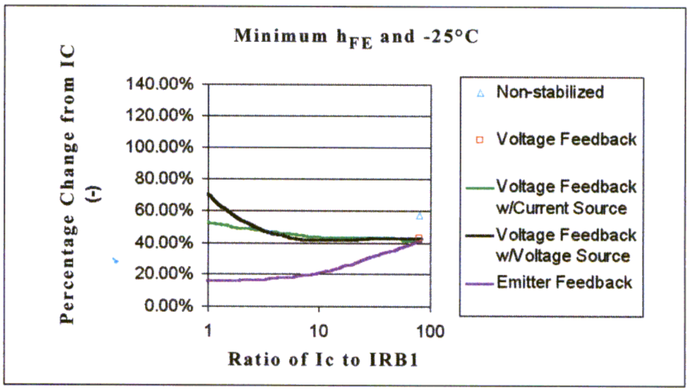

▲ **Figure 12. Percent change in quiescent collector current versus ratio of I_C to I_{RB1} for minimum h_{FE} and T_j = –25 degrees C for the HBFP-0405, where V_{CC} = 2.7 volts, V_{CE} = 2 volts and I_C = 5 mA.**

shown as single points because only the base current is in addition to the collector current. The nonstabilized network has an increase of 129 percent, while the voltage feedback network has an increase of 74.5 percent. The voltage feedback with current source network offers no benefit over the simpler voltage feedback network.

Conclusion

This article discussed the circuit analysis of four commonly used stabilized bias networks and one nonstabilized bias network for the bipolar junction transistor. In addition to the presentation of the basic design equations for the bias resistors for each network, an equation was presented for collector current in terms of bias resistors and device parameters. The collector current equation was then differentiated with respect to the three primary temperature dependent variables resulting in three stability factors for each network. These stability factors plus the basic collector current equation give the designer insight as to how best bias transistors for best performance over h_{FE} and temperature variations. The basic equations were then integrated into an AppCAD module, providing the circuit designer with an easy and effective way to analyze bias networks for bipolar transistors. ■

Acknowledgement

The authors would like to thank Bob Myers at Agilent Technologies in Newark, CA, for his fine work in converting the bipolar biasing equations into a very effective and useful AppCAD module with which various bias networks can be easily designed and evaluated.

References

1. *A Cost-Effective Amplifier Design Approach at 425 MHz Using the HXTR-3101 Silicon Bipolar Transistor*, Hewlett-Packard Application Note 980, February 1981 (out of print).

2. Kenneth Richter, “Design DC Stability Into Your Transistor Circuits,” *Microwaves*, December 1973: 40–46.

3. *Microwave Transistor Bias Considerations*, Hewlett-Packard Application Note 944-1, August 1980, (out of print).

4. *1800 to 1900 MHz Amplifier using the HBFP-0405 and HBFP-0420 Low Noise Silicon Bipolar Transistors*, Hewlett-Packard Application Note 1160, November 1998, publication number 5968-2387E.

5. AppCAD is available from Agilent Technologies through the company’s Web site, www.semiconductor.agilent.com.

Author information

Al Ward is an applications engineer with Agilent Technologies Wireless Semiconductor Division, 1410 E. Renner Road, Suite 100, Richardson, TX, 75082. He may be reached at 972-699-4369, or via e-mail at al_ward@agilent.com. Bryan Ward was a summer “SEED” student with Agilent Technologies.

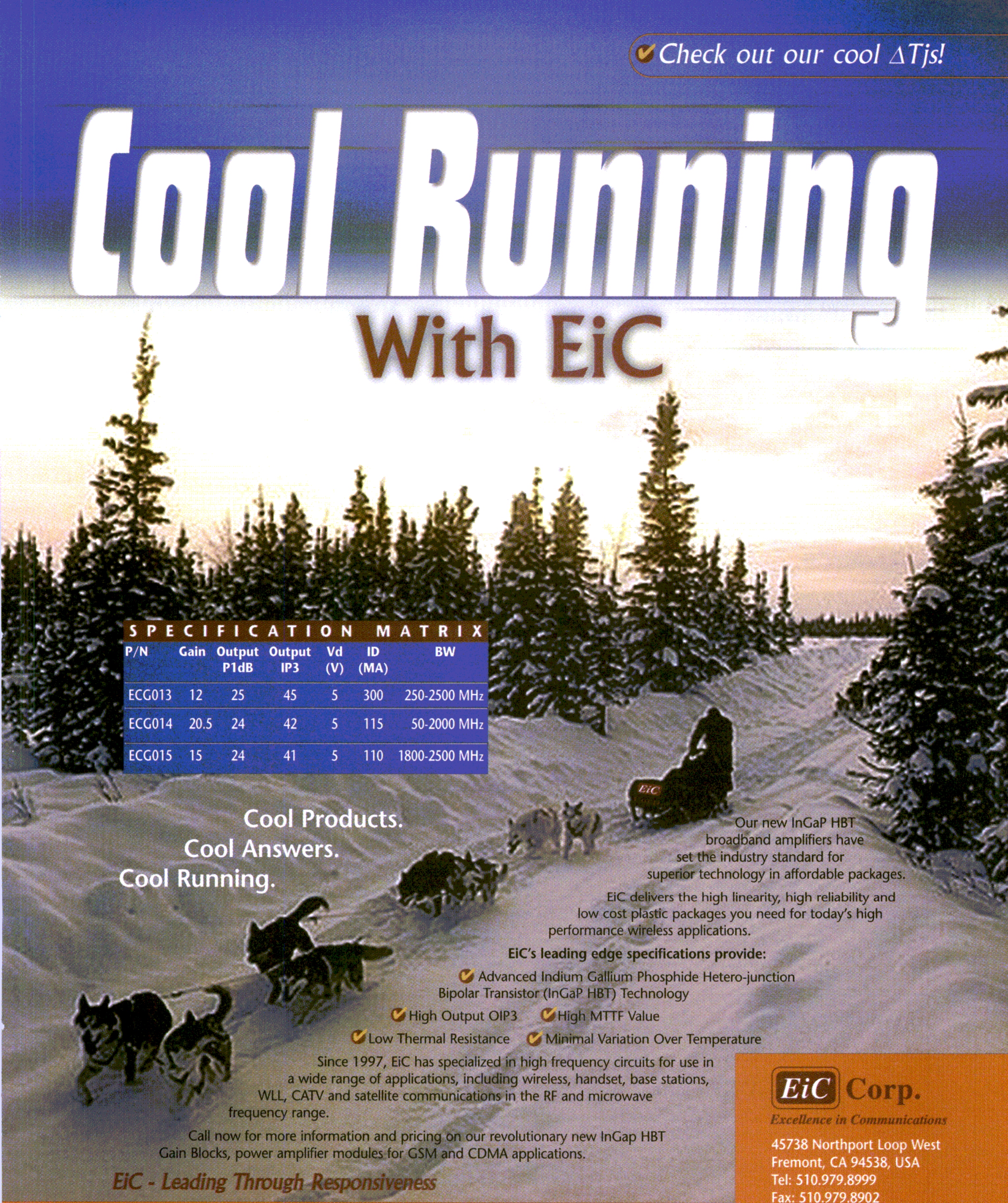

SPECIFICATION MATRIX

P/N	Gain	Output P1dB	Output IP3	Vd (V)	ID (MA)	BW
ECG013	12	25	45	5	300	250-2500 MHz
ECG014	20.5	24	42	5	115	50-2000 MHz
ECG015	15	24	41	5	110	1800-2500 MHz

EiC Corp.
Excellence in Communications

45738 Northport Loop West
Fremont, CA 94538, USA
Tel: 510.979.8999
Fax: 510.979.8902
E-mail: sales@eiccorp.com

ISO 9001 SGS Q17541
UKAS Quality Management 005

Visit us on the web at:
www.eiccorp.com

Call today and learn about our accelerated life test data. 510-979-8999 or call your local Avnet Distributor

Circle 31

Appendix

Collector Current at any Temperature (I_C)	$\dfrac{h_{FE}\cdot(V_{CC}-V'_{BE})+I_{CBO}\cdot(1+h_{FE})\cdot A}{h_{ie}+R_B+R_C\cdot(1+h_{FE})}$
I_{CBO} Stability Factor $I_{CBO}=\dfrac{\partial I_C}{\partial I_{CBO}}\Big\vert h_{FE},V'_{BE}=\text{constant}$	$\dfrac{(1+h_{FE})\cdot A}{h_{ie}+R_B+R_C\cdot(1+h_{FE})}$
V'_{BE} Stability Factor $V'_{BE}=\dfrac{\partial I_C}{\partial V'_{BE}}\Big\vert I_{CBO},h_{FE}=\text{constant}$	$\dfrac{-h_{FE}}{h_{ie}+R_B+R_C\cdot(1+h_{FE})}$
h_{FE} Stability Factor $h_{FE}=\dfrac{\partial I_C}{\partial h_{FE}}\Big\vert I_{CBO},V'_{BE}=\text{constant}$	$\dfrac{V_{CC}-V'_{BE}+A\cdot I_{CBO}}{h_{FE}\cdot R_C+R_B+h_{ie}+R_C}-$ $\dfrac{R_C\cdot h_{FE}\cdot(V_{CC}-V'_{BE}+A\cdot I_{CBO})+A\cdot I_{CBO}}{(h_{FE}\cdot R_C+R_B+h_{ie}+R_C)^2}$ where $A=h_{ie}+R_B+R_C$

▲ **Stability factors for voltage feedback bias network #2.**

Collector Current at any Temperature (I_C)	$h_{FE}\left[\dfrac{-V'_{BE}\cdot A-R_{B2}\cdot\left[R_C\cdot I_{CBO}\cdot(1+h_{FE})-V_{CC}\right]}{(R_B+h_{ie})\cdot A+R_{B2}\cdot(h_{FE}\cdot R_C+R_C+R_{B1})}\right]+I_{CBO}(1+h_{FE})$
I_{CBO} Stability Factor $I_{CBO}=\dfrac{\partial I_C}{\partial I_{CBO}}\Big\vert h_{FE},V'_{BE}=\text{constant}$	$(1+h_{FE})-\dfrac{R_{B2}\cdot h_{FE}\cdot R_C\cdot(1+h_{FE})}{A\cdot(R_B+h_{ie})+R_{B2}\cdot(h_{FE}\cdot R_C+R_C+R_{B1})}$
V'_{BE} Stability Factor $V'_{BE}=\dfrac{\partial I_C}{\partial V'_{BE}}\Big\vert I_{CBO},h_{FE}=\text{constant}$	$\dfrac{-h_{FE}\cdot A}{(R_B+h_{ie})\cdot A+R_{B2}\cdot(h_{FE}\cdot R_C+R_C+R_{B1})}$
h_{FE} Stability Factor $h_{FE}=\dfrac{\partial I_C}{\partial h_{FE}}\Big\vert I_{CBO},V'_{BE}=\text{constant}$	$\dfrac{h_{FE}\cdot\{R_{B2}\cdot R_C\cdot[(-R_{B2}\cdot V_{CC}+B)+R_{B2}\cdot R_C\cdot I_{CBO}\cdot(1+h_{FE})]\}}{D^2}-$ $\left[\dfrac{B+R_{B2}\cdot[R_C\cdot I_{CBO}\cdot(1+h_{FE})-V_{CC}+h_{FE}\cdot R_C\cdot I_{CBO}]}{D}\right]+I_{CBO}$ where $A=R_{B1}+R_{B2}+R_C$ $B=V'_{BE}\cdot(R_{B1}+R_{B2}+R_C)$ $C=(R_B+h_{ie})\cdot(R_{B1}+R_{B2}+R_C)$ $D=(R_B+h_{ie})\cdot(R_{B1}+R_{B2}+R_C)+R_{B2}\cdot(h_{FE}\cdot R_C+R_C+R_{B1})$

▲ **Stability factors for voltage feedback with current source bias network #3.**

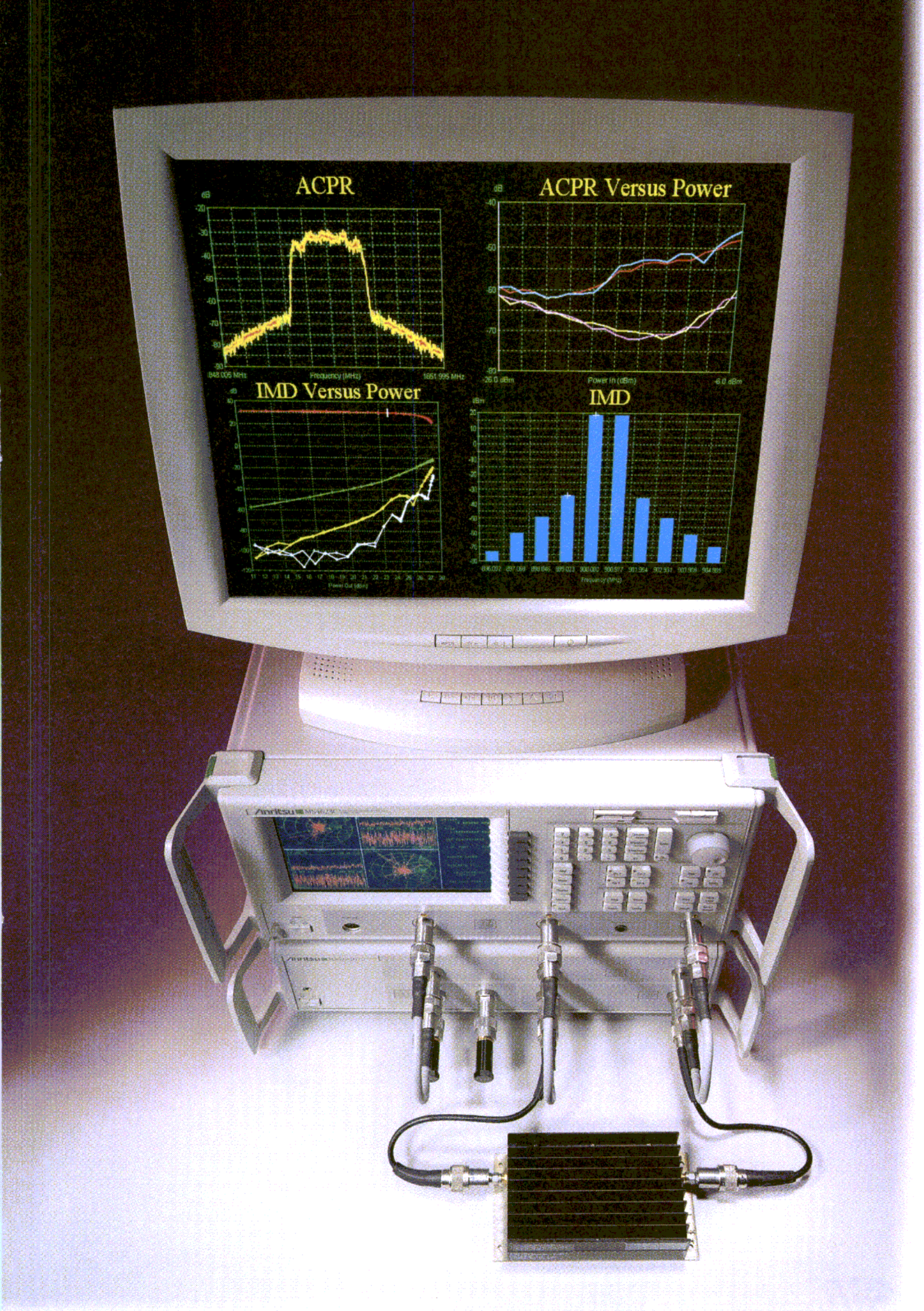

See The True Performance Of Your Power Amplifier.

Scorpion®..You Only Need One!

Anritsu is proud to introduce PATS, an amazing turnkey RF Power Amplifier test like no other on the market. Built upon the Scorpion Vector Network Measurement System (VNMS), PATS tames your toughest measurement requirements with blazing speed, unparalleled dynamic range and ultimate accuracy.

With a single connection, see your Power Amplifier's:

- ACPR
- IMD & PAE
- Compression
- Harmonics
- S-Parameters

The ME7840A is a complete system that includes the following:

ME7840A	**Power Amplifier Test System (PATS)**
Scorpion PA Navigator™	Easy-to-Use Easy-to-Customize Software
Scorpion	Fast Measurements & Ultimate Accuracy
PATS Test Set	Single Connection Flexible Configuration

Whether you're involved with R&D or manufacturing, you only need one PATS to increase your throughput. For a demo, call Anritsu at 1-800-ANRITSU or check out our website. Then, you too, can see your Power Amplifier's true performance.
www.us.anritsu.com/adsmailers/pats.asp

Anritsu

ME7840A Power Amplifier Test System (PATS)

Circle 59

RADIO RECEIVER DESIGN

...the New Definitive Resource For Key Concepts in Receiver Design

order today—www.noblepub.com

Radio Receiver Design

Kevin McClaning and Tom Vito

Hardcover 796 pages ISBN 1-884932-07-X

NP-35 . . . .$89.00

- Provides excellent introductions and technical background on basic as well as advanced component characteristics, featuring "war stories," exercises, design examples and an abundance of useful drawings and tables
- Covers in detail all major components related to receiver design, including cascade interaction
- Serves as a reference tool for students and professionals of electrical engineering, RF and microwave electronics and radio receiver design
- Emphasizes practical and proven concepts that help clarify the role of each component within the design

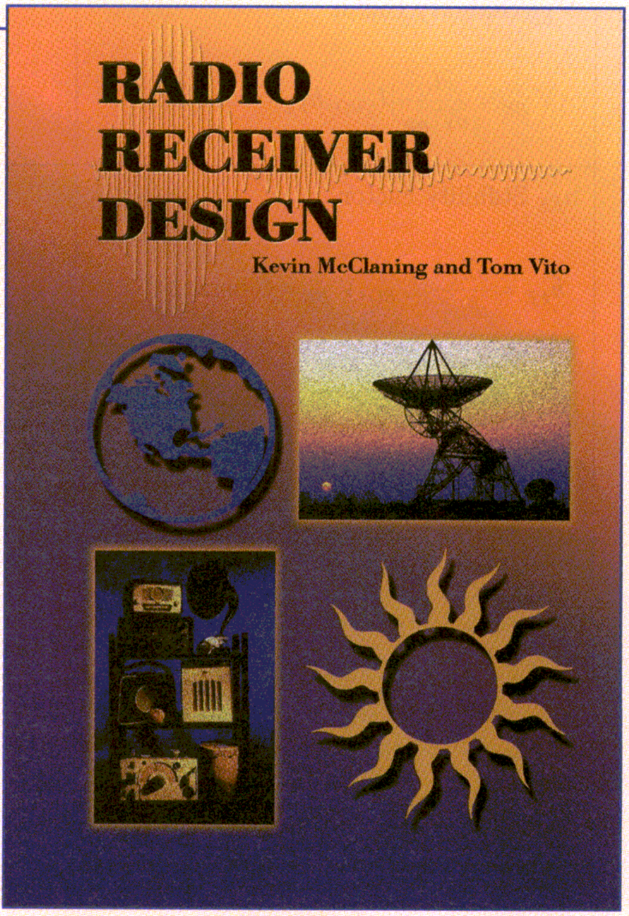

Order NP-35 . . . .$89.00
ISBN 1-884932-07-X

NOBLE PUBLISHING

Noble Publishing Corporation
630 Pinnacle Court
Norcross, GA 30071
Tel: 770-449-6774
Fax: 770-448-2839
www.noblepub.com

European Customers: Please order through
American Technical Publishers
Tel: +44 (0) 1462 437933
Fax: +44 (0) 1462 433678
www.ameritech.co.uk

Dealer inquiries invited.
Price does not include shipping.

Circle 39

Collector Current at any Temperature (I_C)	$\dfrac{I_{CBO}\cdot(-A)+I_{CBO}\cdot h_{ie}\cdot(-B)+D-V_{CC}}{C}$
I_{CBO} Stability Factor $I_{CBO}=\dfrac{\partial I_C}{\partial I_{CBO}}\Big\vert h_{FE},V'_{BE}=\text{constant}$	$\dfrac{h_{ie}\cdot B+A}{C}$
V'_{BE} Stability Factor $V'_{BE}=\dfrac{\partial I_C}{\partial V'_{BE}}\Big\vert I_{CBO},h_{FE}=\text{constant}$	$\dfrac{\dfrac{-R_C}{R_{B2}}-\dfrac{R_{B1}}{R_{B2}}-1}{C}$
h_{FE} Stability Factor $h_{FE}=\dfrac{\partial I_C}{\partial h_{FE}}\Big\vert I_{CBO},V'_{BE}=\text{constant}$	$\dfrac{I_{CBO}\cdot\left[\dfrac{-R_C}{h_{FE}{}^2}-\dfrac{R_{B1}}{h_{FE}{}^2}\right]+I_{CBO}\cdot h_{ie}\cdot E}{C}-$ $\dfrac{I_{CBO}\cdot A+I_{CBO}\cdot h_{ie}\cdot B-D+V_{CC}}{C^2}\cdot\left[\dfrac{-R_C}{h_{FE}{}^2}-\dfrac{R_{B1}}{h_{FE}{}^2}+h_{ie}\cdot E\right]$ where: $A=\dfrac{R_C}{h_{FE}}+R_C+\dfrac{R_{B1}}{h_{FE}}+R_{B1}$ $B=\dfrac{R_C}{R_{B2}\cdot h_{FE}}+\dfrac{R_C}{R_{B2}}+\dfrac{R_{B1}}{R_{B2}\cdot h_{FE}}+\dfrac{R_{B1}}{R_{B2}}+\dfrac{1}{h_{FE}}+1$ $C=R_C+\dfrac{R_C}{h_{FE}}+\dfrac{R_{B1}}{h_{FE}}+h_{ie}\cdot\left[\dfrac{R_C}{R_{B2}\cdot h_{FE}}+\dfrac{R_{B1}}{R_{B2}\cdot h_{FE}}+\dfrac{1}{h_{FE}}\right]$ $D=\dfrac{R_C}{R_{B2}}\cdot V'_{BE}+\dfrac{R_{B1}}{R_{B2}}\cdot V'_{BE}+V'_{BE}$ $E=\dfrac{-R_C}{R_{B2}\cdot h_{FE}{}^2}-\dfrac{R_{B1}}{R_{B2}\cdot h_{FE}{}^2}-\dfrac{1}{h_{FE}{}^2}$

▲ **Stability factors for voltage feedback with voltage source bias network #4.**

Collector Current at any Temperature (I_C)	$\dfrac{h_{ie} \cdot I_{CBO} \cdot (-A) + I_{CBO} \cdot (-B) + D}{C}$
I_{CBO} Stability Factor $I_{CBO} = \dfrac{\partial I_C}{\partial I_{CBO}} \Big\vert h_{FE}, V'_{BE} = \text{constant}$	$\dfrac{h_{ie} \cdot A + B}{C}$
V'_{BE} Stability Factor $V'_{BE} = \dfrac{\partial I_C}{\partial V'_{BE}} \Big\vert I_{CBO}, h_{FE} = \text{constant}$	$\dfrac{-1 - \frac{R_1}{R_2}}{C}$
h_{FE} Stability Factor $h_{FE} = \dfrac{\partial I_C}{\partial h_{FE}} \Big\vert I_{CBO}, V'_{BE} = \text{constant}$	$\dfrac{I_{CBO} \cdot E + h_{ie} \cdot I_{CBO} \cdot \left[\dfrac{-1}{h_{FE}^2} - \dfrac{R_1}{R_2 \cdot h_{FE}^2}\right]}{C} - \dfrac{I_{CBO} \cdot B + h_{ie} \cdot I_{CBO} \cdot A - D}{C^2} \cdot \left[h_{ie} \cdot \left(\dfrac{-1}{h_{FE}^2} - \dfrac{R_1}{R_2 \cdot h_{FE}^2}\right) + E\right]$ where $A = \dfrac{R_1}{R_2 \cdot h_{FE}} + \dfrac{R_1}{R_2} + \dfrac{1}{h_{FE}} + 1$ $B = \dfrac{R_1}{R_2} \cdot \dfrac{R_E}{h_{FE}} + \dfrac{R_1}{R_2} \cdot R_E + \dfrac{R_E}{h_{FE}} + R_E + \dfrac{R_1}{h_{FE}} + R_1$ $C = h_{ie} \cdot \left(\dfrac{1}{h_{FE}} + \dfrac{R_1}{R_2 \cdot h_{FE}}\right) + \dfrac{R_E}{h_{FE}} + R_E + \dfrac{R_1}{R_2} \cdot \dfrac{R_E}{h_{FE}} + \dfrac{R_1}{R_2} \cdot R_E + \dfrac{R_1}{h_{FE}}$ $D = V'_{BE} + \dfrac{R_1}{R_2} \cdot V'_{BE} - V_{CC}$ $E = \dfrac{-R_E}{h_{FE}^2} - \dfrac{R_1}{R_2} \cdot \dfrac{R_E}{h_{FE}^2} - \dfrac{R_1}{h_{FE}^2}$

▲ **Stability factors for emitter feedback bias network #5.**

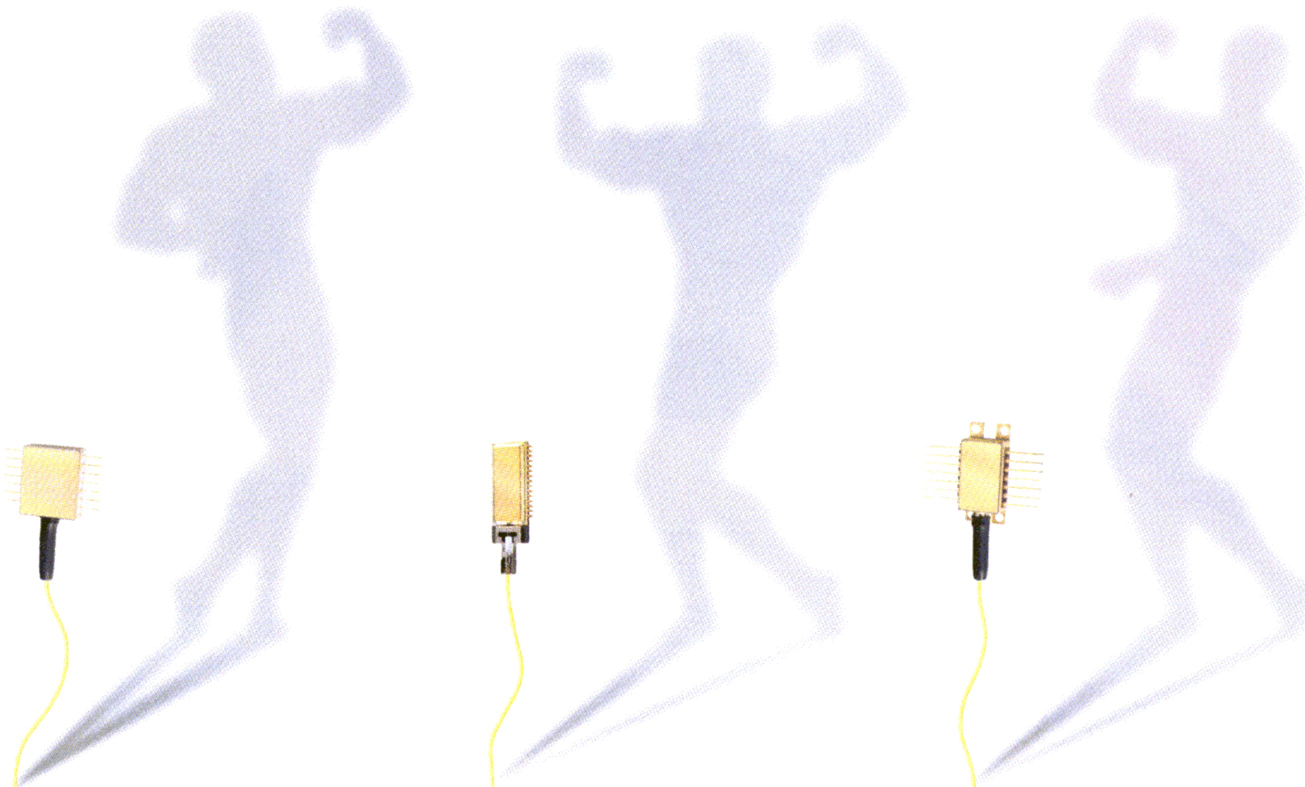

Connector and Termination Construction above 50 GHz

A summary of the design challenges presented by mm-wave interconnects

By Bill Oldfield
Anritsu

This paper discusses the design and construction of connections operating above 50 GHz. Available connectors and their design principles will be discussed, as well as the pros and cons of various backside interfaces. Details of orthogonal connections that work to at least 90 GHz and terminations in coax, microstrip and CPW, operating to at least 110 GHz will be shown and their data presented. Broadband interconnects will also be examined to meet the demanding requirements of 40-gigabit optical systems.

Purpose of an ideal connector

The ideal connector is a lossless, reflectionless port into a circuit. The front side allows connection to another connector or a test instrument. The backside connects to the circuit. Backside design is the most critical feature of connector use and the one over which the user has the most control.

An important feature of connectors is that they must get smaller as frequency gets higher, i.e., if the frequency is doubled, the connector size must be cut in half. Mechanical tolerances must also decrease by half. Only the microwave portions of the connector must diminish with increasing frequency, the outside and connection parts can remain large.

Desired features of a practical connector:

- Low total cost.
- Sum of the material cost plus the assembly cost.
- Coverage of the desired frequency band
- In general, the higher the frequency, the smaller and more expensive the connector parts and assembly labor.
- Low loss, including structure loss and reflection loss. At high frequencies, reflection loss can be the greater value. A 10 dB return loss equals a 0.5 dB insertion loss.
- Meets environmental requirements.
- Hermiticity, thermal expansion, outgassing and voltage breakdown.
- Available standards. The SMA connector has no available standards. This is not problematic at low frequencies, but can cause problems at higher frequencies.

Table 1 lists the available connector types that work above 40 GHz and are supported by standards. Other types of connectors, such as GPO, are not supported by standards.

The upper frequency limit is defined as the frequency at which another propagation mode is possible in the coax case the TE_{11} mode. This usually occurs first in the support bead.

Front side interface [1]

The front side interface defines the connector. It is of little concern to the user except in regard to frequency range and compatibility of connection devices. The pin depth of the center conductor relative to the outer conductor is an

Connector type (outer conductor size)	Upper frequency limit	Center conductor size
2.4 mm	50 GHz	1.042 mm (0.041)
1.85 mm V connector	67 GHz	0.803 mm (0.0316)
1 mm W1 connector	110 GHz	0.434 mm (0.017)

▲ **Table 1. High frequency connector sizes.**

important parameter; a positive pin depth can destroy the connector. More details of connector interfaces can be found in the references.

Glass beads

Glass beads provide package hermaticity and mechanical isolation between the fragile backside connection and the exterior world. The center conductor pin is usually small enough to allow its overlap connection to a standard 10 mil alumina substrate. A typical glass bead assembly is shown in Figure 2.

Backside interface [2]

Backside interface is the most critical feature of connector use and the one over which the user has the most control. Most poor results and failures occur at the backside interface. The problem is how to connect to a very small (assuming high frequencies) microstrip or CPW transmission line in a way that will satisfy all of the RF and environmental requirements.

First we have to decide how to connect the coax pin to the substrate. Figure 3 shows the end view of two traditional methods and a side view of another possibility. The pin overlap design is the most traditional but has no flexibility in the joint and has a capacitive mismatch. It also requires a high skill solder joint. The wraparound is very inductive at higher frequencies.

The other method requires that gold ribbon be prebonded to the coax pin. However, the final connection is an easy gold ribbon bond which is very good from both an RF and an environmental position. It also allows connection to a very small substrate trace.

In all cases, this is the most critical and sensitive area in the connection system. Ground paths must be kept very short. This means that substrates on carriers must not be used if they allow a longer ground path.

Here are guidelines for dealing with high frequency interconnects:

- Keep the coax entry size as small as possible and have an air dielectric.
- Compensate every change in transmission line size.
- Aside from compensation steps, all transmission lines should be 50 ohms.
- Keep bond connections very short. A 10 mil bond wire gives 10 dB return loss at 90 GHz.
- Provide for stress relief at the coax-substrate interface.
- Keep ground paths short. Beware of carriers. The ideal ground path length is zero.
- Keep everything as simple as possible.

Here are guidelines for dealing with substrates:

- 10 mil microstrip will work above 70 GHz, but using 7.5 mil will cause fewer problems.
- 5 mil Teflon works very well up to 110 GHz.

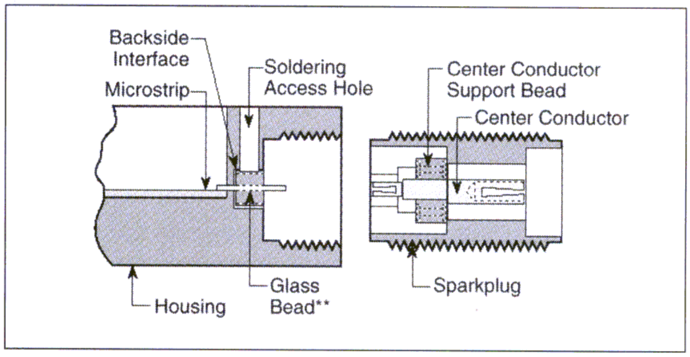

▲ **Figure 1. Typical connector system.**

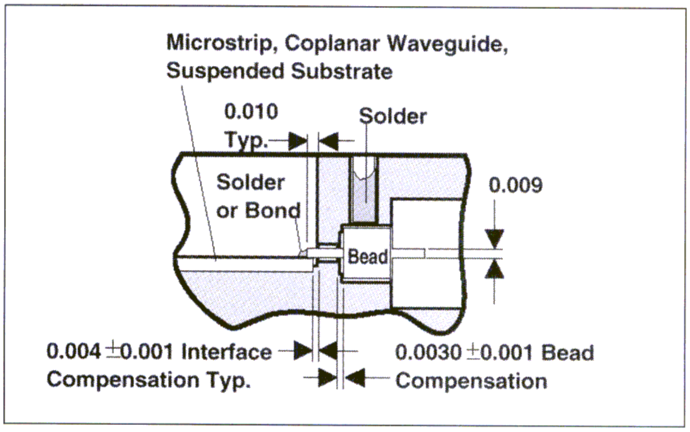

▲ **Figure 2. Glass beads.**

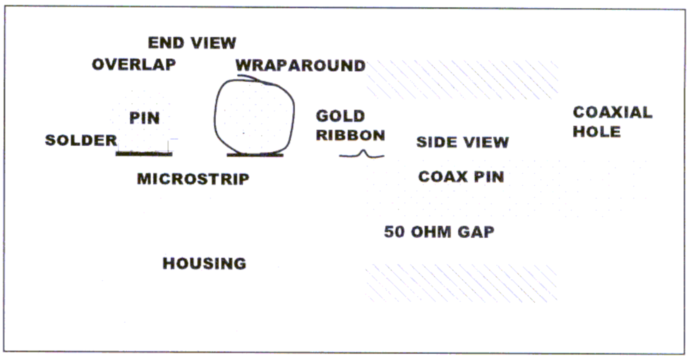

▲ **Figure 3. Coax pin to microstrip connections.**

- 5 mil Quartz is very low loss to 110 GHz and has a nice wide trace.
- CPW must be very small to work well. Thin substrates are best.

Orthogonal connections

Orthogonal connections are particularly useful when using MMICs in high frequency subsystems, allowing connections to be made anywhere in the assembly as opposed to only the perimeter when using standard connections. The examples shown use UT47 coax cable, which can support frequencies up to 110 GHz.

Superior Service

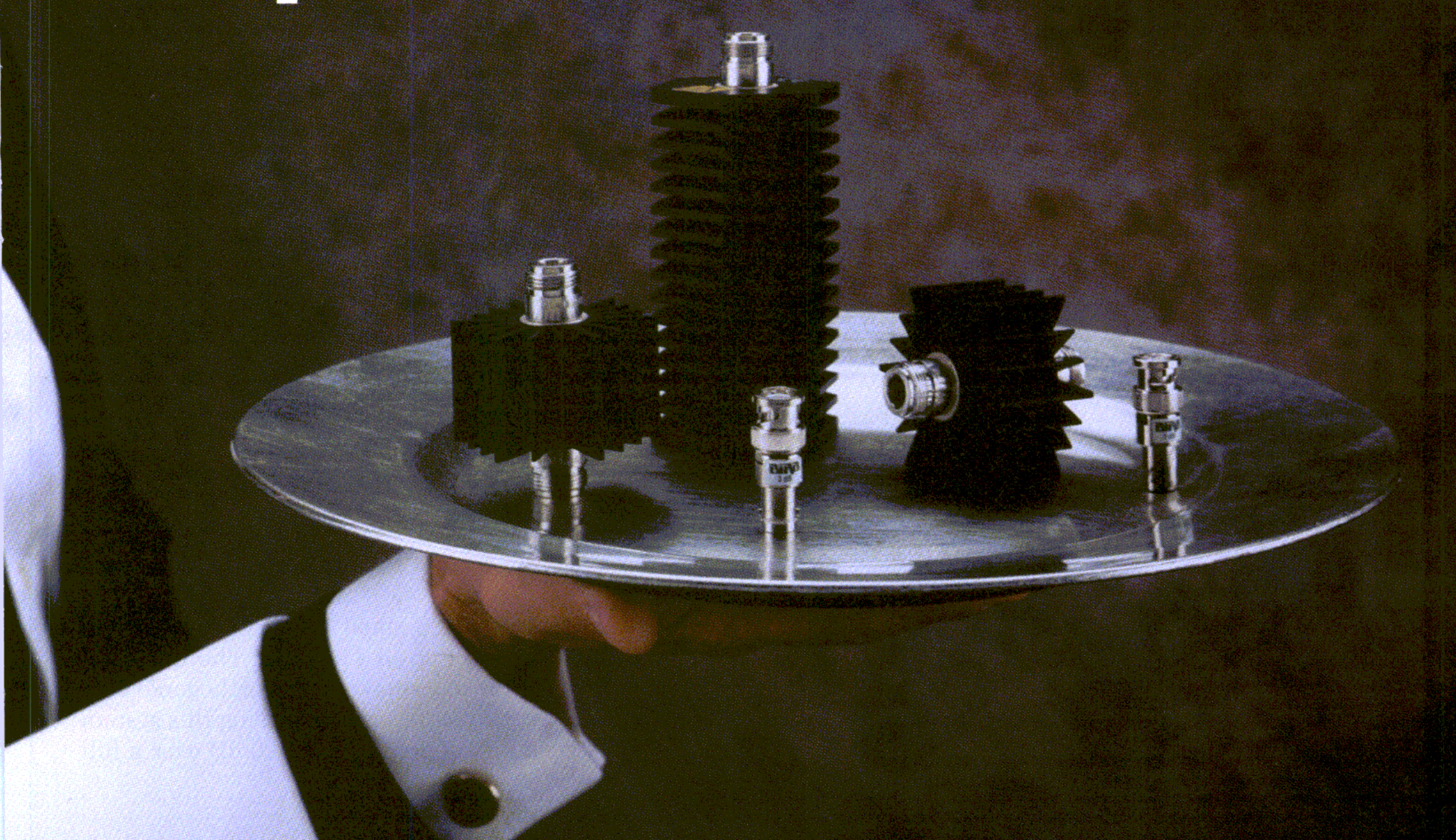

At Bird Component Products we take pride in our excellent customer service. Our technical staff is always ready to identify practical solutions to your product needs and our engineering turnaround on new products is one of the best in the industry. From new products to our proven designs, we are determined to exceed your expectations.

Cellular and PCS Frequency Ranges	Standard and Custom Applications
✓ Attenuators	✓ Divider / Combiners
• convection and conduction cooled	• rugged weather-tight available
• low intermodulation distortion	• many configurations available
✓ Terminations	✓ Couplers
• convection and conduction cooled	• compact and cost effective
• low intermodulation distortion	• ideal for Cellular and PCS applications

BIRD COMPONENT PRODUCTS, INC.

10950 72nd Street North, Suite 107 Largo, Florida 33777-1527
Phone: 727-547-8826 Fax: 727-547-0806 www.birdfla.com E-mail: sales@birdfla.com

BIRD TECHNOLOGIES GROUP

Circle 69

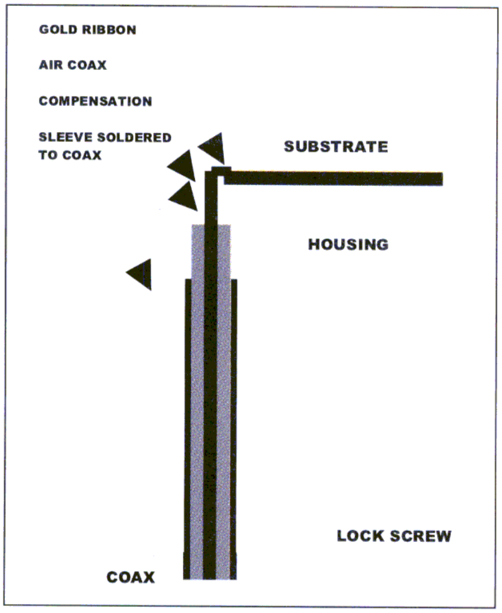

▲ **Figure 4. Orthogonal connection.**

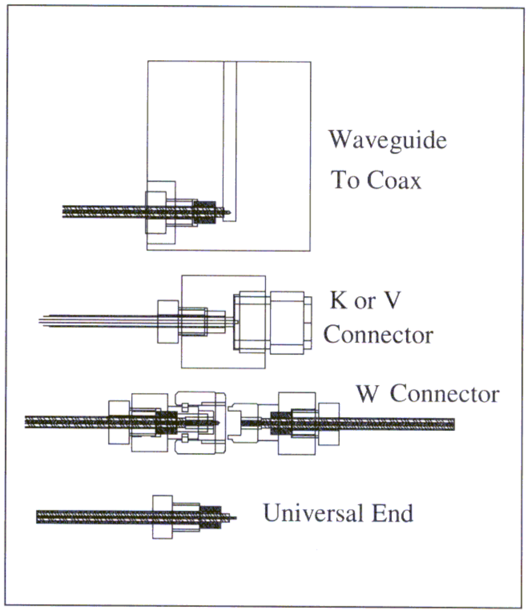

▲ **Figure 5. Universal connection system.**

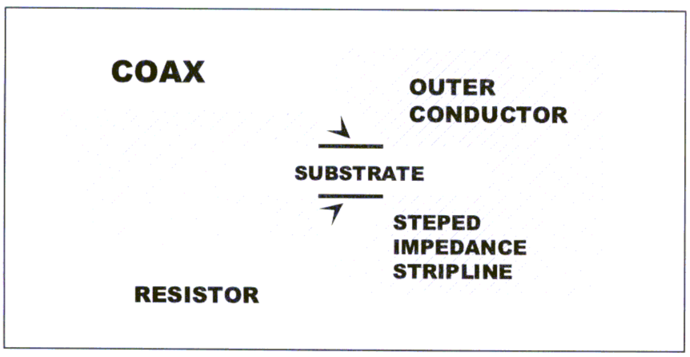

▲ **Figure 6. Planar resistor coaxial termination.**

The assembly shown in Figure 4 can give return losses in the order of 20 dB to 60 GHz and 16 dB to 90 GHz. The design can be modified for an orthogonal feed through and can also be used as a standard axial connection. The other end of the coax can be adapted to waveguide, a 1 mm connector or other type of coax connector.

An alternative connection system

One of the problems with building components at higher frequencies is that the connectors on the component do not always match the available test equipment. This is the case, for instance, if the test equipment is waveguide and the component is coax. One way to solve this problem is to use coax cable as the bridge. UT47 coax with a "universal end" is the ideal size: it is thin with a small center conductor and can support frequencies up to 110 GHz. The universal end is the same as the one shown in the orthogonal connection. Waveguide to coax transitions using this system can have a return loss of greater than 20 dB over a full waveguide band.

Terminations

The ideal termination is a reflectionless transition from the transmission line impedance to ground. This is usually is realized as a resistor in the value of the transmission line impedance and surrounded by the proper topology. The most commonly used terminations are the coax variety used to terminate external ports. Terminations used internally in subsystems are usually in microstrip or CPW topologies. High frequency CPW terminations are easy to make. Microstrip terminations usually become increasingly reflective above 20 GHz.

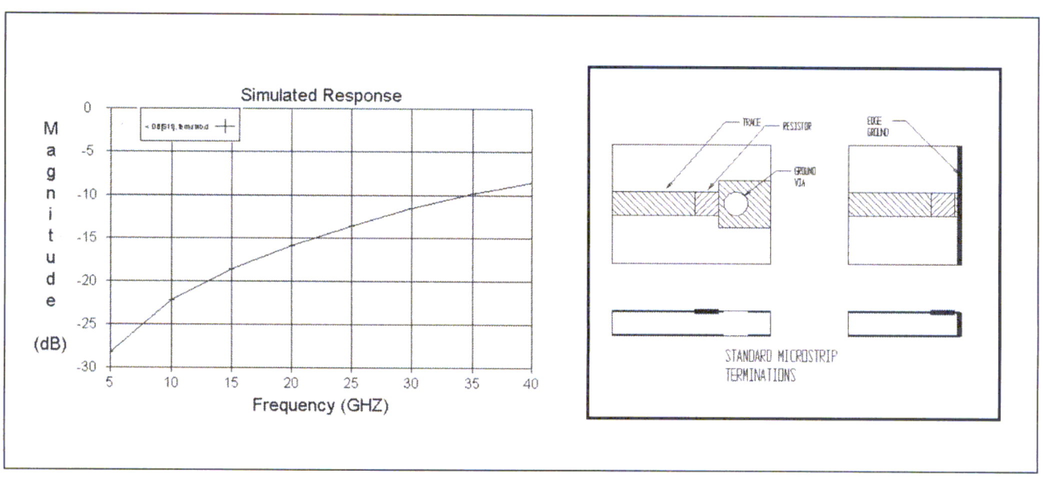

▲ **Figure 7. Microstrip terminations.**

Coaxial terminations

Traditional coax terminations use rod resistors that are about the same size as the coax center conductor of the connector associated with them. At higher frequencies, as the center conductors become smaller, rod resistors become difficult to fabricate and are fragile. An alternative design uses planar substrates and a semi-stripline, semi-coax topology. The

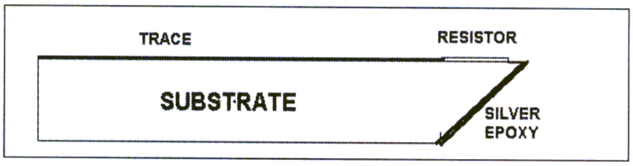

▲ **Figure 8. Improved microstrip termination.**

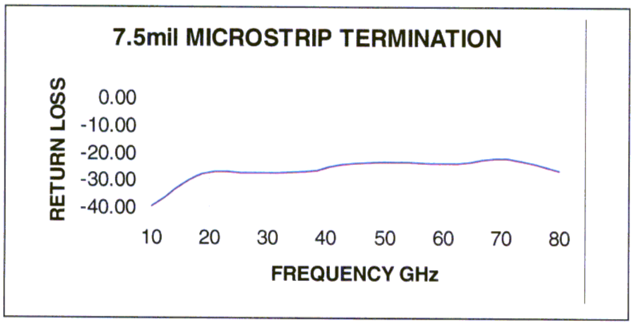

▲ **Figure 9. Improved microstrip termination performance.**

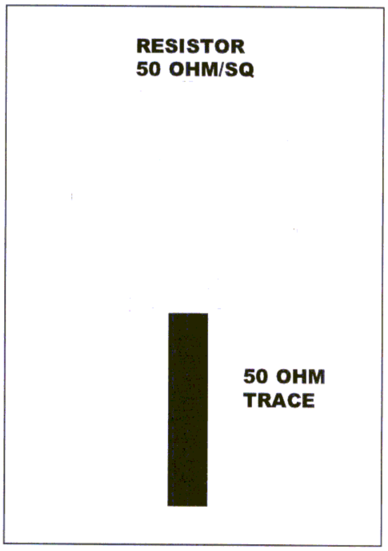

▲ **Figure 10. Improved microstrip termination performance.**

alumina substrate is easy to fabricate and also serves as a support for the center conductor, eliminating the support bead and its associated mismatch. Terminations using this design can have return losses of greater that 40 dB to 40 GHz and 35 dB to 60 GHz. The design has been used to 110 GHz.

Microstrip terminations

Standard microstrip terminations give poor results at higher frequencies, as shown in Figure 7. Designs using open circuit stubs work well for narrow bands even at higher frequencies

A design that works well at high frequencies is shown in Figure 8. The tapered ground plane provides the correct topology for a broad band termination.

With the proper shaping of the substrate, the return loss of this termination is greater than 25 dB to 40 GHz and 20 dB to 80 GHz. The best substrate thickness for use above 70 GHz is 7.5 mil alumina or 5 mil Teflon.

CPW terminations

CPW terminations can work well to high frequencies and are easy to fabricate. CPW substrates are not easy to design at high frequencies as they tend to mode jump. The best performance is achieved using thin alumina substrates with another dielectric and some lossy material attached to the bottom side of the alumina.

Dot terminations

Dot terminations are high frequency, high return loss microstrip terminations that do not require a ground but have a low frequency limit. They consist of an input trace and a circle of resistance material. The resistance is 50 ohms per square.

The size of the dot determines the low frequency limit of the termination. Dot diameters up to 15 times the trace width will perform to the upper limit of the microstrip. Minimum diameters of the dot should be at least three times the trace width. A dot termination can give 25 dB return loss from 8 to 110 GHz.

Broadband interconnects

The 40 gigabit optical modulator will dramatically increase the need for broadband high frequency interconnects. DC to 80 GHz connectors and interconnects with low loss and low reflections will be in great demand. Substrates mounted on carriers of standard design will not meet these requirements. This section discusses designs that will meet these interconnect requirements.

Carriers are a very convenient method of mounting multiple devices. They can be processed outside of the housing and can be replaced without destroying the entire subsystem contained within the housing. Carriers can be made of material that matches the expansion coefficient of the substrates, thus allowing the housing to be made of a more common material. They also provide flat surfaces, which allow easy bonding compared to the

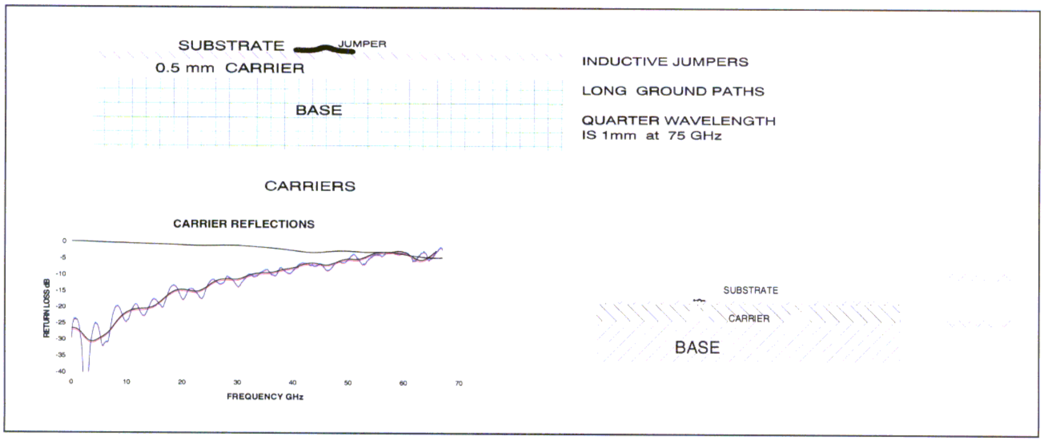

▲ **Figure 11. Standard carriers.**

SAWTEK OSCILLATORS REALLY DELIVER

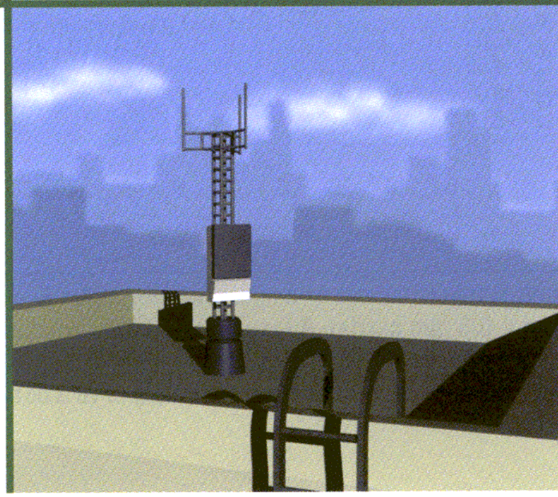

Sawtek...Your Total SAW Solution!

Sawtek's voltage controlled SAW oscillators deliver the specs your need for low g-sensitivity, very low noise floors and low phase noise. The new single-ended sinewave oscillator is ideal for broadband applications such as SONET, LMDS/MMDS point-to-point and multi-point microwave systems. Look to Sawtek's proven Surface Transverse Wave (STW) technology for those outdoor installations where environmental conditions make vibration immunity an issue. When your designs demand a better solution and aggressive cost-effectiveness, demand oscillators from Sawtek. They really deliver.

- **Frequencies from 400 MHz to 2.4 GHz**
- **Low phase noise/jitter (-105 dBc/Hz at 1 kHz offset typical)**
- **Very low noise floor (-165 dBc/Hz starting at 300 kHz offset typical)**
- **Superb vibration immunity for STW versions (5×10^{-10}/g typical maximum)**

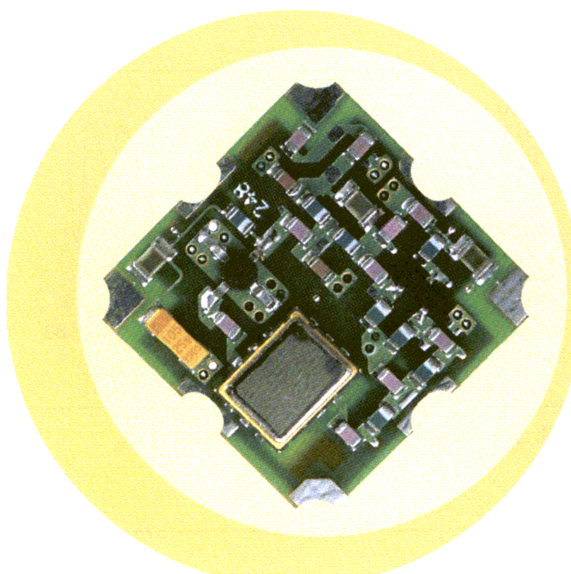

SAWTEK INCORPORATED

www.sawtek.com

Phone: (407) 886-8860 • Fax: (407) 886-7061
E-Mail: info@sawtek.com

Visit Sawtek at booth #2117 at the MTT-S Show.

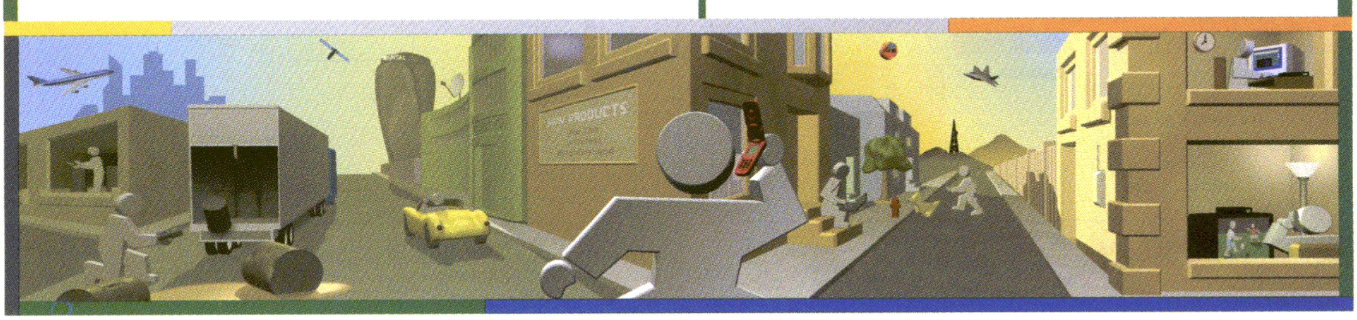

Circle 85

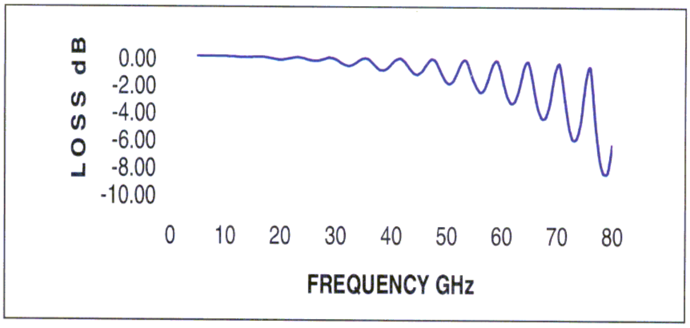

▲ **Graph 1. Insertion loss of a microstrip through line mounted on a 0.5 mm carrier. A long ground path formed by the carrier causes the problem. The results are similar whether connecting to another substrate or to a coax connector.**

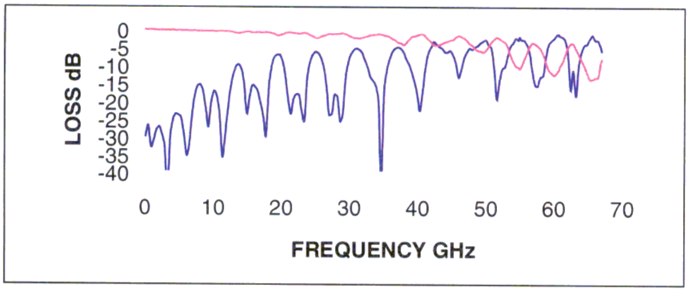

▲ **Graph 2. Measured efffects of the carrier gap.**

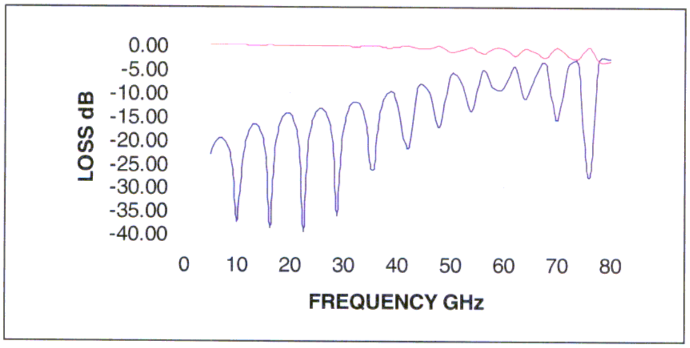

▲ **Graph 3. Simulated effects of the carrier gap.**

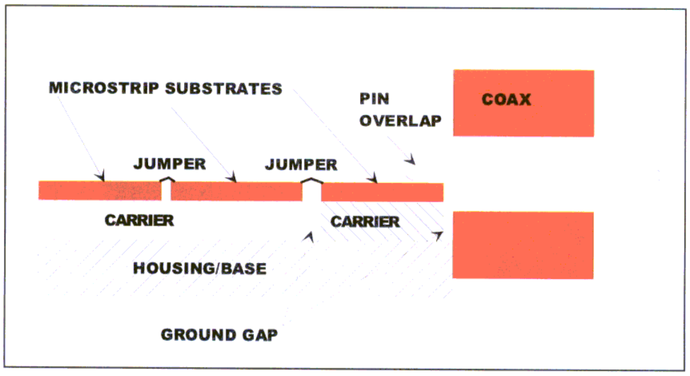

▲ **Figure 12. Ground gaps.**

housing cavity when devices are mounted directly into housing. However, the carrier introduces a long ground path, which seriously degrades high frequency performance.

Figure 11 shows the details of a standard carrier assembly and the performance of a single gap. The two reflection traces are standard frequency domain and frequency gated by time. Notice the good agreement. Time domain is a very useful tool for measuring this type of mismatch.

The carrier gap can be located internally in the housing or at a connector port. Both gaps cause equivalent problems. Graphs 2 and 3 show both simulated and measured effects of a carrier. In general, the measured data seem to be worse than the simulated data.

Figure 12 also shows both type of gaps in addition to the gap formed by two substrates mounted on the carrier. This gap (Graph 4) also gives a significant mismatch at higher frequencies. The standard pin overlap causes a sizable mismatch at higher frequencies. All of these design features must be refined in order to obtain good high frequency performance.

Solutions

Narrowband designs can vary the ground path solution so that the mismatches occur outside of the narrow frequency band. Broad band solutions, however, require that long ground paths be eliminated.

Carrier to housing

The easiest solution is to bridge the gap with a microstrip line, as shown in Figure 13. The line can be preattached to the carrier and connected to the housing or the next carrier by various methods including screws, conductive epoxy, solder or conductive rubber. Conductive rubber can cause problems at high frequencies. The bridge line can also be assembled into the system after the carriers are mounted.

Another method, which is patented, is shown in Figure 14. A flexible ribbon spring, held in place by conductive rubber, fills the gap between carriers and with the trace jumper ribbon, forms a 50-ohm transmission line. This system is flexible, requires no ground solder-

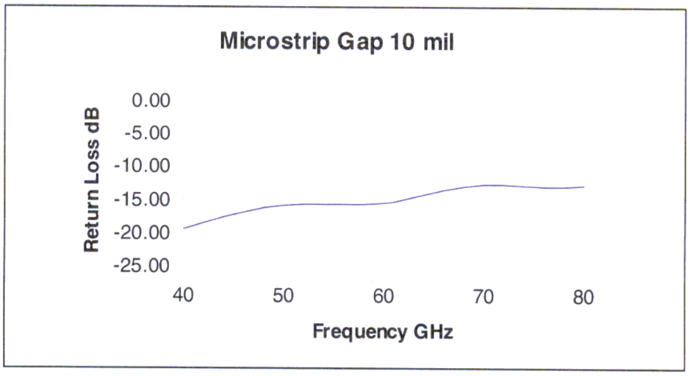

▲ **Graph 4. Carrier gap as shown in Figure 12.**

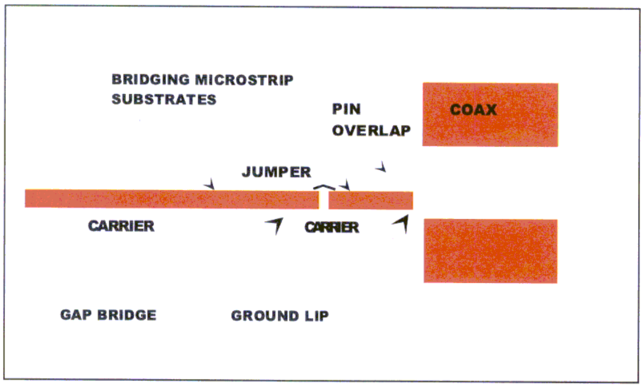

▲ **Figure 13. Bridging substrates.**

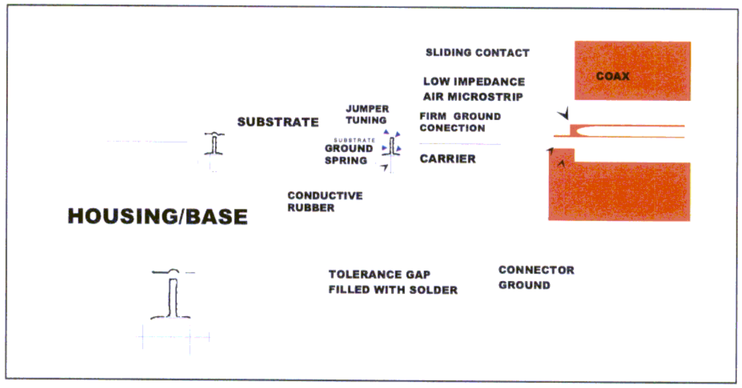

▲ **Figure 14. Alternative designs.**

ing and gives very good performance up to 90 GHz.

Carrier to connector

The best solution to this connection is to have a ground lip at the coax interface and a microstrip substrate cantilevered from the carrier and connected to the ground lip. This is shown in Figures 13 and 14. The ground lip can be part of the housing or incorporates into the connector as a newly developed connector. The connector also contains a glass support bead and the required compensation steps. The connector therefore solves the problems of the hermetic seal and ground. The connector is shown in Figure 15. The connector eliminates the hassle of soldering a glass bead into the housing. A sliding contact is used to connect the coax center conductor to the microstrip trace. This allows a flexible connection and eliminates the capacitive mismatch of the pin overlap design. The sliding contact is bonded to the microstrip trace.

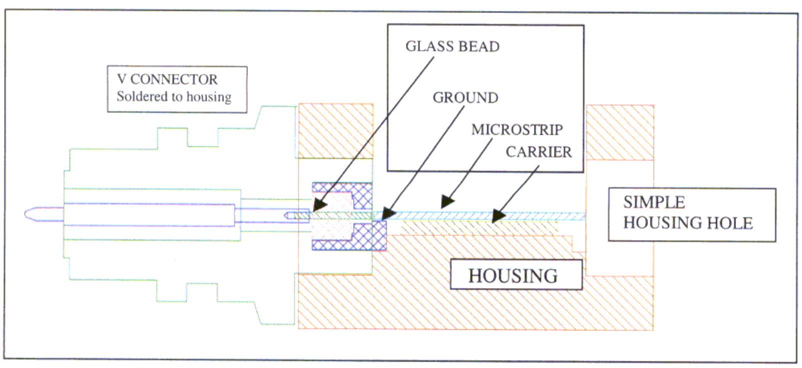

▲ **Figure 15. Connector for substrates on carriers.**

Conclusion

Carriers can be used at high frequencies, but care must be taken to eliminate long ground paths. Ground gaps can be bridged using cantilevered substrates. Gaps between substrates cause a significant mismatch above 40 GHz. ■

References

1. "The Connector Interface," *Microwave Journal*, March 1996.

2. "Backside Interface," *Microwave Journal*, March 1997.

Author information

Bill Oldfield is a staff engineer at Anritsu Company (formerly Wiltron). His career has mostly been focused on connecting, calibrating, modifying or terminating 50 ohms. He may be reached via e-mail at boldfield@anritsu.com.

CST DESIGN STUDIO™

CST MICROWAVE STUDIO™ and **MAFIA 4**
have benefitted from over 20 years experience in the area of numerical field calculation, and have firmly established CST's place at the forefront of CAE software houses.

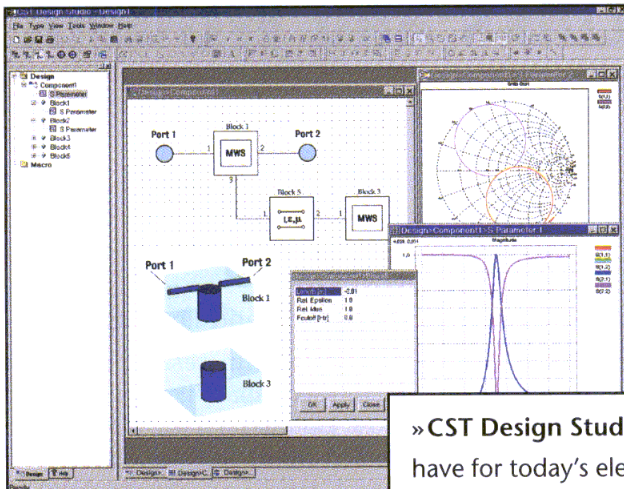

The Interface of CST DESIGN STUDIO™
A high Q coaxial filter structure split into two non-resonating waveguide parts. The combination of both S-matrices together with an analytical transmission line model allows quick parameter studies.

CST DESIGN STUDIO™ can radically speed up the analysis and optimization of complex or highly resonating structures.

How does it work?
CST DESIGN STUDIO™ enables the breaking down of complex systems into smaller components. Each of these components can then be analyzed by the simulator best suited to the particular application domain. Finally everything can be combined in CST DESIGN STUDIO™ to obtain the S-parameter results for the entire system.

»**CST Design Studio** is a must have for today's electrical design engineer. Its interface with Microwave Studio is flawless and compliments it very well. A large diversity of waveguide structures is easily realized by defining a few parameters. In addition, the powerful Graphical User Interface allows S-parameter models to be effortlessly assembled, simulated and optimized with other passive structures.«
Frederic Lecuyer, RF Antenna Design Engineer, Radio Frequency Systems, Inc., a customer of CST of America, Inc.

MAFIA 4

The new modules have been introduced into the Mafia family of codes: MAFIA-TL3 for low frequency problems with parts in motion, and MAFIA-H3, for the calculation of transient heating processes.

RJ45 connector

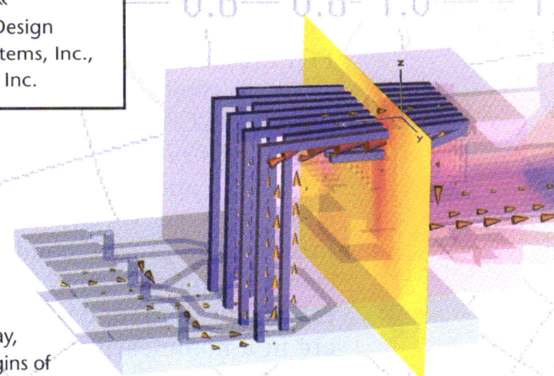

Time Domain Reflectometry (TDR), exclusive to the Time Domain, is an important method in the HF design of interconnectors. It delivers valuable information, such as signal delay, impedance jumps, and the origins of reflections. Probes inside the structure can record the time dependent behaviour of the propagating signals.

Radiation of a mobile phone from the inside of a BMW.
Growing attention is being paid to 3D field simulation by the automobile industry. Areas of particular interest include antennas' radiation patterns and emc problems.

Compatibility of Dual Use Standardized FQPSK with Other Data Links and WCDMA

By **James A. McCorduck,** Entech Engineering
and **Dr. Kamilo Feher,** University of California, Davis and Digcom Inc.

This article discusses the benefits of interoperability of FQPSK systems with future and legacy data links. Specifically, the benefits of forward interoperability with 3G wireless systems, such as WCDMA up to 40 Mchips/sec, are described. Other proposals of forward interoperability with future data links include an enhanced ultra-bandwidth efficient FQPSK and 16-state FQAM architectures. Since FQPSK based systems have been proven in commercial and government systems and extensively tested and evaluated by the Department of Defense and NASA, the analysis of backward interoperability with legacy data links, such as GSM, is also included in this discussion. Interoperability is further facilitated by standardization of the FQPSK systems by the Inter-Range Instrumentation Group (IRIG-106-00 for FQPSK-B), and NASA/JPL recommended FQPSK for standardization by the International Consultative Committee for Space Data Systems (CCSDS).

Interoperability of FQPSK [1–3] with WCDMA and other transceivers offers a wide variety of solutions, including improved bandwidth efficiency, frequency agility for higher bit rate applications and the ability operate in a nonlinearly amplified (NLA) environment. Several corporations (licensees of Feher-patented technologies) have developed a wide bit rate range of products. This article explores the benefits of FQSPK products when incorporated into a WCDMA 3G wireless system in this article. The benefits include a 40 Mchips/sec [3] capability, and significant growth in research as compared to the 5 Mchip/sec capability, which is currently in use in most commercial CDMA applications. In addition to the readily available, dual-use products, NASA developed ultra high bit rate FQPSK systems and demonstrated the performance of these systems with satellite links in the 300 Mb/sec to 1 Gb/sec rate [4, 5]. FQPSK systems also provide more promise as an interface to the 3G systems. The second part of this article illustrates the interoperability with other future FQPSK transceivers, resulting in better spectral efficiency and performance. With a goal of both forward and backward interoperability, the third part of this article covers backward interoperability with legacy data links. Utilizing differential encoding (DE) and differential decoding (DD) techniques, interoperability with GSM-based transceivers is discussed [5].

Interoperability of FQPSK with WCDMA

Since interoperability with CDMA systems may be essential for integration into the next

System	1. DDSS mode: BPSK, OQPSK, FQPSK 2. clear mode: BPSK, OQPSK, FQPSK
Data rate (Kbit/s)	256, 560, 660, 772, 1544, 2110
Chip rate (Mc/s)	16.984, 30.88, 30, 35
PN code	2**16 length
Carrier recovery	Decision-directed, phase difference approximation, digital phase shifter (i.e., vector rotator)
Convolutional coding and interleaver	Viterbi decoder
IF signal (MHz)	70

▲ **Table 1. Specifications of an experimental setup circuit for testing FQPSK transceivers up to 35 Mchips/sec with DSSS CDMA [6].**

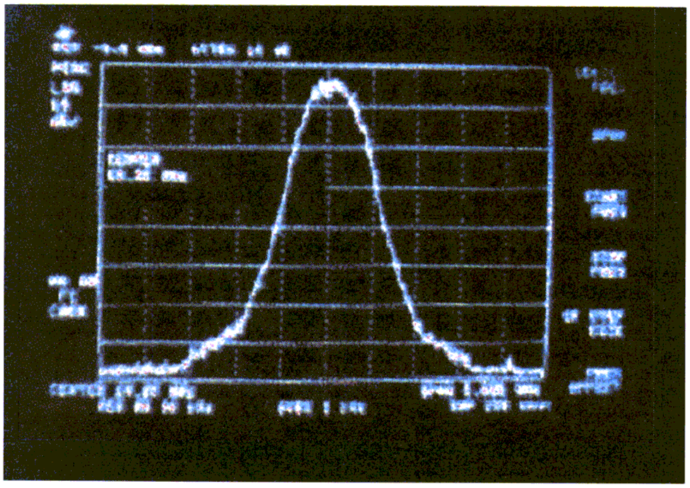

▲ **Figure 1(a). FQPSK-B spectrum at 1Mb/s and f_c = 70 MHz. This is the spectrum of the recently licensed FQPSK (IRIG-106-00, and recommended for by the International CCSDS) [12].**

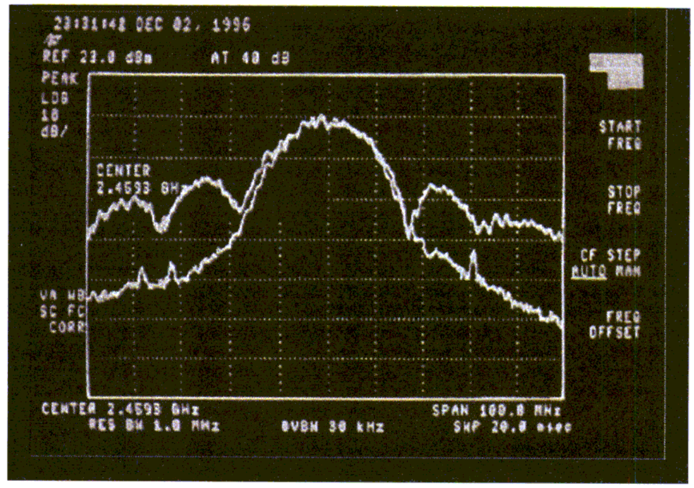

▲ **Figure 1(b). Spectrum for FQPSK (lower trace) as compared to filtered QPSK (upper trace) with WCDMA. In this setup, FQPSK is operating with a bit rate of 1.544 Mb/sec with a chip rate of 16.84 Mchips/sec. Both transceivers are operating in an NLA RF system [6].**

generation of wireless communications, the benefits of interfacing FQPSK with WCDMA systems is discussed.

Experimental results show FQPSK operation at 16.984, 30.88, 35 and 40 Mchips/sec with various bit rates, confirming bit rate agility [4]. Table 1 shows the specifications of an experimental circuit setup that allows the user to use both FQPSK and DSSS CDMA. Figure 1 shows the spectrum of the hybrid FQPSK/WCDMA system. These figures demonstrate that FQPSK has been measured and evaluated for WCDMA systems. Since FQPSK has been experimentally proven to data rates up to 1 Gb/sec [5], and proven to operate with WCDMA up to 40 Mchips/sec, the integration of these systems is feasible. Using Equation (1) as an approximation for the relationship between the chip rate f_{chip} of the CDMA access method and the bit rate f_b of the transceiver, the amount of growth for this system integration is [1, 6].

$$G_p = \frac{BW_{RF}}{BW_{MOD}} = \frac{f_{chip}}{f_b} \tag{1}$$

where BW_{RF} is the RF bandwidth of the signal and BW_{MOD} is the modulated signal bandwidth. For example, if 70 MHz is the RF signal and the approximate bandwidth of the FQPSK signal, which supplies about a 1 Mb/sec data rate, is 1 MHz (at –60 dB), then the chip rate is approximately 70 Mchip/sec (assuming the same processing gain). Because potentially higher frequency RF signals result in significantly higher chip rates, the FQPSK architecture is ideally suited for growth in capacity. Figure 2 shows that there is no BER penalty for employing FQPSK transceivers at 30 Mchips/sec in a CDMA system.

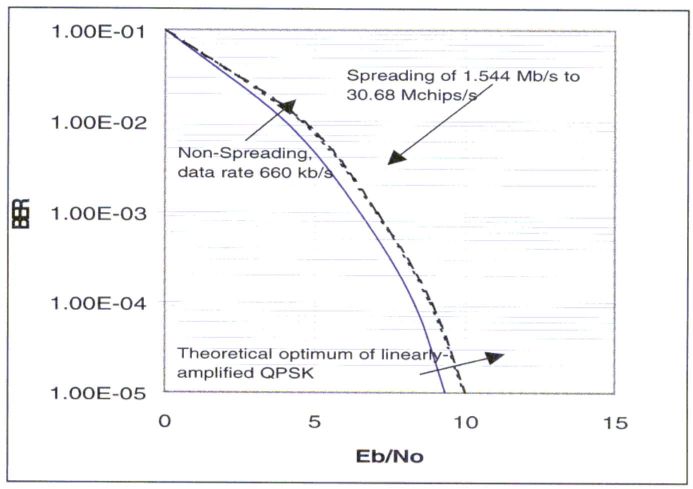

▲ **Figure 2. Effect of the WCDMA 3G+ system's integration with FQPSK on the BER performance of transceiver systems. There is no notable performance penalty for incorporating spread spectrum into the transceiver architecture [4].**

Interoperability of FQPSK with future data links

Because future data links, such as enhanced FQPSK and FQAM transceivers, show promise of significantly better performance than the currently installed transceivers, interoperability of these architectures with the standardized FQPSK systems (IRIG-106-00) is essential. Both of these proposed systems employ the current IRIG 106-00 standardized FQPSK architecture as a building block to the respective proposed transceivers.

Figure 3 shows the proposed architecture of 16-state FQAM. The processor currently utilized in the IRIG-106-00 standardized FQPSK is also present in this

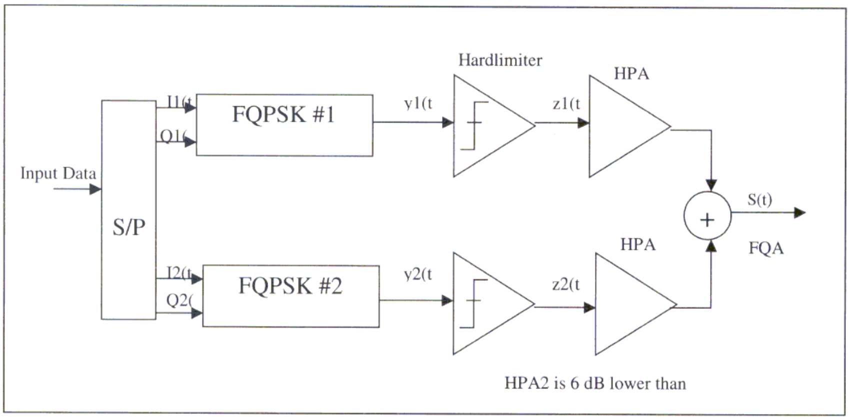

▲ **Figure 3. System architecture for a proposed parallel-type 16-state FQAM data link. This architecture is designed to support NLA environments in the RF spectrum [7].**

architecture. This architecture provides significantly increased spectral efficiency in an NLA environment with minor degradation of 0.8 dB in the SER [7].

Figure 4 illustrates the performance of the enhanced-FQPSK transceiver. The enhanced FQPSK architecture significantly improves the BER performance of the current IRIG-106-00 standardized FQPSK. Figure 4 also illustrates that this proposed architecture improves the ACI of the standardized FQPSK. This improvement in BER performance and spectral efficiency is accomplished by incorporating FEC into the standardized FQPSK architecture [7].

Interoperability of FQPSK with legacy systems

The key to interoperability between the FQPSK-B and GMSK architectures is the addition of the DE in the FQPSK transmitter circuits and DD in the receiver circuits. A DE is added to the FQPSK transmitter architecture for compatibility with a GMSK receiver architecture. Figure 5 shows the proposed configurations of the FQPSK transceiver links with GMSK, MSK, and O-QPSK systems [10].

The algorithm for the DE is [2, 8, 9]:

$$I_{2n} = b_{2n} + \overline{Q}_{(2n-1)} \qquad (2)$$
$$Q_{(2n+1)} = b_{(2n+1)} + I_{2n}$$

for n>0 and where I_2, I_4, I_6, … and Q_3, Q_5, Q_7, …

The DE and DD algorithms convert the NRZ data sequences between amplitude and phase based systems.

As Figure 5 illustrates, the FQPSK architecture can be integrated with the GMSK systems as either a transmitter or receiver [8]. When FQPSK is inserted as a transmitter, the composite system outperforms the GMSK system by approximately 1 dB at P_e = 1E–5. The spectral efficiency is also improved, since the benefits of the FQPSK transmitter characteristics are fully employed in this configuration.

FQPSK update

This section describes spectrally efficient Feher's patented FQPSK first and second generation technology developments, commercial and government "dual-use" FQPSK products and test and evaluation results and standardization (CCSDS and IRIG 106-00). US and international customer requirements, recent deployments and standardization programs are also discussed. Numerous government and commercial systems/pro-

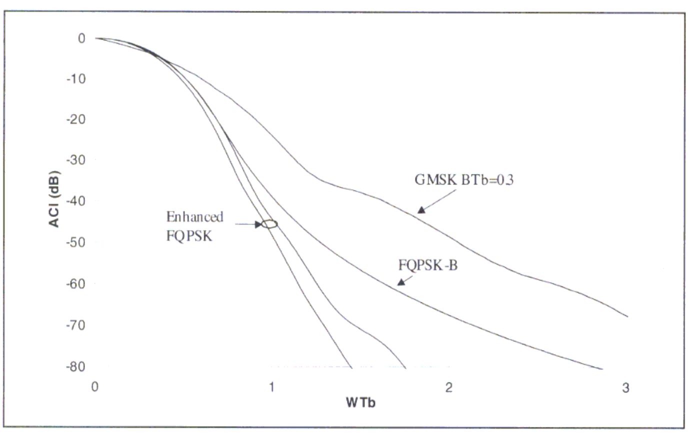

▲ **Figure 4 (a). Adjacent channel interference performances of the enhanced FQPSK (variation L1 and L2, from the left curve to the right, respectively), FQPSK-B and GMSK NLA systems. The GMSK receiver uses a fourth order Gaussian bandpass filter equal to 0.6 and a transmitter filter bandwidths equal to 0.3. Enhanced FQPSK uses a much simpler receiver [10,11].**

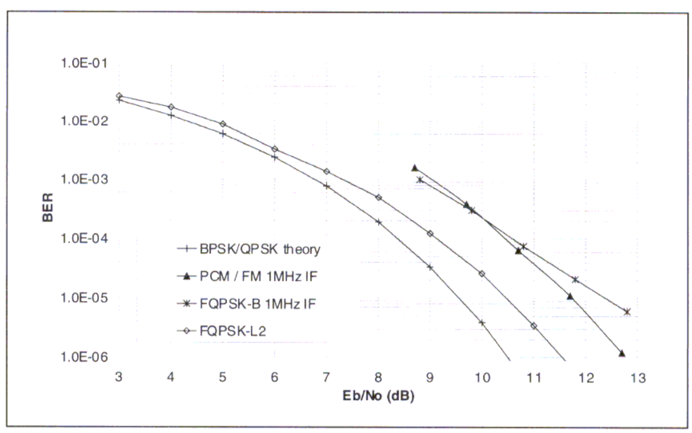

▲ **Figure 4(b). BER for the enhanced FQPSK (variation L2) and 1 Mb/s FQPSK-B and PCM/FM. The BER performance of FQPSK-B and PCM/FM was measured for a 1Mb/s signal and a 1 MHz IF filter bandwidth. The demodulator of FQPSK-B was a nonoptimized modified QPSK demodulator; the PCM/FM was limiter detected [10,11].**

Commercial	L3 Communications, Inc.	EIP Microwave
	Telemetry East - Aydin	Iota/NeoSoft
	Conic	Emhiser Research Inc.
	Interstate Electronics Co. (IEC)	Applied Signal Techology
	Microdyne	Broadcast Microwave Syst.
	Lockheed Martin	INTEL Corporation
	RF Networks, Inc.	Analog Devices
	Herley Industries-Vega	Semco
	Tasc-Litton	Centraxx
	Tybrin	
U.S. Department of Defense	SBIR (US Air Force)	CRADA-U.S. Navy-Pt. Magu
	ARTM-US Air Force - Edwards	FIRST
	CRADA	FIT
	US Navy China Lake and TGRS	Telemetry RCC
NASA	TCA w/ JPL - NASA	
	300 Mb/s - 600 Mb/s FQPSK	
	NASA:Goddard and NASA/JPL	
Standarization	AIAA	ESA
	CCSDS	FIT
	SFCG	Telemetry IRIG 106-00
Universities	New Mexico State University	
	University of California, Davis	
	California Institute of Technology (Cal Tech)	

▲ **Table 2. List of Feher patented FQPSK licensees and Feher patented GMSK licensees, manufacturing companies and cooperating U.S. Department of Defense, NASA, AIAA, international CCSDS programs/customers and member organizations of the FQPSK consortium (1995–2000).**

grams have immediate and/or near term requirements for spectrally efficient telemetry systems, data links and other spectrally efficient wireless and broadcasting applications. First generation Feher patented FQPSK doubles the spectral efficiency of PCM/FM telemetry, Feher patented GMSK and alternatives, and second generation FQPSK could quadruple the spectral efficiency of these systems. This section includes the use of FQPSK for applications such as telemetry, data links, clear mode, TDMA, CSMA and CDMA, OCDMA, WCDMA and OFDM–COFDM.

Recent R&D achievements and study results demonstrate that enhanced performance first generation FQPSK systems have a 1 dB improved BEP performance as compared to that of inter-operable and fully compatible IRIG 106-00 standardized FQPSK-B bit rate agile 1 Mb/s to 20 Mb/s range transmitters and receivers. Preliminary results of noncoherently demodulated FQPSK systems will be compared with the performance of coherently demodulated FQPSK systems. Fast synchronization and re-synchronization time issues will be also addressed.

Further, adaptively equalized FQPSK systems, with ultra fast dynamic adaptive equalizers, designated as FE, are also discussed. Progress in nonredundant error detection (pseudo-error) based controlled adaptively equalized and SMART antenna -diversity and FE multiple array FQPSK systems is also presented. Low redundancy (5 to 10 percent range) FEC combined with FQPSK is demonstrated to lead to an approximately 5 dB increase in the data link margin.

A key technology overview of several FQPSK-based programs operated and implemented in the 100 kb/s to 40 Mb/s range, and NASA's FQPSK implementations in the ultra high bit rate in the 300 Mb/s to 1 Gb/s range are also highlighted.

Table 2 [13] shows the current licensees for FQPSK.

Conclusion

This article highlighted interoperability with 3G and 3G+ wireless systems by showing established experimental results with WCDMA systems. Growth in channel capacity was also demonstrated for an FQPSK transceiver integrated with the 3G wireless systems. This added capacity is due to FQPSK's proven high bit rate and increased spectral efficiency without any significant degradation in BER perfor-

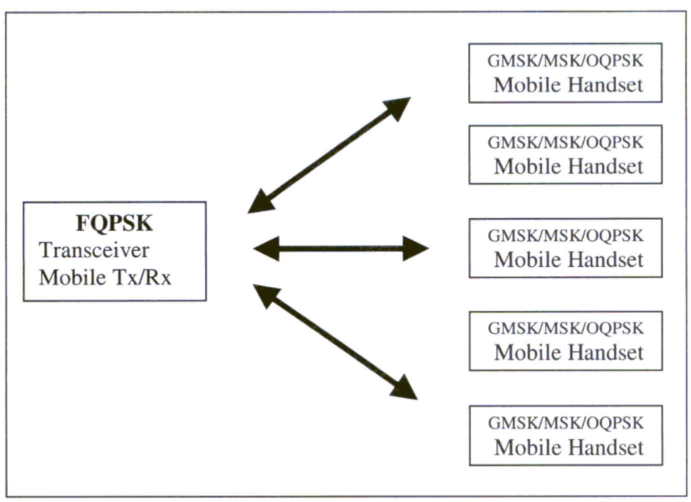

▲ **Figure 5. Proposed architecture for the interoperability of FQSPK with legacy data links. The FQPSK hardware can be implemented for both transmitter and receiver applications, as well as for future spectrally efficient data links [10, 14].**

mance. Interoperability of FQPSK with future data links was also described. Specifically, the proposed enhanced-FQPSK and the 16-state FQAM transceivers will provide better BER performance, increased spectral efficiency and QAM operation (from FQAM transceiver) with an NLA in the transmitter without significant spectral spreading. This article also showed that FQPSK-B systems can be made compatible with legacy data links, such as GMSK systems, by employing differential encoding and decoding. Particularly, improved BER performance and increased spectral efficiency are added benefits of constructing a composite FQPSK/GMSK transceiver. ■

References

1. K. Feher, *Wireless Digital Communications: Modulation & Spread Spectrum Applications,* Prentice Hall: Englewood Cliffs, NJ, 1995.

2. IRIG STANDARD 106-00 "Telemetry Standards," Secretariat of Range Commanders Council, U.S. Army, White Sands, NM, January 2000. (Note: for higher bit rates, when better bandwidth efficiency is required, the IRIG 106-00 telemetry standard specifies the use of Feher's patented FQPSK-B. This standard has been approved for public release and distribution is unlimited).

3. K. Feher, et al.,"Feher Patented FQPSK, Feher Patented GMSK (FGMSK) and Feher Patented FQAM," U.S. Patents 4,339,724; 4,567,602; 4,644,565; 5,491,457; 5,784,402, post-patent improvements and other U.S. and international patents pending, including international application published under the Patent Cooperation Treaty (PCT); international public. no. WO 00/10272; World Intellectual Property Organization; international publication date February 24, 2000 (PCT internat SN: PCT/US99/17995) and international public. no. WO 00/13382 publication date March 9, 2000 (PCT internat SN PCT/US99/19909). For Feher patented FQPSK, FGMSK and FQAM technology transfers and licensing information on an equal-opportunity, non-discriminatory basis with uniform terms and at a fair market price, see author information at right.

4. K. Feher, M. Yu, D. Lee and W.C.Y. Lee, "Innovative Modulation Approaches Enhance CDMA and GSM Performance," *Wireless System Design,* October 1996.

5. P. Ghuman, S. Koubek, T. Winkert, A. Gray, N. Lay and T.Y. Yan, "Ultra High Bit Rate (up to 1 GBIT/S) Bandwidth Efficient FQPSK All-Digital Modulator/ Demodulator Architectures and NASA Implementations," International Telemetering Conference 2000, San Diego, CA, October 23–26, 2000.

6. W. Gao, K. Feher and D.J. Lee, "Interference Performance of Ultra-High Rate (up to 40 Mchips/s) FQPSK Based W-CDMA," *Applied Microwave & Wireless,* March/April 1997: 24–32.

7. Wei Gao, Shih-Ho Wang and K. Feher, "Blind Equalization for FQPSK and FQAM Systems in Multipath Frequency Selective Fading Channels," International Telemetering Conference 1999, Las Vegas, NV, October 25–28, 1999.

8. M.P. Fitz, "Bit Error Probability Analysis of a Digital PLL Based Demodulator of Differentially Encoded BPSK and QPSK," *IEEE Transactions on Communications,* Vol. 42, No. 1, January 1994: 17–21.

9. W.J. Weber, "Differential Encoding for Multiple Amplitude and Phase Shift Keying Systems," *IEEE Transactions on Communications,* Vol. Com-26, No. 3, March 1978: 385–91.

10. J. McCorduck, M. Haghdad, J.S. Lin, K. Aflatouni, W. Gao and K. Feher, "Peformance Enhancements of IRIG-106-00 Standardized FQPSK-B in a Complex Interference RF Frequency Selective Faded Environment and Interoperability with Legacy Data Links," European Telemetry Conference 2000, Garmisch-Partenkirchen, Germany, May 22–25, 2000.

11. J.S. Lin and K. Feher, "Spectrum and BER Performance of a Set of FEC Coded Enhanced FQPSK," International Telemetering Conference 2000, San Diego, CA, October 23–26, 2000.

12 M. Haghdad and K. Feher, "Performance of FQPSK Transceivers in a Complex Real-Life Interference Environment," International Telemetering Conference 2000, San Diego, CA, October 23–26, 2000.

13. K. Feher, "Spectral Efficiency of Commercial Wireless and Telemetry Systems is Doubled with IRIG-106-00 Standardized FQPSK and is Quadrupled with FQAM," International Telemetering Conference 2000, San Diego, CA, October 23–26, 2000.

14. J. McCorduck and K. Feher, "Compatibility of IRIG-106-00 Standardized Feher-Patented FQPSK with Other Data Links and Wideband W-CDMA," International Telemetering Conference 2000, San Diego, CA, October 23–26, 2000.

Author information

James A. McCorduck is an engineer with Entech. He recently obtained his master's degree in engineering at the University of California-Davis. He can be reached at 8061 Cantata Way, Antelope, CA 95843; Tel: 916-338-4482; Fax: 916-332-5507; E-mail: engtec@aol.com.

Dr. Kamilo Feher is a professor of engineering at the University of California-Davis. He also heads Digcom, a digital communications development, consulting and intellectual property licensing organization. He can be reached at 44685 Country Club Drive, El Macero, CA 95618; Tel: 530-753-0738; Fax: 530-753-1788; E-mail: feherk@yahoo.com.

For FQPSK Consortium, FQPSK-GMSK licensing and technology transfer information, contact Digcom, Inc., c/o Dr. Kamilo Feher, 44685 Country Club Drive; El Macero, CA 95618; Tel: 530-753-0738; Fax: 530-753-1788; E-mail: feherk@yahoo.com; Internet: www.fehertechnologies.com.

SEMICONDUCTORS

5 GHz radio chipset

Raytheon Company's Commercial Electronics division introduces a 54 Mbps radio chipset, called Tondelayo, based on the IEEE

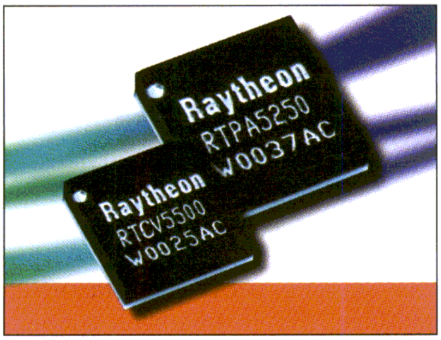

802.11(a) standard for high speed wireless networks in the 5 GHz UNII bands. Features include a power amplifier/switch module; RF, IF and baseband component chips; CardBus and PCI reference designs; and a suite of drivers.

Raytheon Company
Circle #157

Single-chip radio

Analog Devices has released its next-generation OthelloOne™ direct conversion radio chipset for GSM/GPRS cellular phones and wireless Internet devices. Features

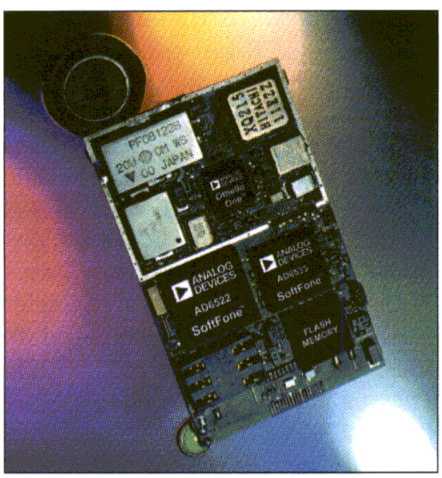

include a complete direct-conversion transceiver on a single chip; LNAs, RF power control and low-dropout voltage regulators; 40 percent reduction in total component count and PC board area compared to original Othello; support for GSM/DCS/PCS voice and GPRS/EDGE data applications; compatibility with Analog Devices SoftFone baseband chipset; 51 total components for a three-band GSM radio; and a 48-lead LFCSP (chip-scale) package.

Analog Devices
Circle #158

MMIC amplifier products

Fujitsu Compound Semiconductor announces the expansion of its Low Noise Amplifier MMIC product line. Fujitsu is introducing two new millimeter-wave, high power

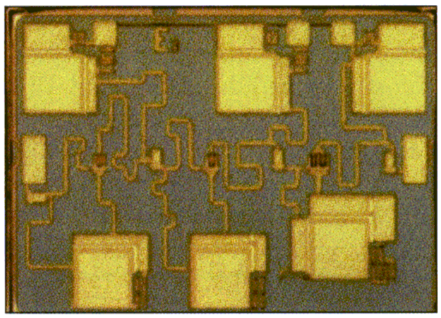

MMIC amplifier products covering the 24 to 40 GHz frequency band with output power of up to 9 dBm. These new devices are designed for point-to-point or point-to-multipoint radio link and Local Multipoint Distribution System applications.

Fujitsu Compound Semiconductor, Inc.
Circle #159

Low noise amplifier

Stanford Microdevices introduces the SLX-2043, a new pHEMT-based low-noise amplifier module suited to 2G/3G wireless infrastructure and fixed wireless applications. This product simultaneously offers low-noise and high-intercept performance, with a typical noise figure of 1.1 dB and a typical output intercept of 34 dBm. The part offers 15 dB of gain, which results in an input intercept of 19 dBm. This LNA offers input and output match without external matching components and is unconditionally stable. It operates from a single 4V supply, dissipating under 0.5 watt, and uses internal gate bias circuitry, making it extremely easy to use in a wide variety of applications.

Stanford Microdevices
Circle #160

Wireless chipset

DMC Stratex Networks will begin volume shipping this month of products powered by its new wireless chipset. The chipset, Vantex™, uses quadrature amplitude modulation (QAM) technology to enable high-capacity and ultra-high-capacity point-to-point wireless radios for cellular transmission and broadband access applications. Vantex delivers wireless modulations from 4 QAM and bit rates from 4 Mbps to 311 Mbps in a single radio.

DMC Stratex Networks
Circle #161

RFIC upconverter

New from NEC and available now from California Eastern Labs is the UPC8172TB upconverter. Designed for use in the transmit chain, it combines low power consumption, high output power and

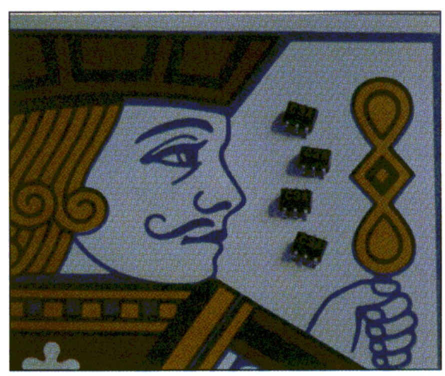

high linearity with operation to 2.5 GHz. The UPC8172TB is manufactured using NEC's 25 GHz f_T UHSO silicon bipolar process, which uses direct silicon nitride passivation film and gold electrodes resulting in consistency and reliability. The UPC8172TB is priced at $1.43 in 12,000-piece quantities.

California Eastern Labs
Circle #162

Bipolar transistor

GHz Technology announces the release of the GHz20060, its newest transistor for linear wireless communication systems. The GHz20060 is a simplified version of GHz Technology's double input matched wider bandwidth 1920CD60. It is a 60-watt (PEP), 26-volt, Class AB bipolar transistor for use in the 1800 to 2000 MHz frequency range, with a minimum power gain of 9 dB.

GHz Technology, Inc.
Circle #163

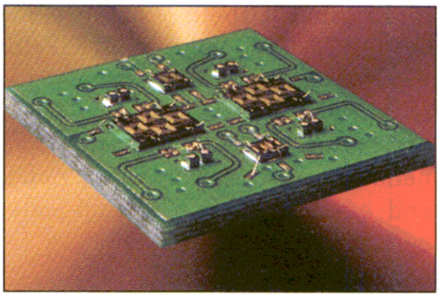

Vector modulators

Alpha Industries has introduced the VM series of vector modulators. These eight-chip, BGA packaged solutions can be integrated into base station MCPA applications to increase bandwidth efficiency and support high-speed data transmission for 2.5G systems. The vector modulator offers 360 degrees of phase control and a large linear amplitude adjustment range.

Alpha Industries
Circle #164

RF power amplifiers

M/A-COM has announced two integrated circuit power amplifiers for use in cellular GSM and DCS GPRS wireless handsets. The MAAPSS0004 and MAAPSS0005 RF power amplifiers, for GSM and DCS bands respectively, meet GPRS specifications and are the first to include all 50 ohm input and output matching in a compact 5 × 5 mm plastic micro leadframe (FQFP-N) package. The devices are priced for high volume applications at less than $1.99 each in quantities of 100,000 or more.

M/A-COM
Circle #165

HBTs for wireless handsets

Kopin Corporation introduces InGaP/GaInAsN HBTs. These structures enhance the performance of HBT transistors within the existing GaAs manufacturing platform. Kopin has been successful in incorporating indium and nitrogen into the base layers of the HBTs and has achieved substantial reductions in turn-on voltage of more than 150 mV with the InGaP/GaInAsN structures, while retaining device characteristics.

Kopin Corporation
Circle #166

Field effect transistor for cellular radio

Ericsson Microelectronics has introduced the PTF10161 GOLDMOS field effect transistor. This new component delivers a minimum of 165 watts RF output at 894 MHz from a 28 volt supply. Typical figures for efficiency and power gain are 50 percent and 16 dB, respectively. The PTF10161 is designed for use in cellular radio applications from 869 MHz to 894 MHz and provides IMD performance to bipolar transistors, largely due to the more linear transfer function of LDMOS compared to the bipolar technology.

Ericsson Microelectronics
Circle #167

Single supply pHEMT

Agilent Technologies has introduced a small-signal E-pHEMT device, the first in a family of high-gain, highly linear and very low noise transistors. The ATF-54143

Products

offers performance, size and design advantages for applications such as tower-mounted amplifiers and front-end LNAs for base stations operating in GSM, E-GSM and W-CDMA systems at 900 MHz and 1.9 GHz. The ATF-54143 device is priced at $1.97 in quantities of 25,000 to 49,999 pieces.

Agilent Technologies, Inc.
Circle #168

TEST EQUIPMENT

Low phase noise dual range synthesizer

Programmed Test Sources has released the new PTS 250SX-51, a versatile dual-range frequency generator offering broad coverage from 1 to 250 MHz, as well as 5 to 20 μs switching between any two frequencies with a resolution of 1 Hz. Output is 13 dBm, and spurious outputs are –70 dB referenced to +13 dBm. The unit can be optionally supplied with two different frequency standards with moderate or high stability (3×10^{-9}/day). SSB phase noise is –123 dBc at 10 kHz offset from the carrier. Where even better phase noise is desired, the unit can be set to produce output frequencies from 1 to 25 MHz. Spurious outputs are again –70 dB, and output of +13 dBm (into 50 ohm) is available. SSB phase noise at 20 kHz offset is –141 dBc. The unit is available with remote control (BCD or GPIB) and manual controls.

Programmed Test Sources, Inc.
Circle #169

Enhanced network measurement system

Anritsu Company has introduced the MS4600/4B option for its Scorpion MS46xx RF Vector Network Measurement System (VNMS). The MS4600/4B extends the noise figure frequency of the VNMS to 6 GHz so it can analyze low noise amplifiers (LNAs) and other devices covering the 5.2 to 5.8 GHz band that are used in applications such as ETC, HIPERLAN, WLAN and ISM. The MS4600/4B is priced at $16,000.

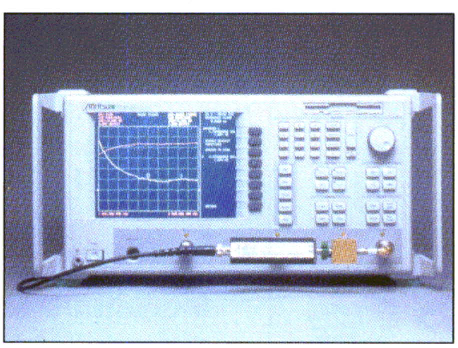

Anritsu Company
Circle #170

Circle 78

Circle 46

CDPD test suite

IFR Systems has announced the release of a new software test suite that tests Cellular Digital Packet Data (CDPD) capabilities on wireless cellular handsets and wireless modems. Designed for use with the IFR 2959 Advanced Multi-mode Cellular Test Set, the software suite allows users to test CDPD performance of mobile phones and modems operating at 19.2Kbps.

IFR Systems, Inc.
Circle #171

Power amplifier test set

Agilent Technologies has unveiled its Handset Power Amplifier (PA) ValiFire system, which helps designers creating power-amplifiers for cell phone handsets to reduce product development time and costs. The system helps shrink the development cycle by reducing the time needed to set up and configure test assemblies and write test code for design verification. It also allows easy comparison and correlation of simulated versus measured results. Prices start at $42,000 for the proprietary software. Pricing for the full system, including hardware and software, starts at $246,000.

Agilent Technologies, Inc.
Circle #172

Field engineering kit

Bird Component Products has introduced its newest field transportable component kit. The plastic case has a retractable handle of

rollers for ease of moving from site to site. Foam shelves are configured for a variety of Bird components including attenu ators, terminations, couplers and divider/-combiners. The kits' dimensions are 25 × 15 × 14 inches and is assembled for easy access and re-stocking.

Bird Component Products
Circle #173

FREQUENCY CONTROL

Monolithic VCO with differential buffered output

Maxim Integrated Products introduces the MAX2753 2.4 GHz monolithic VCO with differential

output, which integrates the oscillator, tank circuit and a matched output buffer, all in the small 8-pin μMAX package. Applications include cordless phones, HomeRF, Bluetooth and other propietary radios operating in the 2.4 GHz ISM band.

Maxim Integrated Products
Circle #174

Commercial PLL

Vari-L Company announces its Model PLL400-915, which generates frequencies from 902 to 928 MHz in 200 kHz steps. The unit typically requires 19 mA of current from a 5.0 V supply voltage. Typical phase noise at 0.5 kHz offset is –84 dBc/Hz and the typical phase noise at 100 kHz offset is –131 dBc/Hz. Phase detector spurious suppression is typically –82 dBc. Typical output power is 4.0 dBm. Second harmonic suppression is typically –13 dBc and third harmonic suppression is typically –27 dBc.

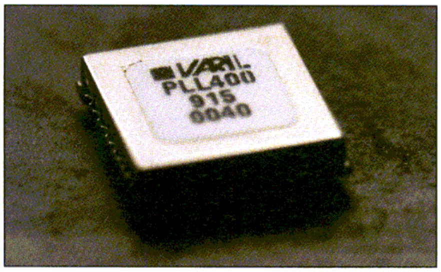

Vari-L Company, Inc.
Circle #175

Crystal ideal for portable and wireless applications

Fox Electronics has introduced a new crystal that provides a cost-effective alternative for portable, wireless and other applications with space and budget constraints. The new Fox FUE crystal measures just 13.4 × 5.08 mm with a profile of 4.6 mm, an exact match to the footprint of Epson's part #MA505. The new crystal offers a frequency range of 3.579545 MHz to 66.6667 MHz; a frequency tolerance of ±50 PPM; a frequency ability of ±80 PPM or less depending on frequency; and an operating temperature range of –20° to +70° C. Prices for the Fox FUE Crystal start at $0.44 in quantities of 10,000.

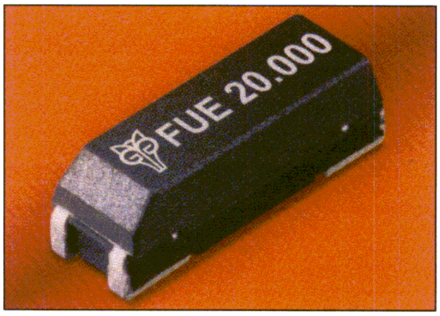

Fox Electronics
Circle #176

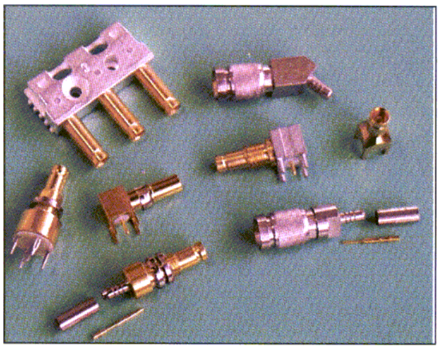

CABLES & CONNECTORS

Mating connector series

Compel Electronics announces the availability of its 1.0/2.3 connector series. With 50-ohm versions operating to 10 GHz and 75-ohm versions operating to 3 GHz, the new 1.0/2.3 line offers threaded, snap-on, slide-in, push-pull and DIN mating configurations. To facilitate numerous applications, designs are available for cable, PCB and bulkhead mounting in straight, U and angled styles. The series also includes in-series adaptors, monitor points and terminations.

Compel Electronics, Inc.
Circle #177

BNC bulkhead jack

Trompeter Electronics announces a 75 ohm BNC separable circuit board jack for interconnecting mother and daughter boards. This connector assembly is ideal for

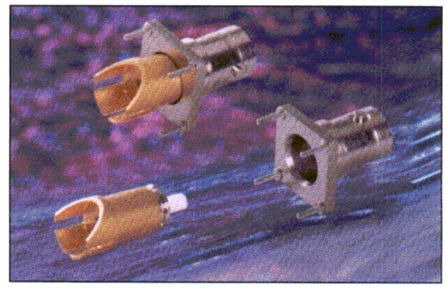

launching high frequency signals directly from the edge of a p.c. board through the motherboard into a coax cable. The UCBJSE20F offers return loss values better than –25 dB up through 3 GHz and handles ~3 pounds of insertion force.

Trompeter Electronics
Circle #178

TNC coaxial connectors

Tru-Connector Corporation has introduced a new series of TNC connectors featuring an expanded

frequency range for military, aviation and telecom applications. The TNC 18 GHz coaxial connectors feature a frequency range that has been extended by modifying their interface dimensions, while conforming to MIL-C-39012 interface standards. Offered as plugs, jacks and receptacles, they can be manufactured to customer specifications. The connectors are priced from $9.95 each, depending upon construction and quantity.

Tru-Connector Corporation
Circle #179

High performance cable assemblies

Times Microwave Systems has introduced its line of flexible 50 ohm Testmate cable assemblies. Designed for operation up to 18 GHz or 40 GHz, Testmate cables feature a proprietary triple shield-

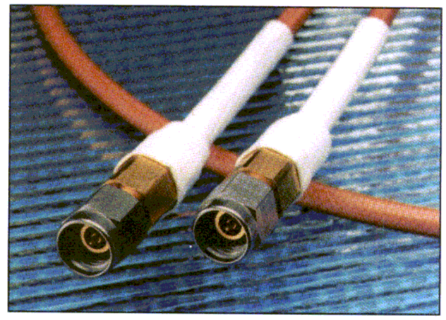

ing system, and several designs offer interchangeable connector heads. Testmate cable assemblies have low attenuation, long term electrical stability and are ruggedized for daily dependability in a wide range of applications including site/field testing, test labs, production line testing, quality/maintenance testing and fixed RF system interconnects.

Times Microwave Systems
Circle #180

PASSIVE COMPONENTS

Ceramic chip trimmers

Johanson Manufacturing introduces the 9344 series ceramic chip trimmer capacitors, economical single-turn, ceramic dielectric capacitors designed for high volume commercial applications. These surface mount trimmers are extremely small in size, and their con-

struction allows them to be used in applications where reflow soldering is part of the manufacturing procedure. The series is available in 5 capacitance ranges from 1.7 to 3.0 pF to 5.5 to 30 pF. They have a

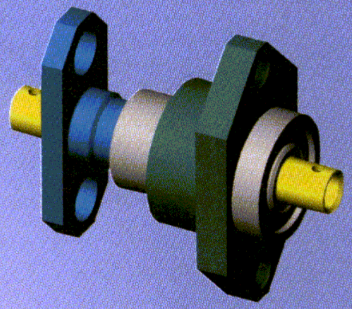

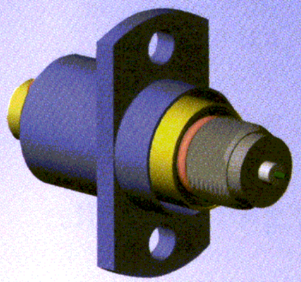

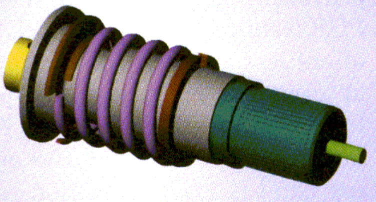

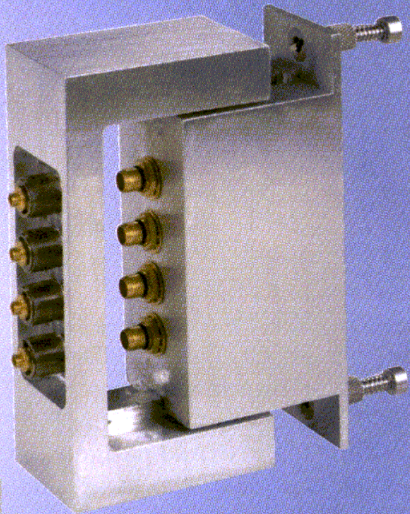

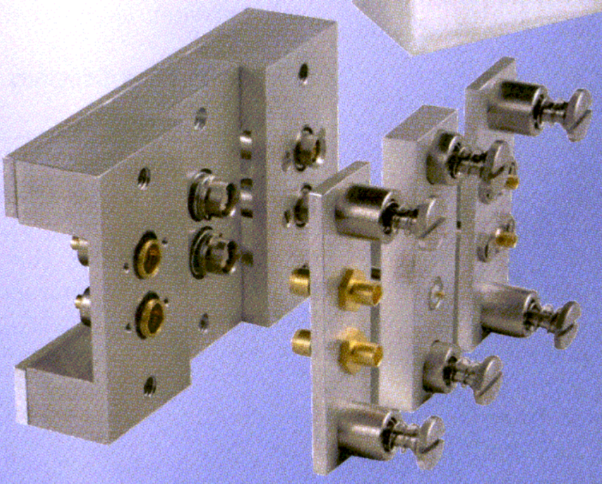

working voltage of 100 VDC and an operating temperature range of -25° C to +85° C. The capacitors are packaged 1,000 pieces on a 7 inch reel. They are priced at $0.24 each at 5,000 pieces.
Johanson Manufacturing
Circle #181

SOFTWARE

Design software update

Applied Wave Research has announced the initial shipments of Microwave Office™ 2001. Improvements in Microwave Office 2001 include new COM-based Design Automation Interface, a new harmonic balance simulator, new layout editing features and design rule checking and new nonlinear and linear models.

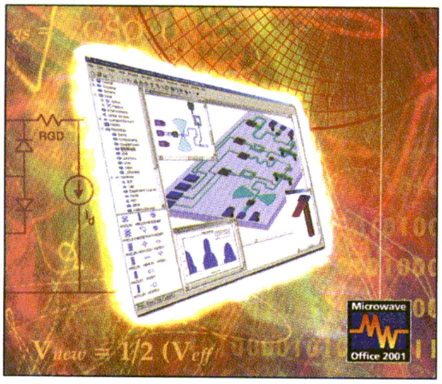

Applied Wave Research
Circle #182

EM simulation

Ansoft Corporation has introduced version 8.0 of its High Frequency Structure Simulator (Ansoft HFSS), a full-wave finite element electromagnetic simulator that enables engineers to design three-dimensional high-frequency structures such as connectors, IC packages and antennas found in cellular telephones, broadband systems and microwave circuits. Additional features of Ansoft HFSS V.8 include common and differential modes, modes-to-nodes, fast sweep, lumped RLCs, macro editor, macro interface and wizards.
Ansoft Corporation
Circle #183

3D EM package

CST of America announces the release of CST Microwave Studio™ version 3.0 – a specialized tool for the solution of 3D EM high frequency problems. Among the 480 new features are: SAR calculation and human data set interface, adaptive mesh refinement, extended dynamic SPICE extraction, surface impedance for metallic losses, parallelisation of solvers for multiprocessor systems, plane waves and RCS calculation.
CST of America
Circle #184

SIGNAL PROCESSING

ENG band filter

Microwave Filter Company introduces a highly selective bandpass filter that passes the full ENG band (1993 to 2107 MHz), while providing suppression of the close PCS frequencies. The model 13969 offers less than 1 dB insertion loss at center frequency and typically less than 2 dB at band edges. Maximum VSWR over the operating band is 1.5:1. Rejection is typically greater than 10 dB at 1988 MHz.
Microwave Filter Company
Circle #185

SMT band pass filters

RLC Electronics's new surface mount filters offer the same frequency response characteristics as RLC's existing MBP micro miniature filters. Units capable of withstanding automated soldering temperatures can also be supplied, if required.

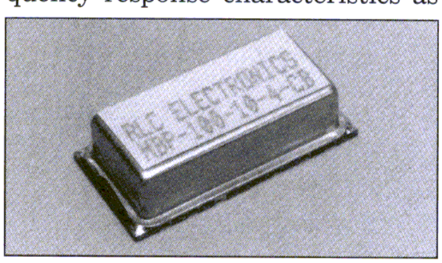

RLC Electronics, Inc.
Circle #186

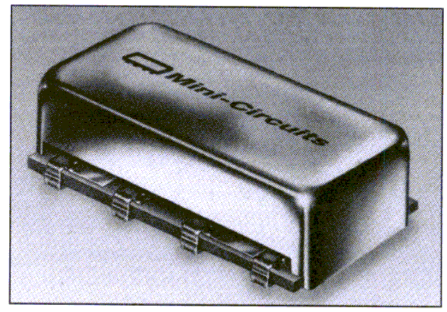

4 way splitter/combiner for CATV frequencies

Mini-Circuits now offers a new JS4PS-9-75 for designers requiring a 4 way 0 degree power splitter or combiner for 75 ohm systems operating in the 50 to 860 MHz band. Equipped with solder plated J leads for solderability and strain relief, this surface mount unit exhibits typically high 25 dB isolation, input matching and output matching with VSWR typically 1.20:1 in/1.3:1 out. Amplitude unbalance is at 0.15 dB typical. Maximum power input is .50 W. The unit is priced at $20.95 each in quantities of 1-9.
Mini-Circuits
Circle #187

Transfer switch

Dow-Key Microwave's newest product, an Ultra-High Power Transfer Switch, extends high power RF coaxial switching. Specifications include a frequency range of DC –2 GHz; maximum VSWR of 1.25:1; maximum insertion loss of 0.25 dB; minumum isolation of 65 dB; and power handling at 4 KW.C.W. up to 1 GHz and 2 KW C.W up to 2 GHz.

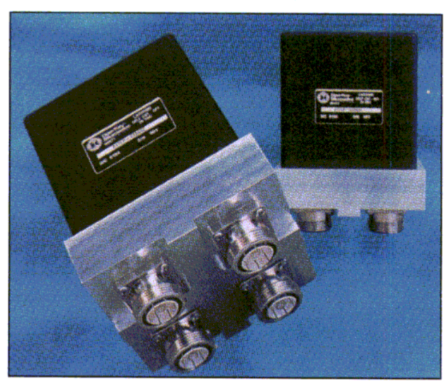

Dow-Key Microwave
Circle #188

NEW PRODUCTS NO. 80

RF/IF MICROWAVE COMPONENTS

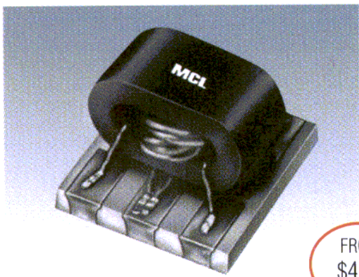

FROM $4.95

2 TO 1100MHz RF TRANSFORMER FOR IMPEDANCE MATCHING

Designed for impedance matching applications, Mini-Circuits low cost TC4-11 RF transformer provides 4:1 impedance ratio (50 ohms primary, 12.5 ohms secondary) in the broad 2 to 1100MHz band. Referenced to midband loss, users can expect 1dB insertion loss in the 5 to 700MHz range and 2dB loss bandwide. This leadless surface mount transformer is housed in an open style aqueous washable package with ceramic base. Absolute maximum RF input power is 0.25W.

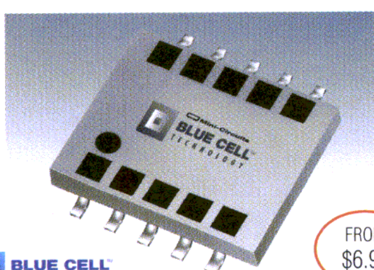

BLUE CELL TECHNOLOGY

FROM $6.95

1900 TO 2400MHz 90° HYBRID IS ULTRA-THIN 0.050" SOLUTION

Mini-Circuits 1900 to 2400MHz broadband QBA-24 is a 2way-90° power splitter developed with high 21dB typical isolation and low 0.54dB insertion loss (typ, avg. of coupled outputs less 3dB). As a splitter, these patented Blue Cell™ hybrid's are capable of handling 20W (max.) power input and are housed in a low profile 0.050" ceramic package with solder plated leads for good heat dissipation and excellent solderability. Available off-the-shelf.

FEATURED PRODUCT

FROM 99¢

DC TO 8GHz MMIC AMPLIFIER HAS HIGH RELIABILITY

The GAL-21 is a newly developed monolithic surface mount amplifier from Mini-Circuits for the broad DC to 8GHz band. When operated at 2GHz/25°C, the unit typically delivers high 13.1dB gain (±0.6dB flat) and maximum output power of 12.6dBm typical (at 1dB comp.). These low cost 50 ohm amplifiers are housed in an industry standard SOT-89 package for excellent heat dissipation and display low 128°C/W (typ, θjc) thermal resistance. Available from stock.

1500 TO 3600MHz SM MIXER SUPPRESSES INTERMODULATION

This level 17 (LO) SYM-36H surface mount frequency mixer from Mini-Circuits targets PCS and ISM applications within 1500 to 3600MHz. Typically at center band, the mixer exhibits high 25dBm IP3 and low 6.3dB conversion loss. Bandwide, L-R isolation is 30dB, and L-I isolation is 34dB typical. Ruggedly constructed in a low cost plastic package with solder plated leads and covered by a 5 year Ultra-Rel® reliability guarantee.

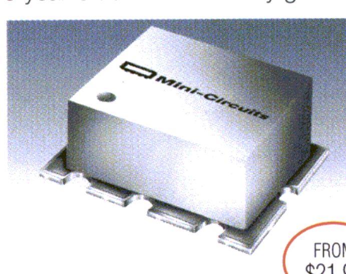

FROM $21.95

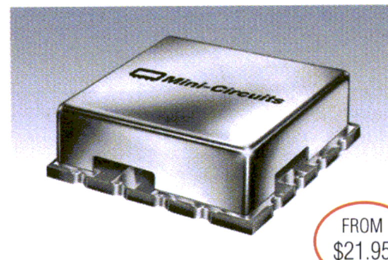

FROM $21.95

1350 TO 2000MHz VCO WORKS FROM 12V SUPPLY

Mini-Circuits new ROS-2000 voltage controlled oscillator features 1350MHz to 2000MHz broad band linear tuning from a miniature 0.5"x0.5"x0.18" industry standard surface mount package. The VCO delivers low -100dBc/Hz SSB phase noise typical at 10kHz offset, good 30-50MHz/V typical tuning sensitivity, and 0.5 to 20V minimum to maximum tuning voltage. Typical power output is +7dBm with output suitable for LO drive to mixers. Affordably priced.

FROM $5.95

13dB "DO-IT-YOURSELF" COUPLER DELIVERS COST SAVINGS

The patented TCD-13-4 from Mini-Circuits needs only a commercially available 50 ohm external chip resistor, and a complete 5 to 1000MHz directional coupler is realized. Designed to lower costs through automated manufacturing, this rugged coupler provides 13.0dB±0.5dB nominal coupling (±0.6dB max. flatness) with 0.7dB mainline loss and 18dB directivity typical midband. The 50/75 ohm "do-it-yourself" TCD family contains 9 units with 9 to 20dB coupling for 5 to 1000MHz.

Mini-Circuits®

US 104 INT'L 114 CIRCLE READER SERVICE CARD

P.O. Box 350166, Brooklyn, New York 11235-0003 (718) 934-4500 Fax (718) 332-4661 For quick access to product information see MINI-CIRCUITS CATALOG & WEB SITE

YONI™ **The Design Engineers Search Engine** *Provides ACTUAL Data Instantly From MINI-CIRCUITS At:* **www.minicircuits.com**

ISO 9001 CERTIFIED

F 347 Rev. Org.

STRENGTH

REPUTATION

Wideband Gain Block Amplifier Design Techniques

Here is a thorough review of the device design requirements for a general-purpose amplifier RFIC

By Chris Arnott
RF Micro Devices

Wideband highly linear gain block amplifiers are becoming a popular, cost-effective alternative to the discrete designs presently used in many systems. These wideband gain blocks offer highly repeatable linear fixed gains with internally matched impedances and minimal external component count, which reduces manufacturing costs.

Replacing existing discrete designs with gain block amplifiers further reduces manufacturing costs by decreasing tuning time during manufacture, as well as reducing initial system design time. System designs can be simplified and completed faster. This reduction in time-to-market can remove costs from product development (and increase profit margins), simply by using gain block amplifiers.

The RF3348 is the first product in RF Micro Devices' RF3340 gain block amplifier series. This series offers low cost gain blocks with performance that exceeds that of previously available units. The RF3348 amplifier is designed to replace more expensive and less reliable discrete amplifiers and permit better distortion performance for a given DC power consumption. This article addresses the methods used to design and manufacture the RF3348 wideband linear amplifier. The amplifier is realized with a simple Darlington amplifier topology. Techniques used in the design of the amplifier include minimization of small signal nonlinear effects while achieving maximum linear amplification, gain flatness and input/output return loss.

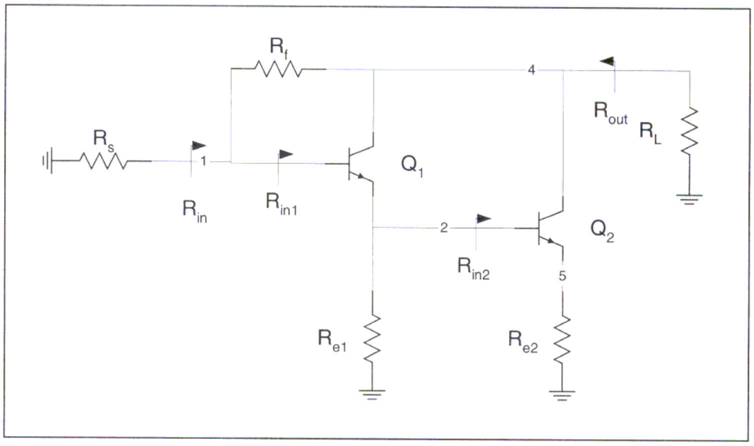

▲ **Figure 1. Simplified Darlington amplifier circuit used for analysis of circuit behavior.**

Amplifier nonlinear design issues

Four distinct distortion-causing mechanisms in realistic amplifiers contribute to signal degradation, voltage compliance and nonlinear device parameters. The device parameters are nonlinear transconductance, nonlinear base-collector capacitance and nonlinear output resistance. These sources of distortion must be addressed with either design techniques or appropriate use of integrated device technology.

- *Voltage compliance.* Power supply level and circuit bias points within the amplifier must be sufficient to allow linear voltage swings for maximum input power drive levels. Overdriving the amplifier to levels exceeding bias conditions will cause voltage clipping in the output signal. Voltage clipping is the result of transistors being driven to "turn-off" during maximum power input signals. The

Johanson high frequency multilayer ceramic capacitors

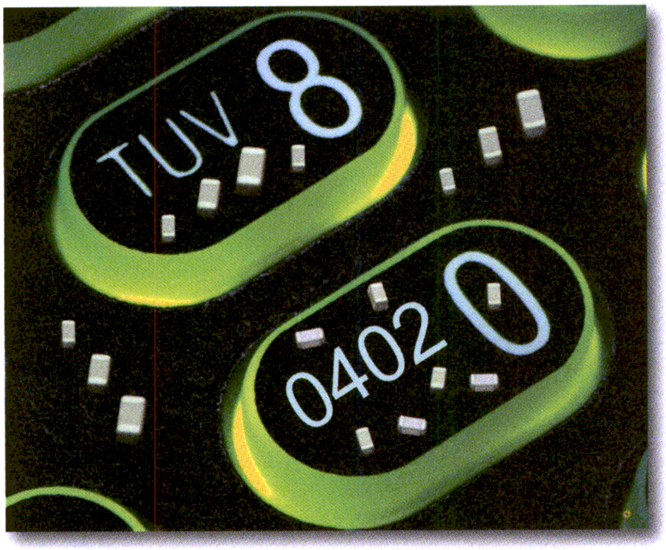

Proven Performance!

Prove it to yourself! Just surf over to our web site at www.johansontechnology.com and download your free copy of MLCSoft®, an industry leading RF modeling and evaluation software. Using MLCSoft® you'll be able to chart critical performance parameters such as Quality Factor, Equivalent Series Resistance and S-parameters for Johansons entire range of high frequency multilayer ceramic chip capacitors from 1MHz through 20 GHz. After you've found the high frequency capacitor that's right for your design, order an engineering kit for in-circuit evaluation.

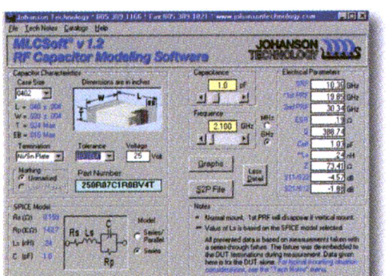

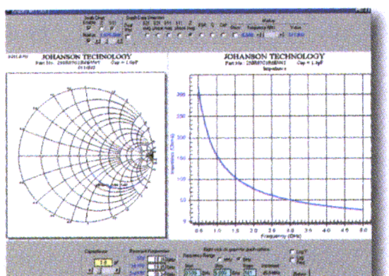

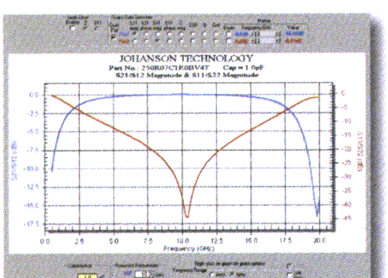

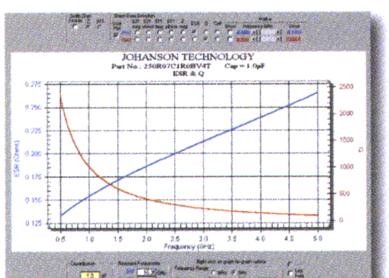

JOHANSON TECHNOLOGY

www.johansontechnology.com

Camarillo, California TEL (805) 389 1166 FAX (805) 389 1821

Circle 58

power supply level must be selected to provide adequate bias and voltage headroom for maximum output power levels. Typically, an RF choke provides amplifier bias by directly connecting the output to the DC level of the power supply. This bias configuration allows the output signal to swing around the average DC level of the power supply. Large negative output swings act as a decreasing power supply and tend to turn the amplifier off, which causes voltage clipping.

- *Nonlinear transconductance.* The exponential I-V characteristics of BJT devices inherently exhibit nonlinear operation when operated in an open loop state. Using emitter degeneration and shunt feedback with adequate bias current can permit the amplifier to obtain very good linear operation.
- *Nonlinear amplifier input/output impedance.* Nonlinear variations in amplifier input/output impedance produce distortion in the output signal. The open loop output impedance of the amplifier is ideally large and constant, but in reality a dependence on bias current and device physical parameters exists. This dependency causes nonlinear loading of the output, which distorts the output signal. In addition, parasitic base-to-collector capacitance exhibits nonlinear characteristics, which distorts the output signal. RF Micro Devices' GaAs HBT technology exhibits excellent input/output impedance due to very high output impedance and almost constant base-to-collector capacitance versus input voltage.
- *Minimizing nonlinear effects by design.* The RF3348 was implemented with a single-ended Darlington feedback amplifier configuration with an emitter degeneration resistor, as shown in Figure 1. The main advantages of the Darlington topology are high, nearly constant gain versus frequency response and good input/output return loss. Feedback resistors R_s, R_e and R_F are used to determine closed loop gain while fixing the input and output impedance to 50 ohms. A properly biased Darlington amplifier circuit minimizes nonlinear device effects with negative feedback.

Small signal amplifier design

Classical feedback amplifier methods of loop transmission analysis [1] are used to analyze the resistor shown in Figure 1. The loop transmission of the amplifier is found by breaking the feedback loop at the base of Q_1 in Figure 1, applying a test disturbance signal to the base and monitoring the return signal. The loop transmission is the ratio of return signal to test signal. The approximate mid-band loop transmission of the amplifier, using Figure 1, is given by

$$T_{mid} \approx -\left(\frac{R_1 \| R_{in_2}}{R_1 \| R_{in_2} + r_{e_1}}\right)\left(\frac{R_L \| r_o \| R_{F2}}{R_e + r_{e_2}}\right)\left(\frac{R_{in_1}}{R_{in_1} + R_f}\right) \quad (1)$$

where R_L is the load resistance, r_o is the open loop output impedance; r_{e1} is the dynamic emitter resistance of Q_1; r_{e2} is the dynamic emitter resistance of Q_2; and R_{in1} and R_{in2} are the impedance looking into the bases of Q_1 and Q_2. The ideal closed loop gain is the ratio of the feedback resistor and source impedance as given by

$$A_{CL_{ideal}} = \frac{-R_F}{R_S} \quad (2)$$

The actual amplifier closed loop gain at mid-band frequencies is given by

$$A_{CL} = A_{CL_{ideal}} \times \frac{-T_{mid}}{1 - T_{mid}} \quad (3)$$

where T_{mid} is the mid-band loop transmission or loop gain of the amplifier.

The characteristics of Equation (3) show the tendency of negative feedback to force the closed loop gain to approach its ideal value for large values of loop gain. This forcing effect can resist amplifier non-linear output fluctuations if $T_{mid} >> 1$ and amplifier operation within voltage compliance. In multiple GHz-wide bandwidth amplifiers, large loop gains are not possible because of possible instabilities. Wideband gain block amplifier designs achieve small signal linearity performance by combining both minimization of device nonlinear effects and negative feedback correction.

Amplifier input/output impedance at mid-band frequencies is mainly determined by amplifier parameters R_f, R_{e2} and R_s. Assuming amplifier input and output loading effects are negligible, R_{INOL} is approximately equal to R_{OUTOL}. The approximately equal value of R_{IN} and R_{OUTOL} is $R_f + R_s$. Using Blackman's theorem, the input impedance of the amplifier at mid-band frequencies is given by

$$R_{IN} = R_{IN_{OL}} \times \frac{1}{1 + |T_{mid}|} \quad (4)$$

The mid-band output impedance is given by

$$R_{OUT} = R_{OUT_{OL}} \times \frac{1}{1 + |T_{mid}|} \quad (5)$$

Negative feedback reduces open loop input/output impedance, as seen in Equations (3) and (4). The same forcing effect that forces the gain of the amplifier to approach its ideal value causes this reduction in amplifier open-loop input/output impedance. This effect is accomplished through voltage sampling at the output and information processing by current summation at the input. Negative feedback thus tends to idealize the input impedance presented to the input current signal while making the amplifier's output appear as an ideal

voltage source. The transformation of the amplifier's input and output into an idealized impedance and voltage source fixes the input/output impedance and minimizes effects of Beta variation, reactive loading and other non-linear variations for frequencies approaching the amplifier's 3-dB bandwidth. In contrast, low bandwidth op-amp type circuits with very high loop gain lower the input/output impedances to very small values and approach the ideal gain with high accuracy. Wideband circuits use these feedback principles to achieve desired gain and input/output return loss by adjusting the loop gain while maintaining stability against oscillations, near constant gain, and input/output return loss with process parameter variation. This loop gain adjustment is analogous to adding input and output ideal series resistance to an amplifier with very high loop gain. Therefore, wideband gain blocks can be realized with highly precise input/output impedance matching.

$$T(f) \approx -\frac{|T_{mid}|\left(1+\frac{j\times f\times \tau_{z_1}}{2\times\pi}\right)\left(1+\frac{j\times f\times \tau_{z_2}}{2\times\pi}\right)}{\left(1+\frac{j\times f}{2\times\pi\times f_{t_1}}\right)\left(1+\frac{j\times f}{2\times\pi\times f_{t_2}}\right)\left(1+\frac{j\times f\times \tau_{in}}{2\times\pi}\right)\left(1+\frac{j\times f\times \tau_{out}}{2\times\pi}\right)}$$

▲ **Equation (9).**

Three non-linear, small signal terms, r_{e1}, r_{e2} and r_o, are present in the loop gain Equation (1). These nonlinear terms cause output nonlinearity when the amplifier is operating with small input signals. Sensitivity analysis assuming small signal operation shows the effects of these nonlinear terms on loop gain [2]. Sensitivity of the loop transmission with respect to r_{e1} is given by

$$S_{r_{e_1}}^{T_{mid}} \approx \left(\frac{r_{e_1}}{R_{e_1}\|R_{in_2}+r_{e_1}}\right)\left(\frac{R_{e_2}+r_{e_2}}{R_L\|r_o\|R_f}\right)\left(\frac{R_{in_1}+R_f}{R_{in_1}}\right) \quad (6)$$

with respect to r_{e2} by

$$S_{r_{e_2}}^{T_{mid}} \approx \left(\frac{r_{e_2}}{R_{e_2}+r_{e_2}}\right)\left(\frac{R_{e_1}\|R_{in_1}+r_{e_1}}{R_{e_1}\|R_{in_1}}\right)\left(\frac{R_{in_1}+R_f}{R_{in_1}}\right) \quad (7)$$

and with respect to r_o by

$$S_{r_o}^{T_{mid}} \approx \left(\frac{r_o}{R_L\|R_f+r_o}\right)\left(\frac{R_{e_1}\|R_{in_1}+r_{e_1}}{R_{e_1}\|R_{in_1}}\right)\left(\frac{R_{in_1}+R_f}{R_{in_1}}\right)\left(R_{e_2}+r_{e_2}\right) \quad (8)$$

Equation (6) suggests the sensitivity of the loop transmission, with respect to r_{e1}, can be minimized if $R_{e1} \,||\, R_{in2} >> r_{e1}$. Since R_{e1} biases transistors Q_1 and Q_2, its value should be large compared to r_{e1}. Equation (7) suggests the sensitivity of the loop transmission, with respect to r_{e2}, can be very small if $R_{e2} >> r_{e2}$. Small r_{e2} is usually the case because large bias current is required in Q_2 to deliver maximum output power. Since R_{e2} approximately determines amplifier open loop gain and greatly effects noise figure, it should be made as small as possible. These criteria on R_{e2} suggest reducing r_{e2} with large bias current in the output-driving transistor Q_2 to improve the linear performance. Loop gain sensitivity, with respect to r_o, shows linearity is improved if $R_L \,||\, R_f << r_o$, as shown in Equation (8). This is the case with very high output impedance RF Micro Devices GaAs HBT devices. Therefore, maximizing R_{e1} and increasing Q_2 bias current with the use of RF Micro Devices' GaAs HBT devices in wideband Darlington topology amplifiers will optimize small signal linear performance.

Small signal amplifier frequency response

An approximate expression for frequency response of the loop gain can be found using the time constant method [2]. Once the frequency-dependent expression for loop gain is found, the closed loop amplifier response is simply obtained by substitution for T_{mid} in Equation (3). The time constant method consists of calculating the time constants at each node within the amplifier, including the frequency limitations of the active devices, f_T. These time constants represent poles and zeros in loop gain frequency response. Transistor unity current gain frequencies are included in the analysis as poles and combine with the time constants for the approximate frequency-dependant loop gain expression is given by Equation (9) above, where f_{T1} and f_{T2} are poles associated with devices Q_1 and Q_2, t_{in} and t_{out} are time constants associated with the amplifier's input/output, and f_{z1} and f_{z2} are locations of parasitic zeros. The remaining poles associated with nodes 2 and 5 can be neglected because the impedance at these nodes is very small and resulting poles are located at frequencies beyond the loop gain unity gain frequency.

The zero described by f_{z1} in Equation (8) is due to the parallel connection between the feedback resistor R_f and parasitic base to collector capacitance of transistor Q_1. Zero and f_{z2} in Equation (8) result from parasitic series inductance and degeneration resistor R_{e2}. Dominant poles in the frequency response are due to both input and output time constants, which are at a much lower frequency compared to the unity current gain frequencies of the transistors. Large parasitic shunt capacitance increases these input/output time constants. Also, these dominant poles have approximately equal frequency locations since the circuit has equal source/load imped-


The Evolution of Broadband
DRWiN™
Dynamically Reconfigurable Wireless Networks
Does Your Antenna Adapt to a Changing Environment?
It does now. Paratek Microwave, Inc. introduces DRWiN™ (Dynamically Reconfigurable Wireless Networks) antennas that adapt to provide flexible and scalable solutions in an ever-changing communications landscape. Paratek's debut DRWiN™ product is the first low-cost passive phased array antenna. This DRWiN™ antenna electronically scans in one dimension, providing rapid beam hopping to a high frequency broadband wireless network subscriber base.
DRWiN™ Antennas Enable Broadband Flexibility and Scalability
▪ Increased capacity
▪ Increased data rates
▪ Software reconfigurable networks
▪ Interference discrimination
Paratek's DRWiN™ antennas are the natural selection in the evolution of broadband.
PARATEK
Email inquiries to drwin@paratek.com
1-866-PARATEK ▪ 443-259-0140
www.paratek.com
Paratek Microwave, Inc. – The Tunable Wireless Company
Circle 84

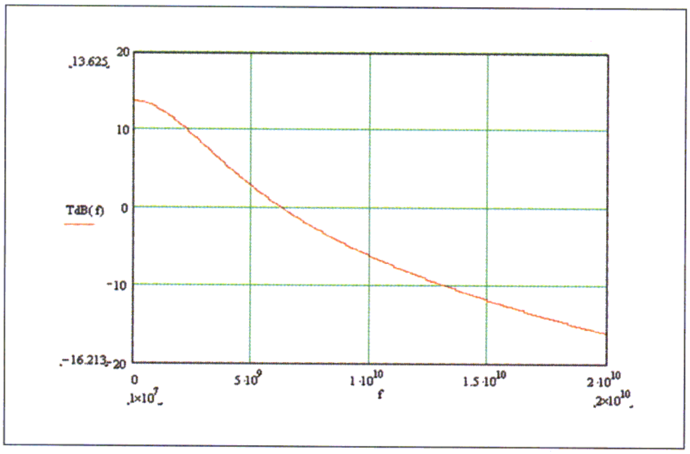

▲ **Figure 2(a). Darlington amplifier loop gain plot.**

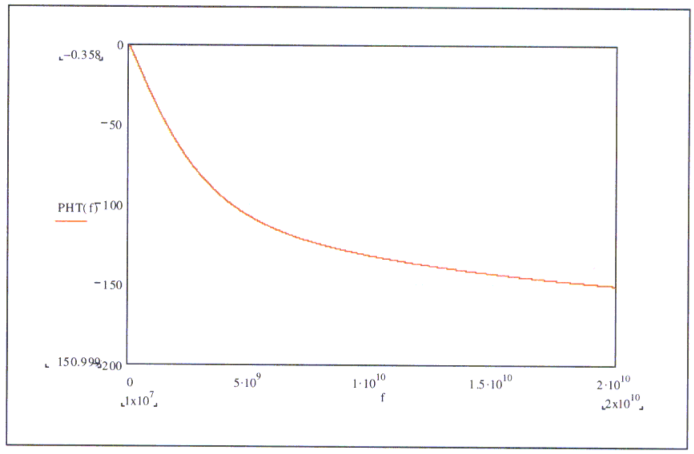

▲ **Figure 2(b). Darlington amplifier loop gain phase plot.**

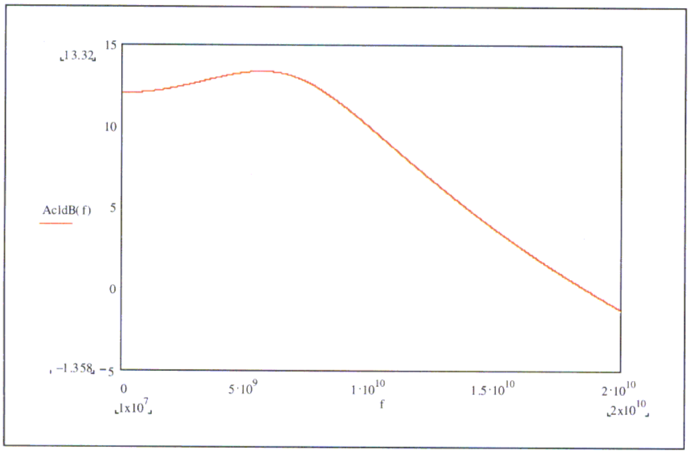

▲ **Figure 3. Darlington amplifier closed loop gain dB magnitude plot.**

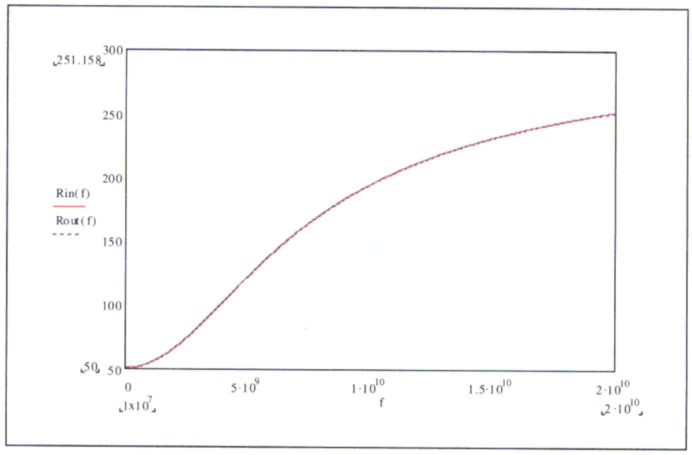

▲ **Figure 4. Plot of the Darlington amplifier input/output impedance vs. frequency.**

ance and approximately equal parasitic shunt capacitance. Therefore, the loop gain expression has a dominant double pole, which causes excessive phase shift and results in low amplifier phase margin. The zeros at f_{z1} and f_{z2} tend to neutralize the poles at f_{T1} and f_{T2} by decreasing loop gain phase shift. Stability against oscillations is secured because the low mid-band loop gain value will reach its unity gain frequency before loop gain phase shift reaches 180 degrees, as shown in Figures 2(a) and 2(b). This results in a stable design that exhibits the gain peaking frequency response as shown in Figure 3.

The amplifier-closed loop gain frequency response exhibits a very flat response with 2 dB peaking and a 3 dB bandwidth of 9.8 GHz. Equation (2) correctly predicts the gain roll off seen in Figure 3 and shows that this decrease in closed loop gain approaches zero as T approaches zero. Adding series resistance to the base of Q_1 further reduces loop gain phase shift. The value of this series resistance is found through circuit simulations. This simple solution improves phase margin and reduces frequency peaking by effectively adding a low pass filter to the amplifier's frequency response.

The maximum stable bandwidth of the amplifier is limited by the unity current gain frequencies of devices Q_1 and Q_2. These device-induced poles in Equation (9) are essentially fixed depending on bias conditions. Attempts to improve bandwidth by decreasing input/output time constants will produce amplifier instabilities when the dominant double pole frequency approaches f_{T1} and f_{T2}. Bandwidth can be slightly improved with careful choice of package type and PCB layout, but care must be taken in order to maintain amplifier stability. RF Micro Devices' GaAs HBT technology possesses an f_T approaching 30 GHz, which is sufficient for this design.

The frequency response of the input impedance is found by substituting Equation (9) into Equation (3) and Equation (4) for the output impedance. The input/output impedance is set to 50 ohms by the loop gain (very precisely for low frequencies), but increases with decreasing loop gain, as shown in Figure 4. This

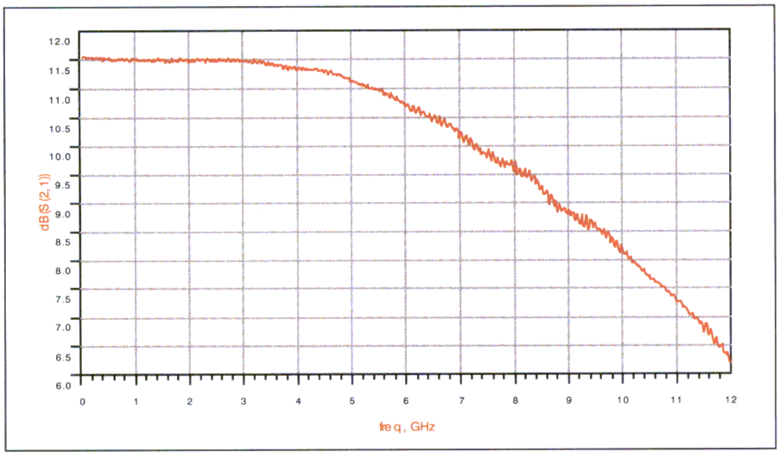

▲ **Figure 5. Measured amplifier gain, S_{21}.**

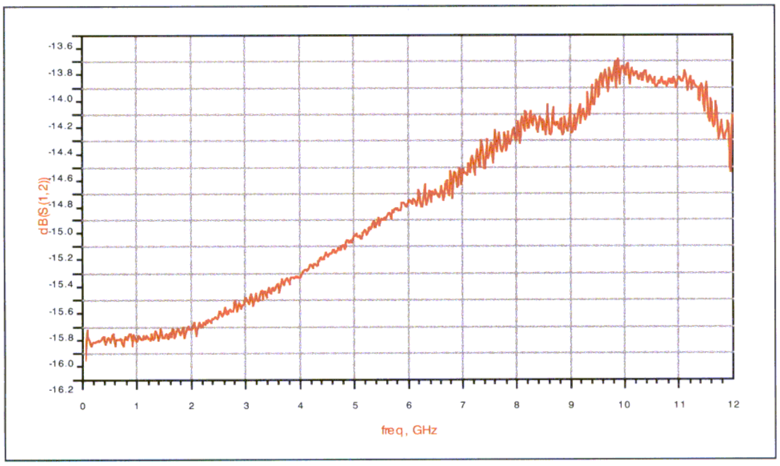

▲ **Figure 6. Measured amplifier reverse gain, S_{12}.**

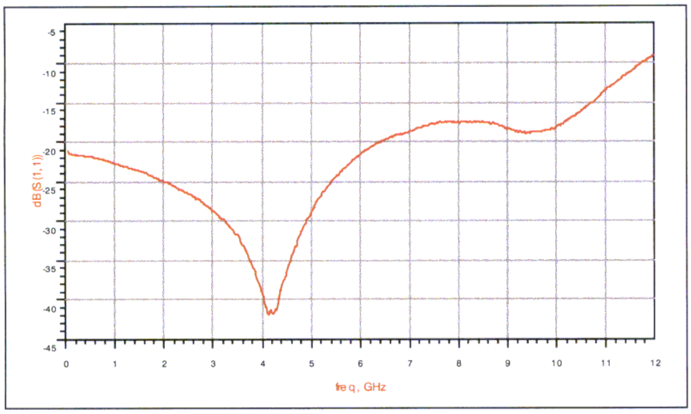

▲ **Figure 7. Measured input reflection coefficient, S_{11}.**

shows how effectively negative feedback fixes the input/output impedance for frequencies within the 3 dB bandwidth of the loop gain. Equations (3) and (4) show that this increase in impedance is expected because R_{in}/R_{out} approaches R_{INOL}/R_{OUTOL} as T approaches zero with increasing frequency, as shown in Figure 2. Amplifier input/output impedance is more sensitive to changes in loop gain compared to closed loop gain due to the inversely proportional loop gain relationship. The closed loop gain of the amplifier is less sensitive because the loop gain correction factor in Equation (2) tends to ratio to unity.

Large signal amplifier considerations

The Darlington amplifier operates in a Class A state. This operating state simplifies amplifier design since constant power is dissipated regardless of input power level. Usually these gain blocks are operated under small signal conditions achieving highly linear amplification. This small signal operation places more importance on output third order linearity instead of maximum output power. Designing the amplifier for output third order linearity allows the assumption of amplifier operation at maximum output levels 10 dB less than the 1 dB compression point. If we assume that the output third order intercept point is 10 dB higher than the 1 dB compression point, then determination of maximum amplifier output power is achieved. We also assume that the maximum deliverable output power from the amplifier is equal to maximum output power of transistor Q_2. Therefore, the bias current in Q_2 must be set at a sufficient level to deliver maximum required output power.

This current can be easily calculated from the specified output 1 dB compression power into the source impedance. This calculated current is the ideal minimum bias current that will deliver maximum specified output power. The final Q_2 bias current will be slightly larger than the calculated value and is easily found with nonlinear circuit simulations. Transistor Q_1 must be biased with sufficient current to drive the base current of Q_2 and voltage swing on R_1. This current is small compared to the current in Q_2, but must be large enough to drive the frequency dependant base current of Q_2 for the amplifier's bandwidth. The final value of the bias current for Q_1 is easily found with nonlinear circuit simulations of output 1 dB compression point versus frequency.

The voltage compliance of the amplifier is evaluated to ensure sufficient voltage head room within the amplifier and eliminate distortion caused by voltage clipping. This can be challenging considering the trend toward decreasing supply voltages. This problem is made worse because the amplifier drives output power directly into system impedance, which causes large output voltage swings that limit the maximum deliverable amplifier output power. Connecting the collectors of Q_1 and Q_2 to the output allows large negative output voltage swings

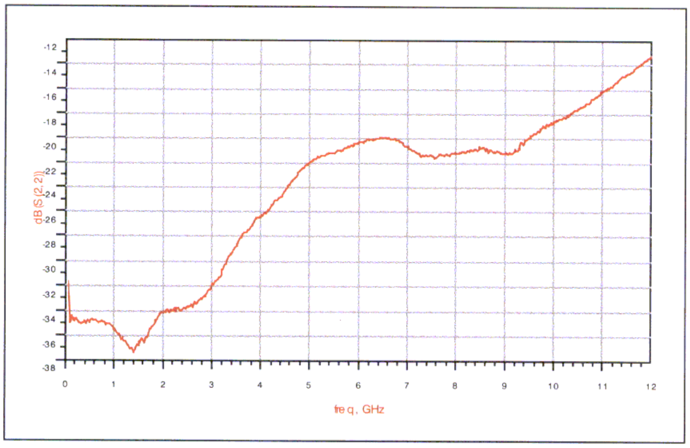

▲ **Figure 8. Measured output reflection coefficient, S_{22}.**

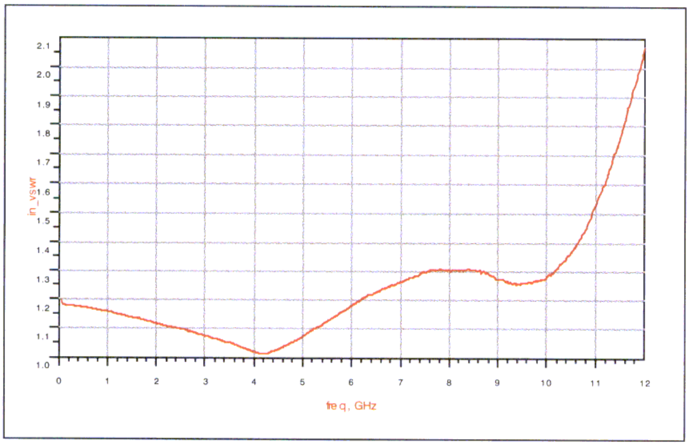

▲ **Figure 9. Measured input VSWR.**

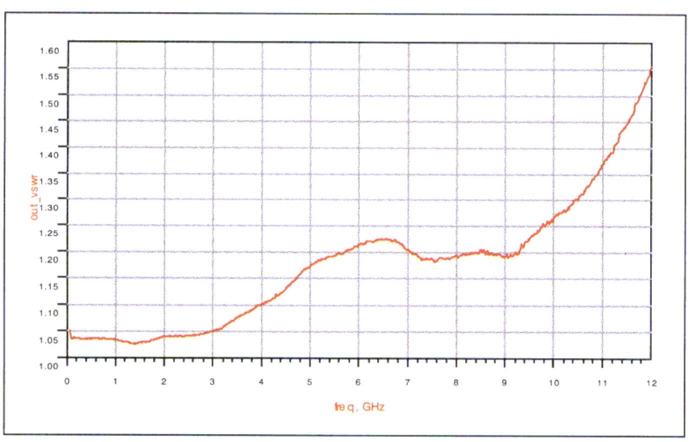

▲ **Figure 10. Measured output VSWR.**

to decrease the collector voltage of Q_2 below its saturation point, which causes severe distortion. Increasing the power supply voltage or decreasing the bias voltage of Q_1 can improve this distortion mechanism. Performing time domain simulations of the circuit and observing the collector current of Q_1 versus time with increasing output power easily detects this effect during large negative output swings. When the collector current of Q_1 approaches zero, the base current of Q_2 approaches zero and turns off the amplifier. The design of the amplifier must include evaluation and compensation of this Q_1 saturation effect to ensure amplifier output power drive capability.

The RF3348 was designed using these general guidelines, which provide a means to calculate the initial values of R_{e1}, R_{e2}, R_f and bias currents. The limitations of these small signal approximations are the inabilities to predict large signal and high frequency device effects accurately. Modern analog circuit simulators accurately predict these effects with sophisticated small and large signal models. All final component and bias values were found using the nonlinear analog circuit simulator Advanced Design System by Agilent Technologies.

Measured results

The RF3348 was evaluated by measuring the amplifier's S-parameters, NF, output 1 dB compression point and output third order intercept point. The scattering parameters of the amplifier were measured using high frequency input/output bias tees and test fixture specifically designed for the ceramic Micro-X package as shown in Figures 5 through 13. The use of this test fixture ensures test data will not include degradation due high frequency PCB and passive component limitations. A frequency range of 50 MHz to 12 GHz with 401 points was used for S-parameter measurements with a source power level of –10 dBm. S_{21}, plotted in Figure 5, shows very good amplifier gain flatness, as predicted by Equation (2). The added series resistance with the base of Q_1 has removed the expected gain peaking in the frequency response. The measured 3 dB bandwidth is 9.5 GHz, which agrees very well with analytical 3 dB bandwidth shown in Figure 3. The reverse gain S_{12} is very flat over amplifier bandwidth with typical magnitude values 5 dB less than the forward gain, as shown in Figure 6, which is an indication of amplifier stability against oscillations.

Measured input/output reflection coefficients S_{11} and S_{22} are plotted in Figures 7 and 8. The measured input return loss of the amplifier is better than 18 dB within the 3 dB bandwidth with a maximum of 42 dB around 4.1 GHz, as shown in Figure 7. This maximum is caused by the large input capacitance of Q_1 resonating with stray input inductance. The measured output return loss is better than 20 dB for entire amplifier 3 dB bandwidth and better than 32 dB up 3 GHz, as shown in Figure 8. Input and output VSWR is better than 1.3 and 1.25 over the entire 3 dB bandwidth, as shown in Figures 9 and 10. The output return loss is more consistent with the analytical approximation given by Equation (4). This results from the very high output

Low Power, Low Noise YIG-Based Synthesizers *for Digital Radios*

"Look to the leader in YIG-Technology"

MICRO LAMBDA, INC.

Micro Lambda, Inc. a leader in the development of next-generation YIG devices now offers YIG-Based Frequency Synthesizers covering the 2-12 GHz frequency range. Designed specifically for Digital Radio ODU's and harsh commercial environments, these synthesizers offer excellent integrated phase noise characteristics over carrier offset frequencies from 10 kHz to 10 MHz.

Tunable bandwidths of either 2 GHz or 3 GHz are available as standard products. This results in fewer numbers of synthesized sources required for a variety of Digital Radio frequency plans. Millimeter-Wave frequencies can easily be obtained using frequency multipliers to obtain output frequencies between 24 GHz through 44 GHz.

Applications include QAM and QPSK modulated Digital Radio's and a multitude of general purpose applications.

FEATURES

- 2 - 12 GHz Frequency Coverage
- Excellent Integrated Phase Noise Characteristics
- Compact Size
- 3-Line Serial Interface
- Low Prime Power
- 500 kHz Step Size
- Internal Memory (last frequency programmed - recall)

MLSL-SERIES SYNTHESIZERS

This series of synthesizers utilize an external 1 to 50 MHz crystal reference oscillator to generate tunable frequencies covering the 2 - 12 GHz range. Output power levels of +12 dBm to +15 dBm are offered depending on frequency, with a standard tuning step size of 500 kHz. Input tuning commands are via 3-Line Serial interface. The size of these compact units is 2.5" x 2.5" x 1.0" without mounting plate and consume less than 6 watts of prime power. The units have an internal memory capability which "recalls" the last frequency programmed when the prime power is removed and reapplied. Standard models include 2-4 GHz, 4-6 GHz, 5-7 GHz, 7-9 GHz and 9-11 GHz. Specialized frequency ranges are easily implemented utilizing the versatile synthesizer architecture.

Cards MasterCard VISA

48041 Fremont Blvd. Fremont, CA 94538 (510)770-9221 mcrolambda@aol.com www.micro-lambda.com

Circle 79

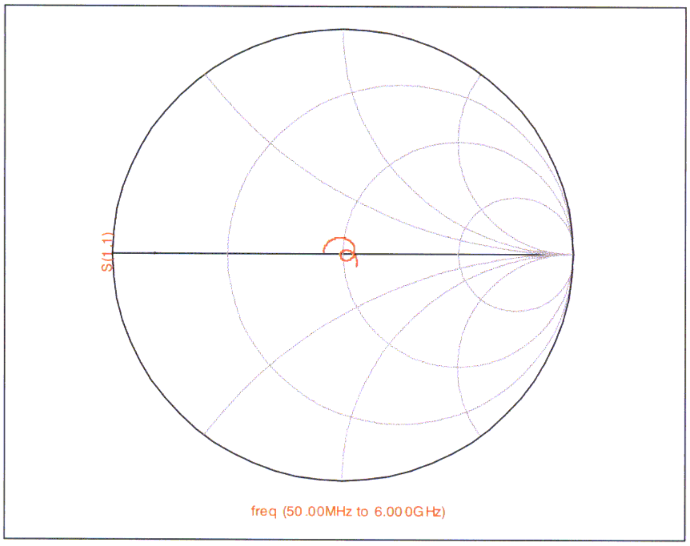

▲ **Figure 11. S_{11} Smith chart plot.**

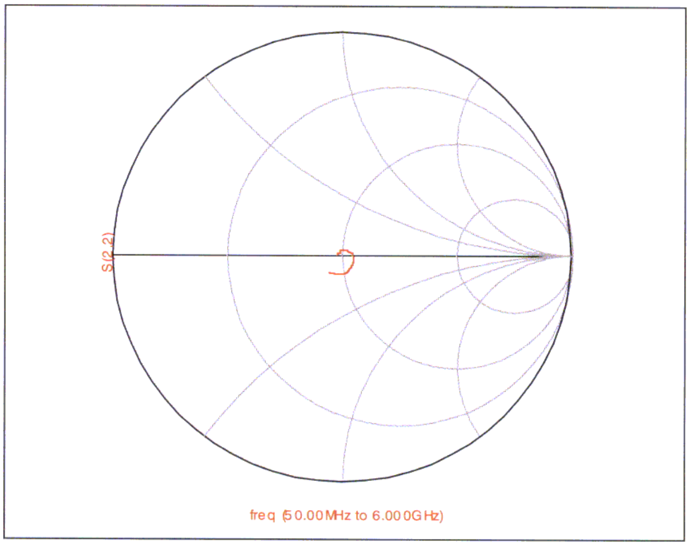

▲ **Figure 12. S_{22} Smith chart plot.**

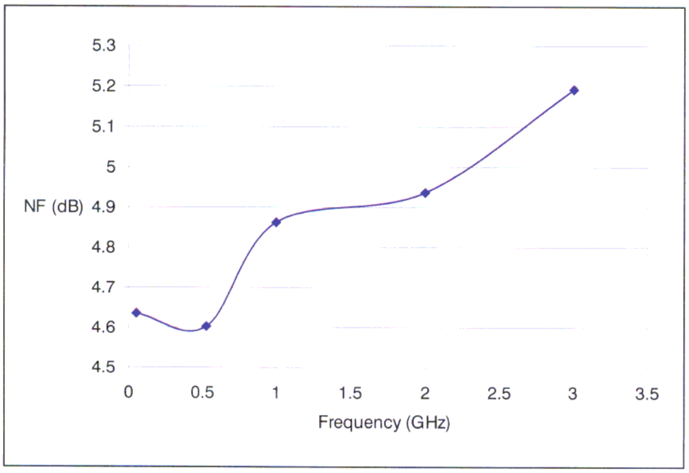

▲ **Figure 13. Measured amplifier noise figure.**

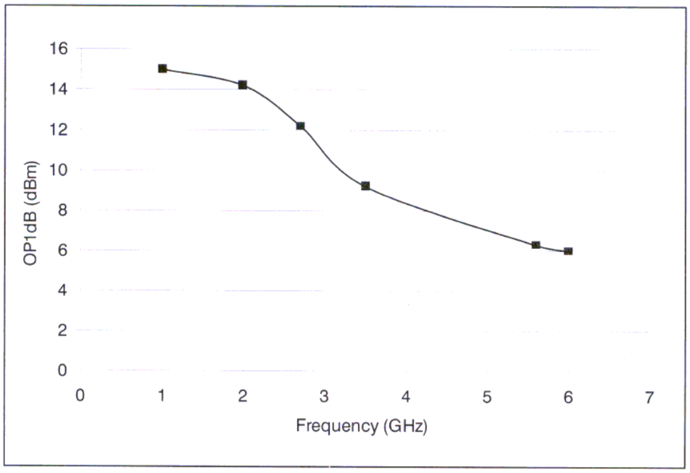

▲ **Figure 14. Measured amplifier output 1 dB compression point.**

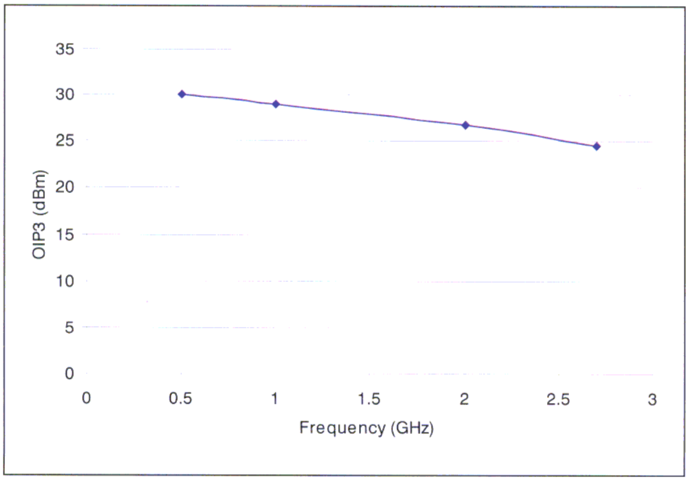

▲ **Figure 15. Measured amplifier output third order intercept point.**

GaAs HBT device output impedance that does not significantly load the closed loop output impedance. This excellent mid-band input/output return loss performance shows how effectively negative feedback can hold the input/output impedance to a near constant value of 50 ohms, as shown in Figures 10 and 11. Only at high frequencies does the input/output return loss begin to decrease with decreasing loop gain, as predicted by Equations (3) and (4). Amplifier noise figure was measured at 1 GHz to 3 GHz, as shown in Figure 12. Noise figure results show the 1 GHz noise figure is 4.7 dB and increases 0.3 dB to 5 dB at 3 GHz, which is consistent with beta roll off of input transistor Q_1.

Amplifier large signal parameters output 1 dB compression point was measured at frequencies 1 GHz to 6 GHz, as shown in Figure 15. Results show the output 1 dB compression point is 15 dBm at 1 GHz and 9 dBm at

6 GHz with a 2 dB decrease from 1 GHz to 2.7 GHz. These results show the effects of Q_2 beta and loop gain roll off for frequencies greater than 3 GHz. The output compression point remains nearly constant up to 3 GHz then rolls off due to decreasing loop gain. The output third order intercept point was measured using the two-tone method [3] at 1 GHz, 2 GHz and 3 GHz, as shown in Figure [illegible]. Results show the amplifier output third order intercept point rolls off by 5 dB at 3 GHz.

Conclusion

This article has presented simple analysis and design techniques for wideband Darlington negative feedback amplifier design. A high performance wideband gain block amplifier was successfully realized by utilizing these proposed design techniques. Results show that the simple mid-band approximations used to predict amplifier performance gives very good correlation with high-frequency measurements. This emphasizes how effectively design properties of negative feedback and optimum device technology can realize high performance wideband gain block amplifiers. These realized amplifiers have very good small signal, noise and large signal performance. Results showed that measured amplifier data meets all required specifications. ■

Acknowledgments

The author greatly appreciates the efforts of Bruce Schmukler, Greg Schramm, Jennifier Ameling and Bryan Sykes in reviewing this paper. The author also thanks Fred Overcashier, John Mckee and Brian White for providing product characterization.

References

1. J.F. Pierce, *Applied Electronics*, TechBooks, 1992.

2. C.L. Phillips, *Feedback Control Systems*, Upper Saddle River: Prentice-Hall, 1996.

3. T.S. Laverghetta, *Handbook of Microwave Testing*, Boston: Artech House, 1981.

Author information

Chris Arnott received a BSEE in 1998 and an MSEE in 1999, from the University of Tennessee at Knoxville. His professional interests are analog and RF circuit design using silicon and GaAs IC technologies. He is a design engineer at RF Micro Devices, designing dual band multimode power amplifier modules for cellular handsets. He may be reached via e-mail at carnott@rfmd.com.

Narrow Band Ultra Low VSWR Cable Assemblies

This article decribes techniques for obtaining the highest possible performance over a limited frequency range

By Bruce Bullard and Eric Houghland
Kaman Instrumentation

Occasionally, a customer contacts our company with a request for cables with ultra low VSWR over a narrow bandwidth. This article will discuss methods for achieving the desired VSWR results.

Figure 1 shows a typical VSWR plot for a Kaman Instrumentation SiO_2 cable connected to a 50-ohm load. In this case, the VSWR highs and lows are primarily a result of discontinuities in the connector. Ideally, the connector is designed for 50 ohms. Also, because of variations of the dielectric constant of materials in the connectors, we see impedance variations. It is primarily these discontinuities and imepdance variations which prevent broadband ultra low VSWR.

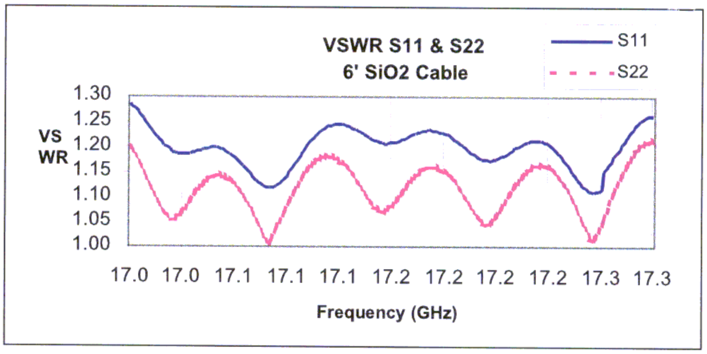

▲ **Figure 1. Typical VSWR for a coax cable.**

A relatively simple model for an SiO_2 coax cable with imperfect glass seals is shown in Figure 2. The characteristic impedance of the cable is easily controlled and is approximately 50 ohms. Each of the glass seals is 52 ohms.

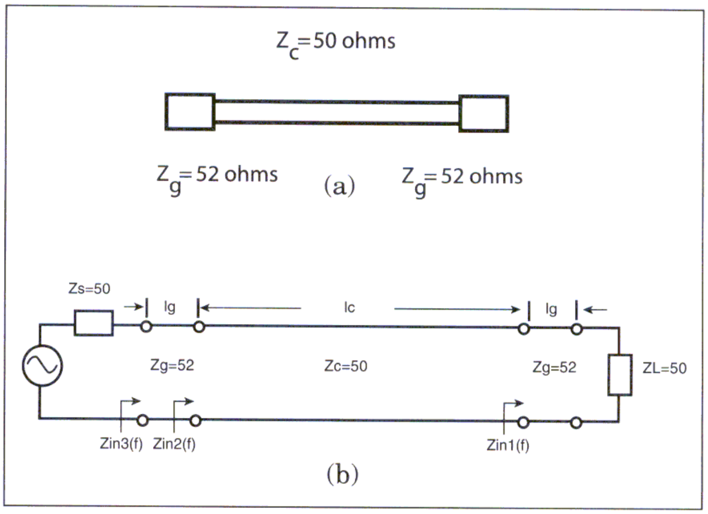

▲ **Figure 2. Simplified coax cable model: (a) phyisical representation; (b) transmission line model.**

The input VSWR to this cable is calculated using transmission line theory (SI units are used in all calculations). In this model, we assume the cable is mated to a perfect source and load impedances of $Z_{S,L}$ = 50 ohms. The following equations (1) describe the cable

l_c = length of cable

$$Zin_1 = Zo_g \frac{Z_L + jZo_g \tan(\beta_g l_g)}{Zo_g + jZ_L \tan(\beta_g l_g)}$$

$$Zin_2 = Zo_c \frac{Zin_1 + jZo_c \tan(\beta_c l_c)}{Zo_c + jZin_1 \tan(\beta_c l_c)}$$

$$Zin_3 = Zo_g \frac{Zin_2 + jZo_g \tan(\beta_g l_g)}{Zo_g + jZin_2 \tan(\beta_g l_g)}$$

l_g = length of glass

$$\beta_g = 2\pi f\sqrt{\mu_o\varepsilon_o\varepsilon_g}$$

$$\beta_c = 2\pi f\sqrt{\mu_o\varepsilon_o\varepsilon_c} = \frac{2\pi}{\lambda_c}$$

$$\rho_{in} = \frac{Zin_3 - Z_s}{Zin_3 + Z_s}$$

$$swr = \frac{1+|\rho_{in}|}{1-|\rho_{in}|}$$

Most readers are familiar with the periodicity of VSWR over frequency. Figure 1 is a typical example of such periodicity. A quick look at the above equations reveals that the dominant factor in the periodicity is the term which appears as the argument of the tangent function. For a given length of cable, the frequency spacing between successive minima is approximated by

$$\beta_{c1}l_c - \beta_{c2}l_c = \pi$$

$$\Delta f = f_2 - f_1 = \frac{1}{2l_c\sqrt{\mu_o\varepsilon_o\varepsilon_c}} \quad (2)$$

Equation (2) is easily rearranged to relate cable length to frequency spacing between nulls

$$l_c = \frac{1}{2\Delta f\sqrt{\mu_o\varepsilon_o\varepsilon_c}} \quad (3)$$

Likewise, for a given frequency, the length of cable required to move between successive minima is approximated by

$$\beta_c l_{c1} - \beta_c l_{c2} = \pi$$

$$\Delta l = l_{c1} - l_{c2} = \frac{1}{2f\sqrt{\mu_o\varepsilon_o\varepsilon_c}} = \frac{\lambda_c}{2} \quad (4)$$

These are only first order approximations. Later measurements indicate second order effects influence the frequency spacing.

Measured vs. predicted VSWR

A sample cable with estimated parameters was modeled and tested. The frequency of interest is 14.0 to 15.0 GHz. The relevant parameters are

$$\varepsilon_g = 3.8 \;\rightarrow\; Z_g = 52\,\text{ohms}$$

$$\varepsilon_c = 1.73 \;\rightarrow\; Z_c = 50\,\text{ohms}$$

$$l_g = 0.07\,\text{inches}$$

$$l_c = 15\,\text{inches}$$

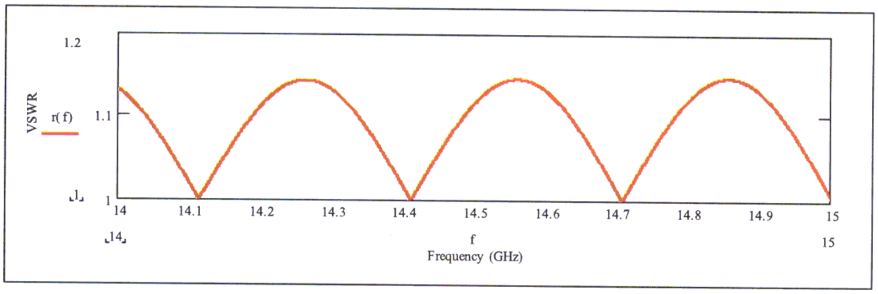

▲ **Figure 3. Theoretical VSWR performance for a 15-inch cable.**

The estimated frequency spacing between successive minima is

$$\Delta f = f_2 - f_1 = \frac{1}{2l_c\sqrt{\mu_o\varepsilon_o\varepsilon c}} = 300\,\text{MHz} \quad (5)$$

The plot of the theoretical VSWR performance in Figure 3 shows the frequency spacing between minima to be roughly 300 MHz. The measured VSWR data in Figure 4 shows an average frequency spacing of 320 MHz at the low end of the band to 250 MHz at the high end of the band.

As noted above, the frequency spacing between nulls decreases with increasing frequency. This occurs as the second order effects, such as junction capacitances between the bulk cable and the connectors, become significant. The graphs verify the primary factor for determination of the frequency spacing between successive minima is the length of cable separating the connectors.

Equation (4) predicts that the minima can be moved with frequency; that is, a VSWR low can be tuned to a specific frequency by cutting off or adding a fraction of a wavelength of cable. For example, to move the minimum at 14.65 GHz to 14.86 GHz (an arbitrary choice), the technician would need to cut off approximately

$$\Delta l = \frac{\lambda_{14.86}}{2}\left(\frac{14.86-14.65}{0.243}\right) = \frac{0.0153}{2}(0.864)$$
$$= 0.0066m = 0.26\,\text{inches} \quad (6)$$
$$\varepsilon_c = 1.73$$

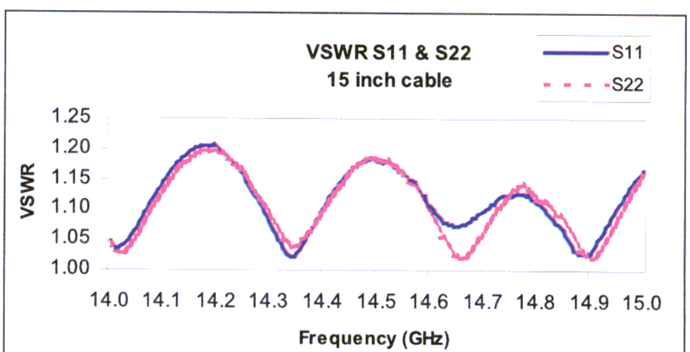

▲ **Figure 4. Measured VSWR performance for a 15-inch cable.**

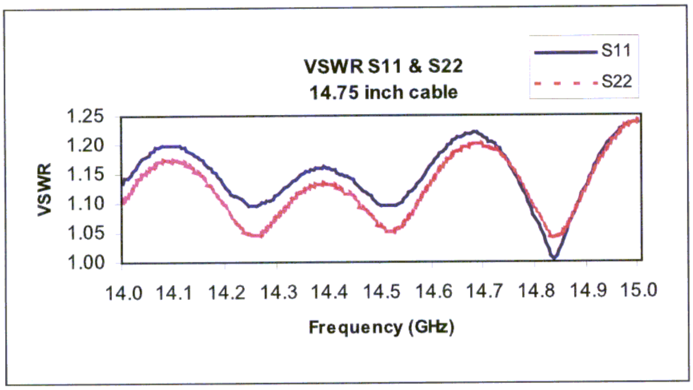

▲ **Figure 5. Measured VSWR performance for the 14.75-inch cable example.**

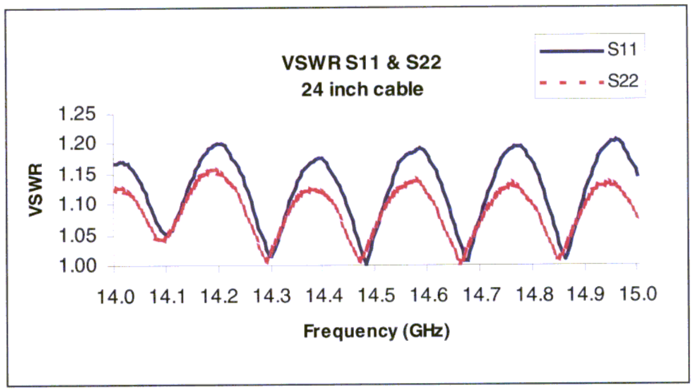

▲ **Figure 6. Measured VSWR performance for the 24-inch cable example.**

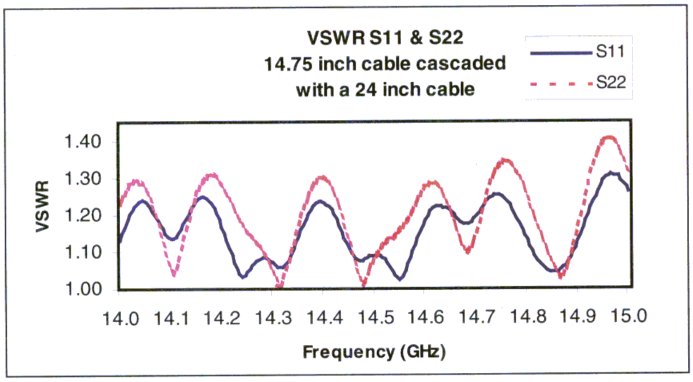

▲ **Figure 7. Measured VSWR cascade for the cables shown in Figure 5 and Figure 6.**

The frequencies are determined as follows:

- 14.86 GHz is the frequency for the desired minimum.
- 14.65 GHz is the first minimum to the left of the desired minimum.
- 0.243 GHz is the frequency spacing between the null to the left of the desired minima and the null to the right of the minima. Using the actual frequency spacing accounts for second order effects.

Note that the frequency spacing between nulls is inversely proportional to the cable length; that is, as the cable is shortened, the frequency spacing increases. Thus, any given null will move upward in frequency as the cable is shortened.

Results

The 15-inch cable was shortened by 0.25 inches. As can been seen in Figure 5, the null at 14.65 GHz has been moved to 14.84 GHz. This not exactly the 14.86 GHz goal, but it is close enough for demonstration.

Cascade of two cables

The goal in designing cables with nulls at specific frequencies is that the cable is mated to a system with a VSWR which has been minimized at the same frequency. An approximation to such a system is a cascade of two cables with minima at the same frequency. The cable of Figure 5 is mated to a second cable, with a VSWR response shown in Figure 6.

The measured VSWR for the cascade of the two cables is shown in Figure 7. As expected, a VSWR null occurs at roughly 14.85 GHz.

Theoretical check

Using Equation (1), a cascade of two cables is modeled and performance comparisons made for variations in the connector impedances. The lengths have been chosen to coincide with nulls at 14.7 GHz. In both cases, the output of Cable 2 is mated to a perfect 50 ohm load, and the input of Cable 1 is mated to a perfect 50 ohm source impedance. (Figures are on the following page.)

Case 1 (Figure 8):

Cable 1:
$Z_{Connector}$ = 52 ohms
Z_{Cable} = 50 ohms
length = 15 inches

Cable 2:
$Z_{Connector}$ = 52 ohms
Z_{Cable} = 50 ohms
length = 30 inches

Case 2 (Figure 9):

Cable 1:
$Z_{Connector}$ = 52 ohms
Z_{Cable} = 50 ohms
length = 15 inches

Cable 2:
$Z_{Connector}$ = 48 ohms
Z_{Cable} = 50 ohms
length = 30 inches

In both cases, the individual cables were tuned for nulls at 14.7 GHz. When cascaded together, a null at 14.7 GHz remained. In Case 1, the impedance mismatches in the connectors were identical and resulted in a lower VSWR for the cascade than shown in Case 2, where the connector impedance of Cable 1 differed from that of Cable 2.

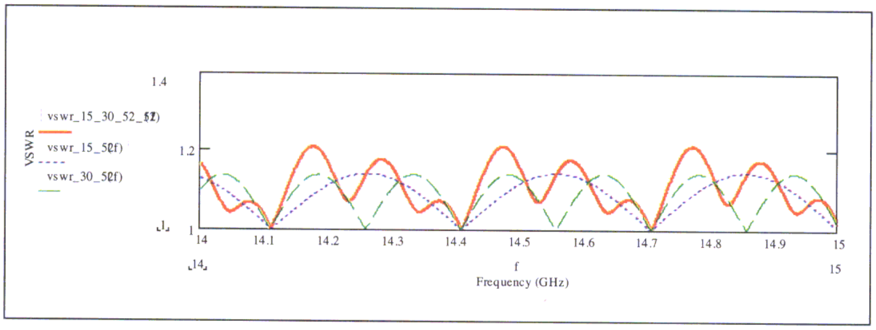

▲ **Figure 8. Theoretical cascade of two coaxial cables with similar connector impedances, tuned for 14.7 GHz.**

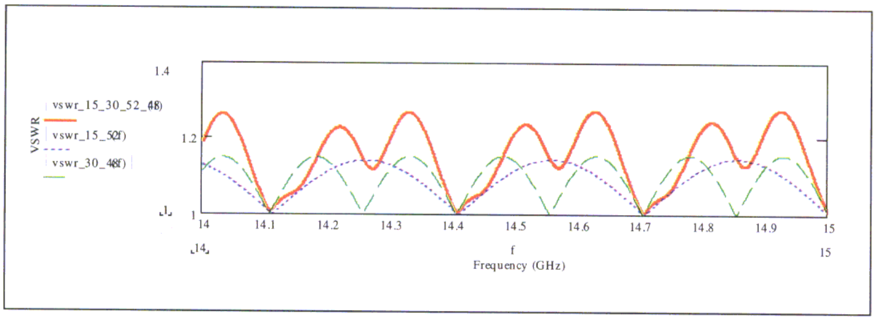

▲ **Figure 9. Theoretical cascade of two coaxial cables with dissimilar connector impedances, tuned for 14.7 GHz.**

Bandwidth

We assume that one-sixth of the frequency band between successive minima has VSWR low enough to meet our needs. Therefore, we estimate the maximum bandwidth of ultra low VSWR for a given length of coax cable as:

$$BW = \frac{1}{6}\Delta f = \frac{1}{6}\frac{1}{2l\sqrt{\mu_o \varepsilon_o \varepsilon_c}} \qquad (7)$$

For the 14.75 inch cable that was built, the estimated bandwidth of ultra low VSWR is 50 MHz, which is in agreement with the measured data. In the case of higher frequency bandwidths, this estimate will have to be reduced as the result of second order effects.

Phase matching

Provided cable of similar dielectric is used, phase matching is possible when two or more cables are matched for VSWR. In general, the absolute phase length of the cables will differ by multiples of 180 degrees, $n = 0,1,2,...$; VSWR matching and phase matching to ±20 percent is easily achieved.

Practical considerations

The basic model is a function of the glass beads in the connectors and the length of cable. As the length of the cable becomes shorter, the glass beads will become more influential. Kaman has found through experience that the model works adequately for cables as short as 4 inches. Bandwidth is inversely proportional to cable length. As such, the longer the cable, the narrower the bandwidth.

The cutoff necessary to move the VSWR minima is dependent on the dielectric constant of the cable. The accuracy of the cutoff will be dependent on how closely the dielectric constant of the cable is known, properly accounting for second order effects.

Second order effects such as junction capacitance are significant at microwave frequencies in the range of 14 to 15 GHz. These effects were compensated for in the determination of cut length by measuring the actual frequency spacing between successive minima about the desired frequency minima.

The actual VSWR performance of cascaded devices will depend on the impedance highs and lows, as well as inductive, and capacitive discontinuities of each device. In the case presented, the cable and connectors were very similar.

Conclusion

VSWR in a coax cable is influenced by the characteristic impedance of the cable, and, generally, the characteristic impedance of the connectors. Building cable and connectors which meet the nominal 50-ohm characteristic impedance will assure good VSWR performance. For applications requiring the best possible VSWR over a narrow band, the cable can be cut to length and VSWR minima can be tuned to a particular frequency. ■

Reference

1. D. M. Pozar, *Microwave Engineering*, New York: John Wiley & Sons, 1990.

Author information

Bruce Bullard received BS and MS degrees in Electrical Engineering from the University of Colorado at Colorado Springs in 1988 and 1991. He is a project engineer with the Microwave Products Group at Kaman Instrumentation, 3450 North Nevada Ave, Colorado Springs, CO, 80907. He may be reached by telephone at 719-442-6957 or by e-mail at bruce_b37@yahoo.com.

Eric Houghland received a BS degree from the University of Southern Colorado in 1992 and is currently pursing an MBA. He is a manufacturing engineer with the Microwave Products Group at Kaman Instrumentation.

2W & 5W DC to 18GHz ATTENUATORS

from **$29.95** ea. (1-49)

Rugged Stainless Steel Construction, High Repeatability, Miniature Size, Low Cost, and Off-The-Shelf Availability are some of the features that make Mini-Circuits "BW" family of precision fixed attenuators stand above the crowd! This extremely broad band DC to 18GHz series is available in 5 watt Type-N and 2&5 watt SMA coaxial designs, each containing 15 models with nominal attenuation values from 1 to 40dB. Built tough to handle 125 watts maximum peak power, these high performance attenuators exhibit excellent temperature stability, 1.15:1 VSWR typical, and cover a wealth of applications including impedance matching, reducing power levels when testing higher power amplifiers, wide band matching during intermodulation measurements, and providing a 2W or 5W termination load for power amplifiers. Call Mini-Circuits today and capture this next generation of performance and value!

Mini-Circuits...we're redefining what VALUE is all about!

MODELS (Add Prefix BW-)

2W SMA	5W SMA	5W Type-N	Attenuation (dB) Nominal	Accuracy*
$29.95	$44.95	$54.95		
S1W2	S1W5	N1W5	1	±0.40
S2W2	S2W5	N2W5	2	±0.40
S3W2	S3W5	N3W5	3	±0.40
S4W2	S4W5	N4W5	4	±0.40
S5W2	S5W5	N5W5	5	±0.40
S6W2	S6W5	N6W5	6	±0.40
S7W2	S7W5	N7W5	7	±0.60
S8W2	S8W5	N8W5	8	±0.60
S9W2	S9W5	N9W5	9	±0.60
S10W2	S10W5	N10W5	10	±0.60
S12W2	S12W5	N12W5	12	±0.60
S15W2	S15W5	N15W5	15	±0.60
S20W2	S20W5	N20W5	20	±0.60
S30W2	S30W5	N30W5	30	±0.85
S40W2	S40W5	N40W5	40	±0.85

*At 25°C includes power and frequency variations up to 12.4GHz. Above 12.4GHz add 0.5dB typ. to accuracy.

ALL MODELS IN STOCK

Mini-Circuits®

US 108 INT'L 118
CIRCLE READER SERVICE CARD

P.O. Box 350166, Brooklyn, New York 11235-0003 (718) 934-4500 Fax (718) 332-4661 For quick access to product information see MINI-CIRCUITS CATALOG & WEB SITE

YONI™ ***The Design Engineers Search Engine*** *Provides ACTUAL Data Instantly From MINI-CIRCUITS At:* ***www.minicircuits.com***

***ISO 9001** CERTIFIED*

F 331 Rev Orig.

MTT Society Prepares For its 2001 International Microwave Symposium in Phoenix

Microwave Week, the largest international conference of microwave engineers, scientists and exhibitors, will be held in Phoenix, AZ, May 20–25, 2001. In addition to the technical program, panel sessions, short courses and workshops are planned. As in previous years, the conference combines the MTT International Microwave Symposium (IMS) with the sessions of Radio Frequency Integrated Circuits (RFICs), as well as the annual Automatic RF Techniques Group (ARFTG) conference.

Microwave Week is accompanied by an exhibition of the latest components, design tools and technologies from numerous companies and vendors in the RF/microwave/wireless industry. This year's symposium and exhibit promise to be the largest ever, according to the organizers, making IMS2001 an event not to be missed.

IMS Technical Program

IMS workshops and short courses are planned for Sunday and Monday (May 20–21). The regular sessions begin on Tuesday, May 22, the official start of the MTT-S. This year's technical program will feature 357 papers, arranged in six parallel sessions. The 2001 symposium focuses on the following topics:

- MEMS components and technologies
- High power amplifiers for commercial applications
- Microwave photonics
- Smart antennas
- Broadband communications systems
- Invited sessions on emerging technologies

New this year are three interactive forum sessions in which 196 papers will be presented and discussed. Panel sessions will be held at lunchtime each day from Monday through Thursday during Microwave Week. The workshop program offers 20 workshops and five short courses on various areas of interest to RF and wireless engineers. Topics for discussion include:

2001 IEEE MTT-S Registration and Attendance Information

Advanced conference registration via fax or e-mail runs through April 27, 2001. The online registration deadline is May 4, 2001. Registration choices include MTT symposium, RFIC symposium, ARFTG conference, panel sessions, workshops, guest programs and the awards banquet. To obtain conference and housing information, directions and schedules, or to register online (telephone registration is not available), please use the following contact information:

For information, call 781-769-9750
To register, go to http://www.mtt-sregistration.com

To register by mail or fax, please use your advance program flyer, or if you did not receive one, you may obtain an electronic version at:

http://www.ims2001.org

- Low cost fabrication and manufacturing techniques
- Communication theory
- Next generation wireless
- Thermal and material issues at microwave frequencies

Short courses and educational activities will highlight RF MEMS, power amplifiers — Classes A through S, nonlinear measurements, linear power amplifiers and fast method of moments.

IMS Panel Sessions

Panels sessions are held at lunchtime Monday through Thursday of Microwave Week. Each day one of the following issues will be discussed: RF CMOS for Bluetooth, one chip radio, automotive radar, university–industrial interactions and commercial exploitation of the 92 to 96 GHz spectrum.

Plenary Session

The plenary session, featuring a keynote address by Dr. Dennis Roberson, Chief Technical Officer of Motorola, and the 2001 Electromagnetics Award, will be held Tuesday, May 22, in the Phoenix Symphony Hall.

Radio Frequency Integrated Circuits Symposium (RFIC)

The technical activities for this year's symposium are scheduled for Monday and Tuesday of Microwave Week. The Monday panel session on RF CMOS for Bluetooth will feature discussions on systems architectures and technological barriers to implementing low-cost Bluetooth receivers. A reception for all RFIC Symposium attendees is hosted by the RFIC Steering Committee and several vendors and will take place on Sunday, May 22, from 6:00 PM to 10:00 PM at the Crown Plaza Hotel.

57th ARFTG Conference

The ARFTG conference will be held May 24–25. A joint session on Thursday, May 24, will address recent developments in electromagnetic field probing techniques using scanned near-field probes, atomic-force microscopes and direct or indirect electro-optic sampling methods. The theme for the main event on Friday, May 25, is "Best Practice and Strategies for RF Test." The program will address alternatives, trade-offs, practical considerations and particular examples of industrial methods used to perform testing.

Microwave Applications and Product Seminars (μAPS)

The microwave application and product seminars are designed to provide technical information related to the latest products of interest available to the microwave community. The seminars are open to all conference and exhibit attendees and will be held on the exhibit floor in Phoenix Civic Plaza on Tuesday, Wednesday and Thursday, May 22–24. CAD tools, simulation techniques, active and passive components and system applications will be in introduced in 30-minute presentations.

IEEE MTT-S Awards Banquet

The annual awards banquet will take place on Wednesday, May 23, from 7:30 PM to 10:00 PM at the Hyatt Regency. Traditionally one of the highlights of Microwave Week, the evening will consist of a dinner, awards presentation and entertainment by Native American dancers.

IEEE Women in Engineering Reception

If you'd like to share your thoughts, experiences and background to promote the Women in Engineering Forum, meet with a panel of distinguished women from academia and industry on Wednesday, May 23, at the Hyatt Regency. For more details on this event, please e-mail kavitag@lucent.com.

■

Information about the IEEE MTT-S Microwave Week

IMS Conference Hours
May 20-25: 8:00 AM - 5:10 PM

Registration Hours
Saturday, May 19: 2:00 PM – 6:00 PM
Sunday, May 20: 7:00 AM – 6:00 PM
Monday, May 21 – Wednesday, May 24: 7:00 AM – 5:00 PM
Thursday, May 24: 7:00 AM – 3:00 PM

RFIC Symposium
Tuesday, May 22: 8:30 AM – 5:00 PM

ARFTG Conference & Exhibition
Friday, May 25: 7:30 AM – 5:00 PM

IMS and μAPS Exhibition Dates and Hours
Tuesday, May 22: 9:00 AM – 5:00 PM
Wednesday, May 23: 9:00 AM – 5:00 PM
Thursday, May 15: 9:00 AM – 3:00 PM

For additional conference information, visit
http://www.ims2001.org

Product Focus – Devices for Fiber Optics and Optical Communications

Optical driver amplifiers for OC-192

CTT Wireless has announced a series of solid-state optical driver amplifiers for OC-192 fiber optic communications. The amplifiers are

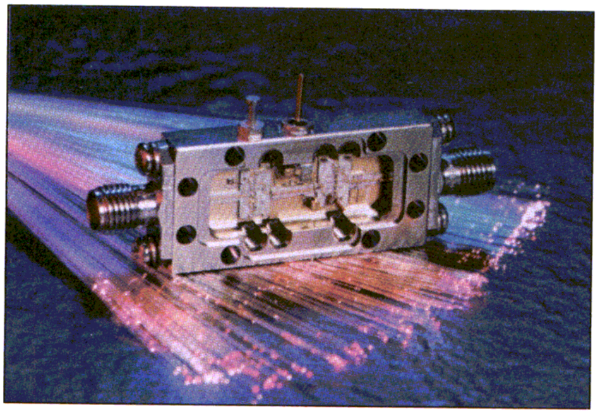

designed for use in 10 Gb/s and other high-speed applications up to 20 Gb/s. The basic amplifier provides 18 dB gain and a minimum power output of +10 dBm from 10 MHz to 15 GHz with a flatness of ±2.2 dB. To accommodate other optical modulation formats, the company offers custom integration of the amplifier and other components into subsystems that include mixer, phase shift and attenuator functions at frequencies up to 40 GHz. These amplifiers incorporate high gain, low noise MIC thin-film modules eutecticallyl bonded to metal carriers for maximum efficiency and durability.

CTT Wireless
Circle #190

Laser diode test systems

Racal Instruments' Broadband Group offers laser diode burn-in and reliability test systems. The Photonics ET-48 test system allows users to subject complete packaged laser diode assemblies, including output fibers and connectors, to a wide range of test temperatures while monitoring key operational parameters. The system provides individual control of device drive currents and TEC temperatures and monitors forward current and voltage, front facet optical output, photodiode output, TEC voltage and

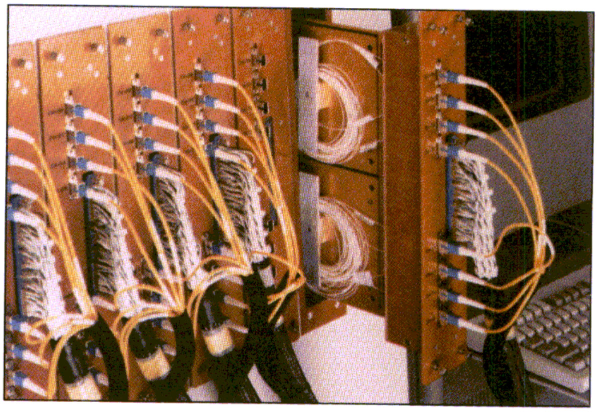

current and device thermistor temperatures. A 48-channel configuration is available. The computer-controlled environmental test chamber combines specialize modular fixtures for packaged or Chip on Submount (CoS) devices with high-volume airflow to ensure even temperature distribution. Cooling options include closed-cycle refrigeration or liquid nitrogen operation. A Graphical User Interface with sources code is provided for system control.

Racal Instruments
Circle #191

Optical return loss meter

Telecom International Services has added a new Optical Return Loss Meter Adapter to its product line. The adapter, a completely passive unit, tests the optical return loss (ORL) for fiber

and DWDM systems. It used with an existing optical loss test set, power meter and source, which connect to appropriate ports on the adapter. The fiber being tested connects to the fiber under test (FUT) port of the ORL adapter. The power meter reading is them used to calculate the optical return loss.

Telecom International Services
Circle #192

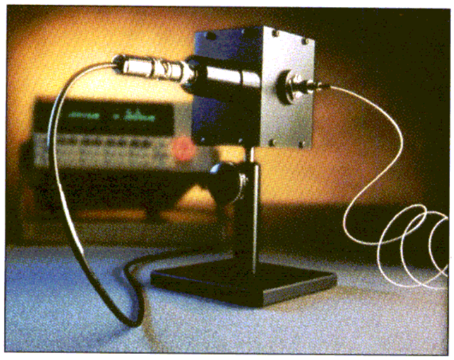

Integrating sphere

Keithley Instruments has made an agreement with Labsphere to offer a custom-designed integrating sphere optical head. The Model 2500INT Integrating Sphere facilitates direct optical measurement of laser diode output power when used with certain types of electronic test instrumentation. The sphere will be offered as part of Keithley's L-I-V (Light Intensity-Current-Voltage) Test System, designed to test laser diode modules for DWDM and other fiber optic communication systems. The sphere features two ports with three detector choices to cover wavelengths from 500 to 1700 nm. Initially, the detectors offered will be silicon, germanium or cooled InGaAs types. The system starts at $2995 with the exact price determined by the desired configuration.

Keithley Instruments
Circle #193

Low toxicity epoxy

Fiber Optic Center offers the AngstromBond® AB9119epoxy system for fiber optic systems. The two-part heat-cured epoxy is formulated to provide a strong bond to glass, metal and ceramic with coloration appropriate for high performance optical terminations. The AB9119 epoxy has less potential to cause dermatitis than most commonly-used heat cure epoxies used in these applications.

Fiber Optic Center
Circle #194

IrDA transceiver

Vishay Intertechnology has announced three additions to its MicroFace family of IrDA-compliant transceivers. Models TFDU4202, 4203 and 4204 feature a wide supply voltage of 2.4 to 5.5 V and are operational down to 2 V. The TFDU4203 features reduced power consumption and a maximum operating distance of close to 70 cm. The TFDU4202 can operate without an external current limiting resistor when a 3.3 V supply is used,

Burn out
or burn with passion?

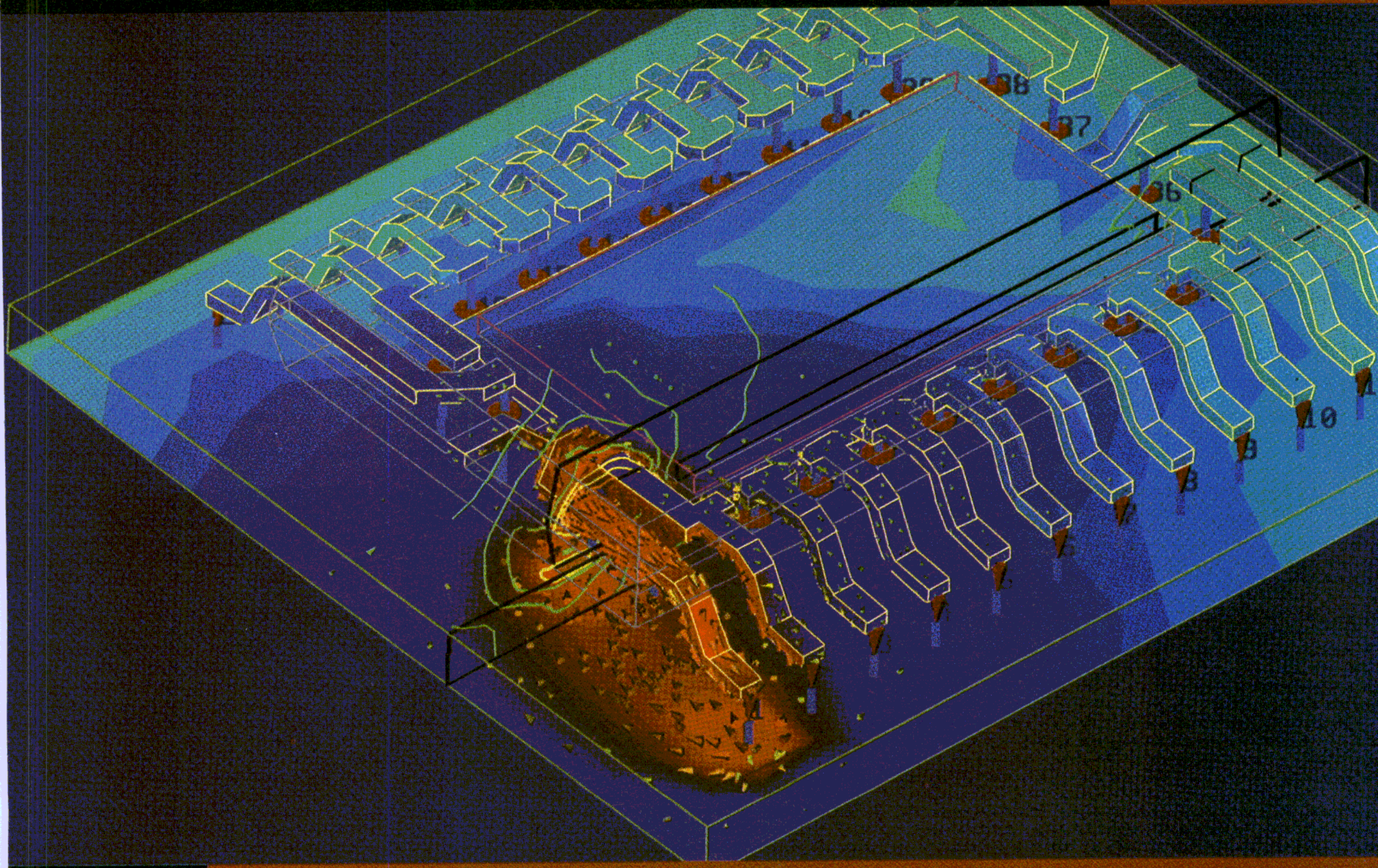

3D EM Simulation

→ Electromagnetic engineers with a passionate disposition? At CST we've found this to be quite the norm. This attitude ensures our technical leadership in the field of 3D EM simulation: The incorporation of the Perfect Boundary Approximation™ (PBA) technique allows an accurate modeling of curved surfaces while maintaining the unparalleled performance of the FI method in the time domain.
CST MICROWAVE STUDIO™'s typical applications include the simulation of waveguides, couplers, filters, power splitters, multiplexers, switches, planar structures, coax and multipin connectors, MMIC packages, RLC-extraction, and all kinds of antennas.

Circle 35

CST
COMPUTER SIMULATION TECHNOLOGY

CST. CHANGING THE STANDARDS.
CST of America, Inc. · Wellesley, Massachusetts · **http://www.cst-america.com**
To request literature or a free demo CD, **781-416-2782**, or **info@cst-america.com**

enabling a range exceeding 1 m. It features a split power supply that only requires a regulated supply for the receiver circuitry, while high IR current is provided by a less-regulated supply or directly from the battery. The TFDU4204 has input and output logic levels adapted to 1.8-V logic. This model operates to 70 cm with low power consumption and it includes the split supply feature. All three devices consume 0.01 μA in the shutdown mode.

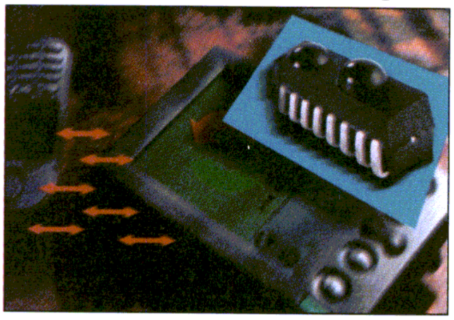

Vishay Intertechnology
Circle #195

Parallel-to-fiber converter

Faraday offers an interface card, the PI-005 which converts parallel (270 Mb/s) to fiber (1300 nm) for transmission distances up to 7 km. For two-way links, the complimentary receiver modules are packaged in the PO-005 card. These two products add fiber optic capability to the company's family of data transfer interface cards.

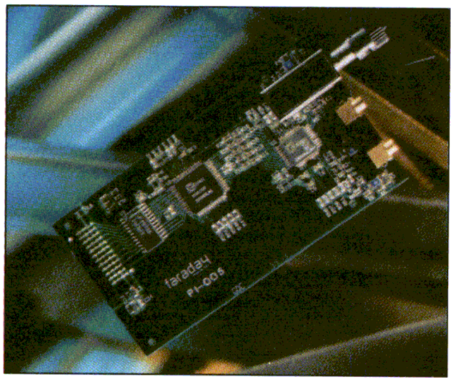

Faraday
Circle #196

Line interface transceiver

TDK Semiconductor introduces the 78P2241B line interface transceiver IC for coaxial and fiber communications. The device operates at either 3.3 or 5 V and consumes less tan 110 mA of supply current. The new IC adds a line-code violation (LCV) detector not provided in earlier versions. Other features include clock recovery and transmitter pulse shaping functions for applications using 75-ohm coaxial cable at distances up to 1100 feet and speeds up to 51.84 Mb/s. The device is fabricat-

ed using a BiCMOS process and supports applications including E3, DS3, STS-1, DSLAMs, digital multiplexers, SONET Add/Drop multiplexers, PDH equipment and ATM/WAN access for routers and switches. The IC is offered in PLCC or TQFP packages. Pricing is $31.00 each in 10,000 unit quantities.

TDK Semiconductor
Circle #197

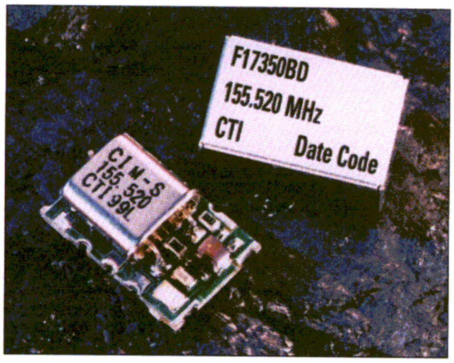

VCXO for optical networks

Champion Technologies expands its FT17000 Series SMT VCXO line with 3.3 and 5 V supply voltage, plus 10E and 100E PECL (Positive Emitter Coupled Logic) outputs. Frequency stabilities are available from ±30 ppm over 0° to +70° C to ±50 ppm over –40° to +85° C. The tuning deviation range is ±80 to ±120 ppm. Typical jitter is 1 ps RMS with <450 psec rise and fall times. Applications include SONET, add/drop multiplexers, WDM and DWDM transmission equipment.

Champion Technologies
Circle #198

Transimpedance amplifier

Applied Micro Circuits has introduced an OC-768 transimpedance amplifier fabricated using silicon-germanium (SiGe) technology. The S76800 will successfully handle data rates up to 48 Gb/s in RZ and NRZ data streams. The device is engineered for a single –5.2 V supply and low power consumption of 0.6 W.

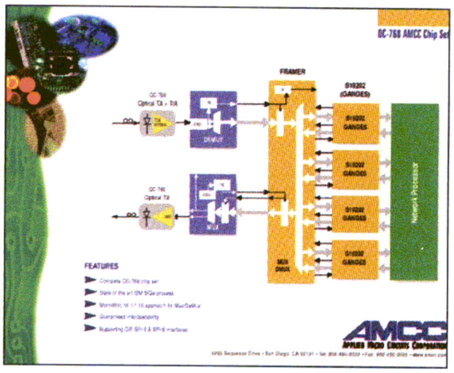

Transimpedance gain is 220 ohms with a 50-ohm single-ended output for efficient clock and data recovery. The S76800 has input noise specified at 4 μA RMS, permitting sensitivity down to 50 μA with 10×10^{-10} BER. The device can interface with a PIN photodiode using ribbon bonding or flip-chip technology. Future products in the family include OC-768 modulator drive, MUX/DEMUX devices and framer.

Applied Micro Circuits
Circle #199

Product Spotlight

Circle 250

Circle 251

Circle 252

Circle 253

Circle 254

How to place Product Spotlight and Classified ads

Our Product Spotlight section allows you to show off your company's products or services in an economical 1/9 page color ad. Ads may be sent camera ready, or we'll make up an ad for you! All you'll need to provide is a product photo, company logo and a description of the product or service you want to advertise.

Our Classifieds section is the place to advertise career opportunities, consulting services, used test equipment and just about anything else. Special Classifieds rates are available and are agency-commissionable if material is supplied. Or, if you prefer, our staff can make up the ad for you. Classified display ads are available in color or black and white in standard ad sizes, or in black and white by column inch.

For more information, please contact Aileen Kronke at 770-449-6774, or by e-mail at aileen@noblepub.com.

Advertiser Index

Tell them you saw it in
Applied Microwave & Wireless!

Applied Microwave & Wireless (USPS 011-596) (ISSN 1075-0207), printed in the U.S.A., is published monthly by Noble Publishing Corporation, 630 Pinnacle Court, Norcross, GA 30071. April 2001. Twelve issues are mailed in the United States for $30, outside the U.S. for $60, or provided free, with a completed and signed subscription form, to qualified professionals engaged in electronics engineering at 1 MHz to lightwave frequencies. Single issues, when available, are $7 in the U.S. and $12 outside the U.S. The material contained in this magazine is believed to be true and correct; however, the responsibility for the contents of articles and advertisements rests with the respective authors and advertisers. Periodical Rate postage paid at Norcross, GA 30071 and additional mailing offices.

Postmaster: Send address corrections to *Applied Microwave & Wireless*, 630 Pinnacle Court, Norcross, GA 30071.

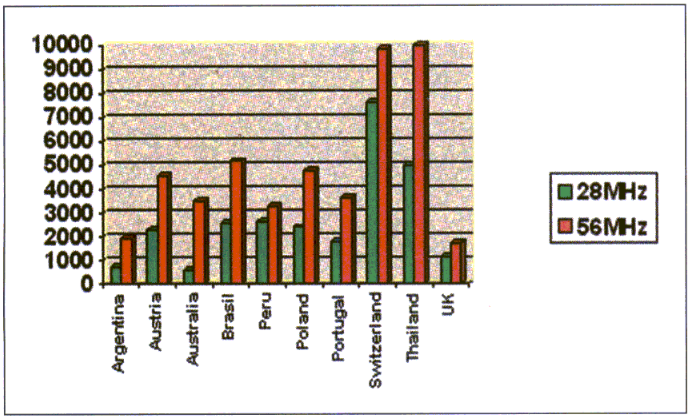

▲ **Figure 1. Comparison of yearly cost of a point-to-point 26 GHz license in various countries (in US$).**

Encouraging spectral efficiency through license fees

The most popular method of charging for spectrum usage is based on the frequency band used and the necessary bandwidth on a link by link basis. This directly equates to more efficient usage of scarce frequency resources, which simplifies frequency allocations and increases potential link densities within a given area for a fixed available frequency resource. Using higher modulation schemes for the same capacity will generally provide cost savings in the license fee. This method should be encouraged to attract spectrum users to deploy more spectrally efficient equipment.

Comparison of license fees

Figure 1 shows the typical yearly cost of a point-to-point 26 GHz license in various countries. The comparison between a 28 MHz and 56 MHz bandwidth charge demonstrates the method of charging according to the bandwidth used. In some cases, the difference is as much as 500 percent. This charging method encourages the use of spectrally efficient radio systems, particularly for large users of spectrum. For example, 100 STM-1 links deployed in Australia using a bandwidth of 28 MHz would cost the operator US$61,000. A similar deployment using a bandwidth of 56 MHz would cost US$340,000: a difference of US$279,000.

Another method used to allocate spectrum has been to auction to the highest bidder. This method has been used in Australia, Canada, the UK and the US for mostly LMDS/LMCS or point-to-multipoint services. The cost of spectrum has varied in each of these auctions. In Canada the cost has been the equivalent of US$25,000 per MHz yearly (10 years); in Switzerland, the cost was US$59,000 per MHz yearly. The costs of these licenses are proportionately higher; therefore, the importance of using spectrally efficient equipment is more apparent.

Conclusion

The inability to implement enough wired or fiber solutions to meet the explosive demands for high-speed data places an increasing importance on wireless solutions. Wireless solutions are creating new industries that depend on radio spectrum. However, radio spectrum is a scarce resource and must be used wisely. Significant improvement in spectrum reuse can be achieved by using high-order modulation systems.

Auctions of spectrum and license fees result in costs that operators must bear in order to do business. This encourages efficient use of the spectrum. Wireless has the benefit of fast and easily reconfigurable deployment in repsonse to changing needs. However, because there are alternative methods of delivering similar services, the license charge should not be cost prohibitive because that would discourage the use of wireless as a method of delivery. ■

Maximimizing the Potential of Radio Spectrum with High-Order Modulation

By Peter Gibson
DMC Stratex Networks

Global telecommunication deliberization has increased the demand for licensed radio spectrum. New operators and new services require fixed service spectrum to enable them to bypass the incumbent national operator's (PTT) access network. In particular, the new wireless services for Broadband Wireless Access (BWA) and 3rd generation mobile (UMTS) require point-to-point radio relay as the most economic method to connect customers to the point of presence (POP).

A recent ERC Report recognized that in certain frequency bands, the growth in demand for spectrum may lead to more and more congestion. It is therefore important to consider the development of more spectrally efficient systems to ensure that radio spectrum, a scarce resource, is conserved and utilized in an efficient and economically viable way.

New terrestrial services

Applications that are attributable to the increased demand for fixed terrestrial spectrum include alternative telecommunication providers, competitive local exchange carriers (CLECs), infrastructure services for mobile systems (UMTS/IMT-2000) and the LMDS/LMCS or WLL services that are necessary to deliver broadband services to small- and medium-sized businesses. Demand also continues for existing terrestrial spectrum from other radio services, such as satellite and broadcast services. This further emphasizes the need to explore better spectrum conservation techniques to use the spectrum in the most efficient manner, thus preserving this limited resource.

Spectral efficiency

The development of efficient spectrum utilization techniques will increase the availability of spectrum to meet increasing demand. One effective method of increasing spectral efficiency is to use less bandwidth for a given capacity. A higher order modulation scheme is required to make this possible.

Peter Gibson joined DMC Stratex Networks in February 1998, from the UK's Radiocommunications Agency (RA). At RA, he was responsible for assigning and licensing fixed terrestrial links to the numerous UK operators.

As DMC's manager of regulatory affairs Peter's primary responsibilities include the development of ETSI standards for new technology developed by DMC Stratex Networks, and global approval of new products promoting spectral efficiency to both regulators and operators. DMC Stratex Networks can be reached by telephone at 408-944-1817 or by fax at 408-944-1648.

For a 155 Mbit/s capacity, the minimum bandwidth that can be used currently is 28 MHz. DMC Stratex Networks has developed an STM-1/OC3 128QAM point-to-point radio that uses half the bandwidth of any existing radios at 18 GHz and above. This is especially important where mixed capacities are deployed in the same sub-band of spectrum. For instance, a single 3.5 MHz occupied channel could block a wider bandwidth system (56 MHz). Using narrower bandwidths reduces the probability that the block of spectrum allocated to an operator is restricted.

Spectral efficiency is particularly important for access networks in which link densities within a given area are expected to be high. Data networks fuel the demand and increased capacities will be attributed to the demand for Internet and other packet data type services.

Modulation schemes

The immediate benefit to using high-order modulation schemes is the saving in bandwidth. The advantage is obvious for a multi-operator environment in which spectrum is shared. Even in situations in which operators have their own exclusive spectrum, it is still advantageous to use bandwidth efficient schemes to limit the blocks of spectrum necessary for each installed network. Bandwidth efficient schemes enable more efficient coordination where guard bands have been introduced between operator allocations. An example is the use of 28 MHz STM-1 systems versus common 56 MHz STM-1 systems between two operators' allocation blocks. A maximum guard band of 28 MHz is sufficient for providing interference-free operation between adjacent links with 28 MHz bandwidth systems. 56 MHz bandwidth systems would need a maximum guard band of 56 MHz to provide sufficient interference protection.

continued on page 131